"Molecular Modeling of Cyclopeptides Targeting Nonstructural Protein (NS5A, NS5B) Of Hepatitis C Virus (HCV)"

Thesis Submitted to

DR NAZIA KANWAL

The Superior University Lahore

In Partial Fulfillment of the

Requirement for the Degree of

MS BIOCHEMISTRY

By

FAREEHA AKRAM

SU92-MSBW-F22-016

2022-2024

Faculty of Sciences

Author's Declaration

I hereby state that my MS. thesis titled **"Molecular modeling of cyclopeptides targeting nonstructural protein (NS5A, NS5B) of Hepatitis C virus (HCV)"** is my work and has not been submitted previously by me for taking any degree from this University,

The Superior University, Lahore,

Or anywhere else in the country/world.

At any time if my statement is found to be incorrect even after my graduation, the university has the right to withdraw my MS degree.

Fareeha Akram

Date: _4th November 2024

Plagiarism Undertaking

I solemnly declare that research work presented in the thesis titled "Molecular modeling of cyclopeptides targeting nonstructural protein (NS5A, NS5B) of Hepatitis C virus (HCV)"is solely my research work with no significant contribution from any other person. Small contribution/help wherever taken has been duly acknowledged and that complete thesis has been written by me.

I understand the zero-tolerance policy of the HEC and University,

The Superior University, Lahore,

towards plagiarism. Therefore, I as author of the above-titled thesis declare that no portion of my thesis has been plagiarized and any material used as a reference is properly referred/cited. I undertake that if I am found guilty of any formal plagiarism in the above-titled thesis, even after awarding of MS/M.Phil. degree, the University reserves the rights to withdraw/revoke my MS/M.Phil. Degree and that HEC and the University have the right to publish my name on the HEC/University website on which names of students are placed who submitted a plagiarized thesis.

Fareeha Akram

Research Completion Certificate

This is to certify that the thesis entitled **"Molecular modeling of cyclopeptides targeting nonstructural protein (NS5A, NS5B) of Hepatitis C virus (HCV)"**submitted by **"Fareeha Akram"**has been accepted towards the partial fulfillment of the requirement for MS/M.Phil. The quality of the work contained in this thesis is adequate for the award of degree.

DR NAZIA KANWAL
Designation:

Signature: _____

Certificate of Approval

This is to certify that the research work presented in this thesis, titled **"Molecular modeling of cyclopeptides targeting nonstructural protein (NS5A, NS5B) of Hepatitis C virus (HCV)"** was conducted by **"Fareeha Akram"** under the supervision of **"Dr Nazia Kanwal"**

No part of this thesis has been submitted anywhere else for any other degree. This thesis is submitted to the Faculty of Sciences, The Superior University, Lahore in partial fulfillment of the requirements for the degree of Master of Philosophy in the field of "**Biological sciences"** in Faculty of Sciences at The Superior University, Lahore.

Student Name: Fareha Akram Signature: _____Fareeha Akram

Examination Committee:

Session Chair: Signature: _____

a) External Examiner: Signature: _____

Prof. Dr. Muhammad Salman Bashir
Professor / Dean
School of Health Sciences
University of Management and Technology, Lahore.

b) Internal Examiner: Signature: _____

c) Supervisor Name: Prof. Dr.Nazia Kanwal Signature: _____

d) Name of HOD: Prof.Dr Uqba Mehmood Signature:

_____

e) Name of Dean: Prof. Dr. Mohammad Naveed Babur Signature: _____

f) Controller Examination: Dr. Muhammad Haris Signature:

_____

DEDICATION

This thesis is dedicated to those who have inspired, supported, and guided me throughout my academic journey in the field of biochemistry. First and foremost, I dedicate this work to my parents and my husband. Their unwavering love, encouragement, and sacrifices have been the foundation of my education. They instilled in me a passion for learning and the perseverance needed to overcome challenges. Without their support, I would not have been able to pursue my dreams and complete this thesis. Their belief in my abilities, even when I doubted myself, has been a constant source of strength.

I also dedicate this thesis to my mentor and supervisor**, Dr. Nazia kanwal**. Your guidance, patience, and expertise have been invaluable to me throughout this research project. Your enthusiasm for biochemistry and commitment to scientific excellence have inspired me to strive for the highest standards in my work. I am deeply grateful for the countless hours you spent reviewing my work, providing feedback, and encouraging me to think critically and creatively. Your mentorship has not only shaped my research but also helped me grow as a scientist.

I would like to extend this dedication to my professors and instructors, whose teachings have laid the groundwork for my understanding of biochemistry. The courses I took under your guidance provided me with the knowledge and skills necessary to undertake this research. Your passion for science and dedication to your students have been an inspiration to me. I am particularly grateful to all my professors sparked my interest in this field and set me on the path to this thesis.

ACKNOWLEDGMENTS

In the name of Allah, the most Gracious, the most Merciful.
I am extremely thankful to Almighty ‘Allah’ who is the entire source of knowledge and wisdom endowed to mankind, for providing me with the acumen and vision to complete this endeavor.

I would like to express my profound gratitude to my supervisor for her wise counsel and encouraging attitude towards this study. I am extremely grateful to him/her for immensely facilitating me during my study period by ensuring the provision of favorable circumstances and conducive environment. This project would not have been possible without her support and expert guidance.

In the end, I would like to extend my deepest gratitude to my family members. Without their encouragement, I would not have been able to complete this endeavor.

Fareeha Akram

ABSTRACT:

Hepatitis C virus (HCV) is a global health concern; it affects approximately 71 million people and results in complications such as cirrhosis and hepatocellular carcinoma. HCV is highly endemic in Pakistan, and many people are infected with this virus while new cases surface every year. There is no available vaccine for HCV. This study focuses on HCV's non-structural proteins NS5A and NS5B, which are necessary for viral replication to discover cyclotides that inhibit the virus. The 3D structures of NS5A and NS5B were obtained from the Protein Data Bank, while physicochemical properties of the proteins were analyzed by ProtParam. The cyclotides were chosen from Cybase, and the 3D structures of the cyclotides were predicted with the help of SWISS-MODEL. Molecular docking was performed with ClusPro, and the structure was visualized with PyMOL. ToxinPred and AlgPred were used to predict the toxicity and allergenicity of the protein. The stability of these complexes was analyzed with the help of molecular dynamics simulation with Desmond. The study suggested that cyclotides Phyb L and Circulin E had the highest binding affinity to NS5A and NS5B with the lowest energy -1037.8 and -1059.7, respectively, which indicates good antiviral properties. Both cyclotides do not possess any mutation, allergic reaction or toxicity. MD simulations suggested that both complexes have good stability and interaction with their respective cyclotides. These results suggested that Phyb L and Circulin E could be potent inhibitors of HCV replication and might serve as lead compounds for designing new antiviral agents. However, more *invitro* and *invivo* experiments should be conducted to support the computational results and to investigate the possibility of using these cyclotides to cure HCV.

CHAPTER 1

INTRODUCTION

The Human Hepatitis C Virus is a worldwide issue. It is an RNA genome virus that severely damages the liver worldwide. HCV causes liver-related diseases in humans like fibrosis, liver inflammation and liver cancer, which is also known as hepatic carcinoma. HCV is a blood-borne viral infection disease **[1]**. It was first noticed in 1989 by Michael Houghton, Harvey Alter, and Charles Rice. It is a long-term and toxic liver disease that occurs in human beings **[2].** Worldwide, there are more than 58 million people who are chronically infected with the hepatitis c virus infection; out of these, 3.2 million patients are teenagers and children **[3].** In 2023, Pakistan stood in second position globally with the highest prevalence of HCV, with 1 out of every 20 Pakistanis infected with HCV **[4]**. The chronic hepatitis c virus infection in 2001 at its peak with 3.6 million infected people; after that yearly, this number declined from more than 200,000 cases per year in the 1980s to around 16,000 cases in 2009 [5]. The mode of transmission of the Hepatitis C Virus is through contaminated blood, through unsterilized medical or other equipment used in piercing, body tattooing and through sexual intercourse **[6]**. HCV is asymptomatic in nature; its symptoms appear a few weeks after getting an infection, prominent symptoms include yellowish skin, pale yellow eyes, loss of hunger, stomach pain, dark urine and blackish stool [7].

Laboratories play a very crucial role in the diagnosis of viruses. The presence of HCV in the human body can be diagnosed through many ways like serological testing (ELISA), also called confirmatory test, which detects anti-HCV antibodies in HCV suspected person's blood; it explains a person is suffering from HCV or not it is a qualitative test to diagnose HCV **[8]**. After the confirmation of HCV in plasma, the most important thing is to quantify the virus in the blood, which is carried out through polymerased chain reaction (PCR), which quantifies the RNA of HCV **[9]**.

The hepatitis c virus's outer surface is covered with core proteins called E1 E2 (which neutralize the antibodies) **[10]**. HCV is 40-60 nm in diameter and belongs to the Flaviviridae

family, and their genus is hepacvirus. Its genome consists of a single ORF 5' end, and 3'end is (UTR) untranslated regions. The translator region consists of ten proteins; three are structural, and seven are nonstructural proteins (p7, NS2, NS3, NS4A, NS4B, NS5A and NS5B**)** [11]. The 30 genotypes of HCV discovered all over the world **[12]**.

HCV is not heritable. It cannot be passed genetically to the next generation. It can only be transmitted through blood. Viral genomes are incorporated into virus particles by the synthesis and replication of viral RNA by the RNA-dependent RNA polymerase (RdRP) protein, NS5B; because HCV NS5B RdRP does not have a proofreading function, there is a significant error rate during HCV replication, which increases HCV genetic heterogeneity and population complexity. The replication stage of HCV is divided into many steps. Initially, the virus enters the hepatic cell and starts to uncoated itself, and translation occurs. The genome of HCV replicates then assembles and releases from the cell to infect another cell. In acute hepatitis, sometimes patients do not need treatment. The immune system fights against the virus, and in chronic hepatitis, patients need medication. The available treatments for chronic hepatitis c virus are acting antiviral drugs like sofosbuvir and daclatasvir **[13]**. NS5A is a nonstructural protein of the hepatitis c virus, which plays a vital role in RNA virus replication, and with the help of other proteins of the cell, it takes part in viral assembly **[14]**. The N terminal amphipathic alpha-helix of NS5A protein has almost three structural domains **[15].** Several reports have shown a connection between HCV NS5A, interferon signalling, and hepatocarcinogenesis. However, the specific function of this protein in the HCV life cycle is still unclear. HCV NS5A has no recognized enzymatic activity **[16]**.The hepatitis C virus (HCV) NS5A protein is a multifunctional protein essential to the pathogenesis and viral replication cycle. Since its discovery, NS5A has been thoroughly studied because of its distinct structure and range of roles in the viral life cycle **[17]**.

An estimated 71 million people worldwide are expected to be affected by HCV, a major cause of chronic liver disease. Belonging to the Flaviviridae family, the virus has a single-stranded RNA genome that codes for a polyprotein. This polyprotein is then processed into two types of proteins: structural (core, E1, E2, and p7) and non-structural (NS2, NS3, NS4A, NS4B, NS5A, and NS5B). NS5A is unique among these non-structural proteins because of its several functions and crucial roles in viral pathogenesis

and reproduction **[18]**. Depending on the HCV genotype, a phosphoprotein called NS5A has between 447 and 447 amino acids. Three domains comprise its structure: Domain I, located at the N-terminus; Domain II, containing a membrane attachment sequence; and Domain III, located at the C-terminus. NS5A's C-terminus is largely conserved and has a zinc-binding motif, but its highly variable N-terminus has many phosphorylation sites **[19].**

The role that NS5A plays in viral RNA replication is one of its primary roles. Viral RNA synthesis is done by a replicase complex that interacts NS5A with other viral proteins, such as NS3 and NS5B. This complex joins the endoplasmic reticulum and other intracellular membranes to form a membranous web structure necessary to replicate the viral DNA effectively. NS5A is involved in the assembly and release of viruses and its function in RNA replication. It aids in constructing new virions by interacting with the core protein and other cellular and viral components. By influencing the host cell's lipid metabolism, NS5A encourages the production of lipid droplets, essential for the assembly and release of infectious virus particles **[20]**.

Moreover, NS5A has been connected to altering signalling pathways in host cells. Cell division, death, and innate immunity are biological processes that NS5A can dysregulate by interacting with different host proteins, such as kinases, phosphatases, and transcription factors. These interactions facilitate the development of chronic infection and HCV pathogenesis. It is appealing to target NS5A with antiviral treatment because of its distinct structure and activities. With the development of direct-acting antiviral medications (DAAs) that specifically target NS5A, the management of HCV infection has been completely changed. When NS5A function is inhibited, viral replication is hampered, and infection-causing individuals eventually clean their viral load **[21]**. NS5B is an RNA-dependent RNA polymerase that uses RNA templates to catalyze the synthesis of viral RNA. The binding of NS5B to the viral RNA template initiates the replication process, followed by the recruitment of nucleotides and the creation of phosphodiester linkages between them. The replication of the HCV genome and the generation of viral progeny depend on this enzyme activity **[22]**.

Thumb, palm, and finger domains are just a few of the many domains that make up the multifunctional protein NS5B. The active site that drives RNA polymerization

comprises all these domains. While the palm domain has conserved motifs necessary for catalytic activity, the thumb domain stabilizes the enzyme. Viral RNA can replicate because the finger domain makes template binding and nucleotide inclusion easier **[23].**Because it promotes viral replication and preserves viral genetic diversity, NS5B is essential to the pathogenesis of HCV. For HCV to develop treatment resistance and adapt to host immunological responses, NS5B's RNA replication fidelity is essential. Moreover, NS5B has been linked to avoiding innate immune responses and altering host cell signaling pathways, which both contribute to the persistence and pathophysiology of HCV**[24]**.

A desirable target for developing antiviral medications is the enzymatic activity of NS5B. HCV infection treatment has been transformed by developing direct-acting antiviral drugs (DAAs) that specifically target NS5B. They interfere with several stages of RNA synthesis and obstruct viral replication. Examples of these include nucleotide analogues and non-nucleoside inhibitors. Combination therapy, including several classes of DAA, has demonstrated high efficacy in maintaining virological response rates and lowering the risk of drug resistance. Hepatitis C virus (HCV) infection continues to be a major global health concern, impacting millions of people globally and placing a heavy strain on healthcare systems. Drug resistance and restricted access to medication are two issues that still exist despite advancements in treatment, such as the development of direct-acting antiviral drugs (DAAs). Therefore, the creation of innovative therapeutic approaches to combat HCV infection is desperately needed. Small cyclic peptides known as cyclotides are usually made up of 28–37 amino acids grouped in a cyclic cystine knot motif, which gives them remarkable stability and resistance to degradation by proteases **[25]**. The cyclic backbone and three conserved disulfide bonds that make up this structural motif give cyclotides exceptional stability and bioactivity. Cyclotides also have a wide range of biological actions, such as cytotoxic, anti-inflammatory, and antibacterial effects, which makes them desirable candidates for drug development. Cyclotides can obstruct the HCV lifecycle at many stages, such as entrance, replication, and assembly **[26].**Cyclotides may prevent the attachment of viruses to host cell receptors or interfere with the fusion of the virus's membranes to prevent their invasion. Cyclotides can impede viral RNA synthesis or assembly by targeting host factors or

viral enzymes necessary for HCV replication. Furthermore, it has been demonstrated that cyclotides have immunomodulatory qualities, which may strengthen human defence mechanism against HCV infection **[27]**.

There is great potential in the development of cyclotides as HCV therapies. Their distinct structural attributes, including stability and bioavailability, render them appealing options for drug discovery. Cyclotides benefit from natural sources, which may lower the possibility of unfavorable side effects linked to synthetic substances. Moreover, cyclotides can be manipulated and refined to improve their pharmacokinetic characteristics, efficacy, and selectivity against HCV. However, in order to fully utilize cyclotides as a therapy against HCV, several issues must be resolved. These include determining the exact mechanisms of action, enhancing formulation and drug delivery techniques and assessing the efficacy and safety of cyclotide-based medicines in preclinical and clinical trials. Furthermore, to enable the broad use of cyclotides, efforts must be made to increase production and lower costs.

AIM AND OBJECTIVES

- To find the antiviral potential of different cyclopeptides against HCV (NS5A, NS5B) proteins.
- To predict the binding affinity between cyclopeptides and NS5A, NS5B proteins.
- To identify the specific amino acid residues on NS5A and NS5B.
- Find peptide base therapeutic drugs which are less toxic.
- Predict the inhibitory function of selected cyclopeptides which can bind to the targeted active site.

CHAPTER 2

LITERATURE REVIEW

2.1 HEPATITIS C

Chronic hepatitis C is the cause of hepatic C. Approximately more than 130–170 million people worldwide suffer from chronic liver disease brought on by the hepatitis C virus **[28].**The tiny virus that caused HCV began in an affected family. A single positive strand of RNA is translated into a complex protein that is divided into ten smaller proteins, three of which are structural and the other six of which are nonstructural**[29].** This process is carried out by means of cell signals. These complex proteins lacked any enzymatic structural motif, in contrast to other complex proteins. Additionally, it was discovered that NS5A is thought to be an essential pathogenic component for a successful viral replication process that involves cooperation and mobilization with a number of host cell components**[30].**

Globally, a large number of people have chronic hepatitis C virus infection. However, there were further options available to those who were unable to respond to treatment or who could not endure it. A large number of patients had taken the other path, and some required supplemental anti-malarial drugs (CAM) in addition to or instead of conventional therapy. The risk of contracting an illness from the (HCV) virus was higher and was predicted to rise sharply over the course of the year**[31]**. Nowadays, antiviral treatments are thought to be authorized and very successful in getting rid of the virus in over half of the patients who are ill. However, ribavirin and pegylated interferon-based therapy were thought to be unsuitable for many HCV patients due to their high cost, length, and significant adverse effects. Thus, there was a clear and ongoing need to create some more alternative medications that operate through different mechanisms so that patients with HCV infection might benefit from treatment and experience a higher rate of recovery. Many of the fundamental processes of HCV

replication have expanded recently because to advancements in cell culture of HCV systems and replication analysis, which could result in the discovery of novel antiviral targets. In order to concentrate on comprehending the life cycle of HCV. These stages mostly involved the virus attaching, entering, and fusing together as the transcription of the viral RNA revealed a posttranslational process. The HCV virus was replicated in order to improve virus assembly and release.

2.1.1 HCV GENOME AND REPLICATION

The HCV virus's structure is essential to the process of replication **[32]** .Its 3-UTR had 225 base pairs, along with a lengthy poly(U)-poly(U/UC) tract and a highly sealed 3´terminal extension consisting of 98 nucleotides that integrated to form three stem-loops. At the 3´end of the NS5B coding sequence, two of the four secure stem-loop structures and the 3´UTR help the RdRp **[33].**

Fig.2.1. HCV replication stages **(1)** Receptor virus binding **(2)** Endocytosis happening virus enter into the host cell **(3)** fusion and coating (4) The process of polyprotein translation occur **(5)** viral proteolytic process occurring **(6)** RNA polymerase catalyze the negative sense RNA template **(7)** HCV particles ASSEMBLE NEAR cytosolic lipid droplets **(8)** maturation of HCV viral lipoparticles **(9)** Release of viral hcv lipoparticles into extracellular compartment.

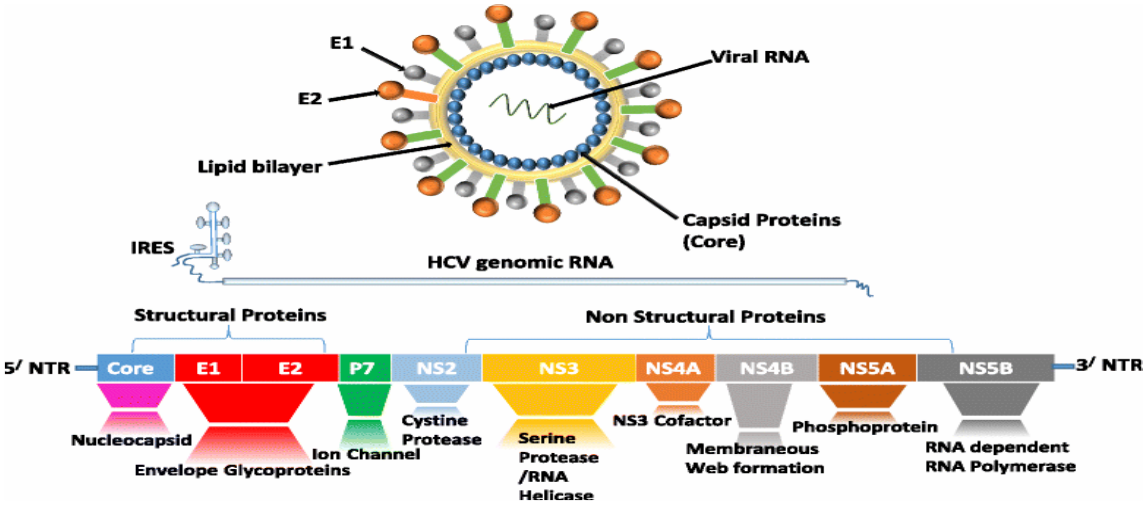

Fig 2.2. Hcv structure and genome

2.1.2 SUSCEPTIBILITY OF LIVER CIRRHOSIS DUE TO HCV

Cirrhosis and hepato-cellular carcinoma are important threats of last-stage chronic hepatitis c caused by HCV **[34]**. HCV is positive-sense molecule of 9.6 kb. The hcv genome contains single-stranded RNA which is translated into a poly-protein containing 3,000 amino acids. The polyprotein after post translation is broken down by both viral and cell proteases to create about 10 small proteins which are known as polyproteins which are comprised of nonstructural NS2, NS3, NS5A,NS5B as well as structural proteins core and E1 and E2 **[35]**.

2.1.3. REDUCTION OF HCV USING ANTIVIRAL INHIBITOR

HCV multiplies as a result of which serious chronic liver disease occurred all over the world and more than 170 million individuals showed highest threats of illness and death. The existing interferon-based the therapies were ideal treatment particularly in diseased patients and reported the estimation of BILN 2061, this inhibitor was biologically accessible when ingested orally during first experimental attempt in human beings. The availability of BILN 2061 to diseased people with HCV genotype

one for two days were lead to a remarkable decline of HCV RNA plasma levels and recognized concept in humans for an HCV protease inhibitor NS3. Furthermore, investigation demonstrated the possibility of the viral-enzyme-targeted drug discovery method for the progress of innovative HCV therapeutics. The existing therapy relied upon both of pegylated ribavirin interferon-α, a treatment that is not well accepted typically linked with less than 50% persistent viral retort rate in diseased individual with genotype one virus. The progressive ant virulent were directly used for HCV were concentrated primarily on inhibitors of the viral enzymes NS3 protease. A small molecule inhibitor profile contained BMS-790052 of protein the HCV NS5A which displayed Picomolar concentration showing an extended variety of the JFH-1 genotype 2 an infectious virus and HCV genotypes in cell culture. At the first stage during clinical attempt in diseased patients with HCV, the analysis of samples having genotypes were performed and compared with standard, recognized with the *in vitro* replicon structure. These results suggested the primary therapeutic confirmation of HCV NS5A inhibitors, a large protein having no function of enzymatic catalysis, but considered as an effective role to the suppress virus replication that presented possible therapeutic treatment created on combinations of HCV inhibitors**[36]**.

2.1.4. PREVENTION OF HCV IN RESPONSE TO INTERFERON AND RIBAVIRIN TREATMENT

The RNA 59 (NTR) and 39 short open reading frames that code for a polyprotein with 3000 amino acids and 9.6 kilobases make up the HCV genome**[37].**Among HCV individuals the 59 NTR region, which was not changed contained ribosome. The ribosomal entrance triggered the synthesis of the viral polyprotein. The NS5A nonstructural protein, which had not identified sequence motif or well-known enzymatic activity, had minute susceptibility until 1995 when it was first associated to IFN treatment in HCV diseased patients. Various individuals of HCV or genotypes exhibited different sensitivity level to IFN treatment. HCV genotypes 1 and 4 are predominantly less sensitive HCV genotypes than 2 and 3 to IFN therapy; the remaining groups showed different mechanism. This therapy created serious problem in the USA where HCV genotype 1 is the most incidence form. The structure and meaning of viral protein of the

genome was determined through changes in HCV genome, these alteration resulted in cooperation with numerous functions of host cell, comprising those occupied in the antiviral accomplishment of IFN in diseased cells.

The viruses that showed resistance to IFN therapy comprised many mutations in the IFN sensitivity-determining region, which might disturb NS5A cooperation by one or additional IFN-induced antiviral effectors. This idea cooperate with and prevent the IFN-induced PKR protein kinase, the IFN-induced antiviral response is mediated through it **[38]**.

Ribavirin therapy is responded to individuals with continual infectivity with hepatitis C virus (HCV). The rate of persistent viral response was less than 50% in cases of HCV genotype 1 infected people. Activation and recruitment of lipid kinase is activated by the NS5A protein is useful for the integrity of replication, an effective oral HCV-protease inhibitor, had estimated as an extra treatment in phase 1 and phase 2. The highest incidence of HCV particularly with genotype 4 was seen in the people of Egypt. The efficiency of PEG-IFN/RBV therapy was determined by both host and viral factors. This study was illustrated to detect virological response in order to identify the variation of*IL28B* gene and mutational changes of HCV core and NS5A regions. Both viral and host genetic factors had been associated in influencing the clinical response to PEG-IFN/RBV therapy for HCV infected individual. Many factors were detected, comprising age, race, liver fibrosis, HCV genotype and HCV RNA levels.

2.1.5. NON-STRUCTURAL NS5A PROTEINS FUNCTION

NS5A that is Nonstructural protein of chronic Hepatitis C virus (HCV) disease is considered an important player of membrane-associated viral replication complex, and was a phospho-protein whose function was not known yet **[39]**. The size of ns5a protein is 56 KD.

2.1.6. STRUCTURE AND PHOSPHORYLATION OF NS5A

NS5A contained three domains which are separated (LCSs).Investigation was done in the first domain and found that it comprised of conserved tetracysteine motif which had an ability to interact with zinc atom. There were two trypsin cleavage sites that are analogous to the two LCSs-persistent with evaluation that these contained flexible

surface showed loops associating domains when length of NS5A were fully analyzed. Atomic absorption spectroscopy investigated that domain was bound to a lone atom of zinc; alteration in the motif of tetracysteine eliminated this interface, and large virus genome replication in sub genomic replicon system, exposing that NS5A function is linked with binding of zinc atom**[40]**. Domain I is zinc binding which comprised on a disulfide bond at the C terminal both the zinc and disulfide are involved to maintain the overall fold. The domain II or domain III was deficient in overall secondary structure when NMR and other biophysical analysis was done, depending upon suggestion that the domains has been essentially out of order. More recently NMR study suggested domain II was expressed and showed indication that it form triple α-helicals in proximity of C terminus.

2.1.7 ROLE OF NS5A IN REPLICATION COMPLEX

The NS5A formed a complex which was localized in plasma membranes and catalyzed the replication of the viral genome **[41]**.In association with the other non-structural proteins, NS5A resides in membranes of cytoplasm with RNA. Differential centrifugation separated fractions of replicon cell membrane comprised both forms of NS5A p56 and p58 were competent for formation of HCV RNA in vitro.

2.1.8 ROLE OF NS5A IN APOPTOSIS

Apoptosis is involved as an intriguing mechanism to eradicate cells having viral particles. There were multiple mechanisms to prevent both intrinsic and extrinsic apoptotic stimuli used by NS5A.**[42]**.

Biochemical approaches mediated the decline of TNF-α signaling which was mediated by a cooperation between (TRADD) and NS5A. TRADD is engaged in the triggering TNF receptor upon ligand binding and form a multimeric complex with the TNF receptor and FADD, the protein of death domain and TRAF2. This multimeric merged after that gave command for many of resulting effectors, comprising caspases and NF-kB. The blocking of these signals was done by NS5A in association to TRADD. Unlike to apoptosis inhibition, stimulation of apoptosis revealed its prominence to NS5A when activated by transcription factor FasL. This provided further understanding because NS5A was not able to attach with FADD engaged to Fas receptor upon ligand binding.

Inherent cell death is stimulated through equilibrium amid pro and other actions, such as the Bcl2 family of proteins contained anti- apoptotic and pro agents that are located in the membranes of mitochondria or nucleus. They form heteromers. NS5A binding resulting in cell loss Bcl2 protein, reducing cells retractile to certain agonists for pro-apoptosis. Different mechanism involved NS5A to target programmed death causing Bcl2 agent member, Bad **[43]**. NS5A had capacity to attach and arrested p53 in the cytoplasm. The action of it was investigated in accelerating cell proliferation, p53 nominated an internal factor which had command to unscheduled DNA synthesis or DNA damage .The p53 attacking viral particles also involved tumor genesis, focusing the importance of this protein for cell survival. The capacity of NS5A to bound to p53 and induced cytosolic seizing which might inhibit DNA linkage so, resulting activation of related genes ending which lead to stop apoptosis **[44]**.

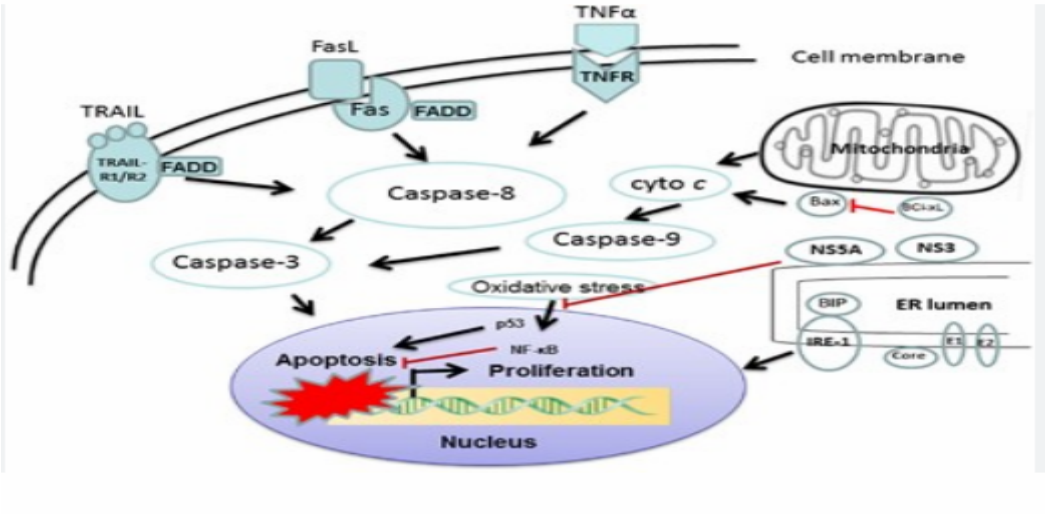

Fig.2.3 NS5A mediates extrinsic and intrinsic stimulated apoptosis

2.2 INTRODUCTION AND STRUCTURE OF NS5B

The viral replication process is central to HCV pathogenesis, and the NS5B protein plays a pivotal role as the RNA-dependent RNA polymerase (RdRp) responsible for viral RNA synthesis**[45]**.With roughly 591 amino acids, NS5B is a multifunctional enzyme that carries the RdRp domain, which is necessary for RNA synthesis. According to structural research, NS5B adopts a "right-hand" shape in which the thumb, fingers, and palm domains are responsible for template recognition, catalysis, and RNA binding,

respectively**[46]**.The presence of conserved motifs essential for nucleotide binding and catalysis in the active site of NS5B renders it a desirable target for the development of antiviral drugs**[47]**.

2.2.1 FUNCTION OF NS5B IN HCV REPLICATION

In order to replicate the HCV genome, NS5B is essential because it catalyzes the creation of new RNA strands utilizing the viral RNA as a template**[48]**.

The viral RNA is translated into a polyprotein precursor during infection, and this precursor is then cleaved to produce distinct non-structural proteins, such as NS5B. On intracellular membranes, NS5B forms replication complexes and engages in host and viral factors-mediated interactions to start RNA replication. Using nucleoside triphosphates as substrates, the enzyme catalyzes the elongation of the viral RNA strand, creating a complementary RNA strand that acts as a template for viral genomes that proliferate. The synthesis of infectious virions depends on this tightly controlled process.

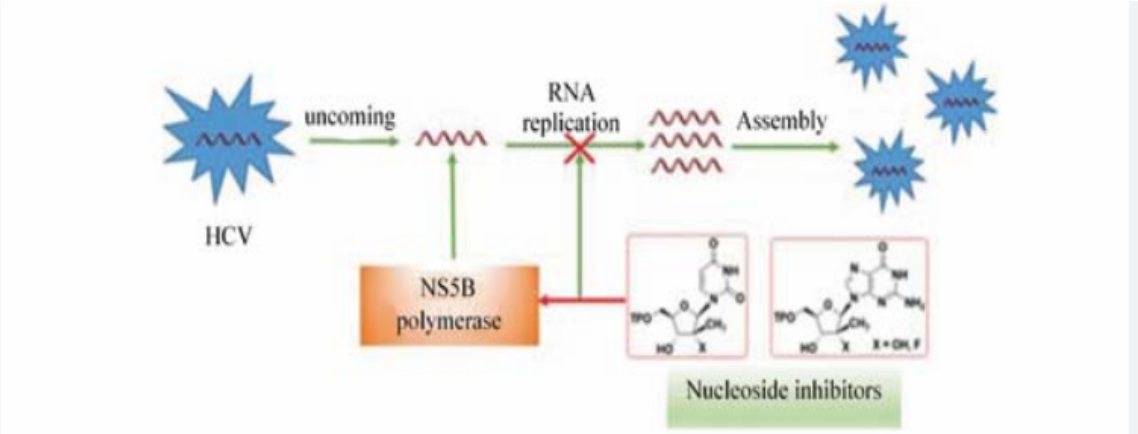

Fig 2.4 regulation of NS5B

During the HCV replication cycle, NS5B activity is strictly controlled to guarantee effective viral RNA synthesis and prevent host immunological reactions. Viral proteins like NS5A and host factors like cyclophilins are among the many elements that affect NS5B function. NS5B localization and activity are also controlled by post-translational changes such ubiquitination and phosphorylation. Determining possible targets for antiviral intervention and understanding the regulatory mechanisms controlling NS5B function are essential for comprehending the dynamics of HCV replication.

2.2.3 TARGETING NS5B FOR ANTIVIRAL THERAPY

The development of antiviral drugs finds NS5B to be a desirable target due to its crucial function in HCV propagation**[49]**. Considerable work has been done in the last few years to find and describe NS5B inhibitors with strong antiviral action. There are now two primary kinds of NS5B inhibitors: non-nucleoside analogs and nucleoside analogs. Analogs of nucleosides, like sofosbuvir, function as chain terminators by imitating natural nucleotides and forcing RNA production to end prematurely. Dasabuvir is one example of a non-nucleoside analog that binds allosterically to NS5B to inhibit its enzymatic activity. Combination therapy, which combines many DAAs to target several stages of the HCV life cycle, including NS5B inhibitors, has completely changed the way HCV is treated and has led to better patient outcomes and high cure rates.

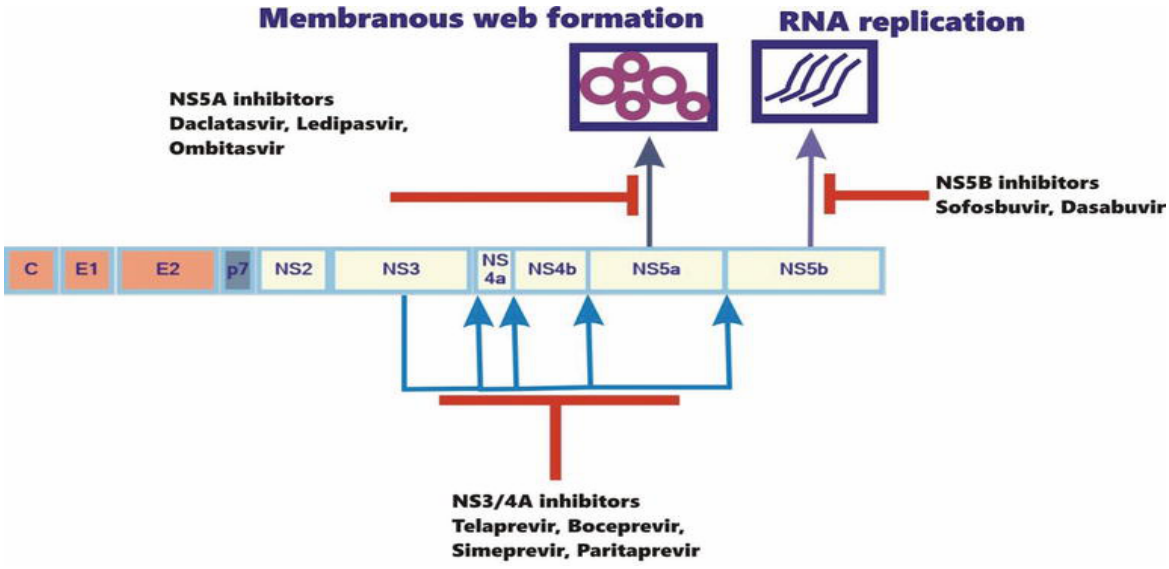

Fig.2.5. Targeting NS5B for antiviral therapy

2.3. CYCLOTIDES ORIGIN

Cyclotides had been originated in some families of plant like *Rubiaceae*, *Solanaceae*, *Cucurbitaceae*, *Fabaceae*, *Poaceae* and *Violaceae*. These above families were also reported to produce peptides of similar sequence and structure. These three families *Cucurbitaceae*, *Rubiaceae* and *Violaceae* still revealed approximately 140 cyclotides.

2.3.1. IDENTIFICATION OF CYCLOTIDES IN REGARDING THEIR BIOPHYSICAL PROPERTIES

The identification of Cyclotides was done on the basis of their chemical and biophysical properties. Cyclotides comprised six conserved cysteine residues and their molecular weight ranges between 2500 and 4000 Dalton. The rate of elution was slow in chromatography that is called reserved high performance liquid chromatography.

2.3.2. STRUCTURES OF CYCLOTIDE

Many previous studies on the kalata B1 peptide structure exposed that it had a compact structure with the lack of free C -and N-terminal groups and three disulfides were present. Kalata B1 was not degraded by enzyme utilization. Firstly, according to head and tail role structure of kalata B1 was revealed but then discarded. The three dimensional structure and full sequence of the kalata B1 peptide was determined after 20 years **[50]**.

The chemical sequencing investigated 29 amino acids and found that kalata B1 were rich in Cys (6), Gly (5) and Thr (5) residues. The enzymatic cleavage studies demonstrated presence of cyclic peptide backbone. Mass spectrometry analysis proposed its molecular weight of about 2892 Dalton. Nuclear magnetic resonance (NMR) spectroscopy data preferentially investigated that six Cys residues formed its arrangement. The two disulfide bonds out of six were considered in formation of an internal ring and a third disulfide bond entered their connecting backbone segment[51]. A motif formed which was later given the name “cyclic cysteine knot” **[52]**.

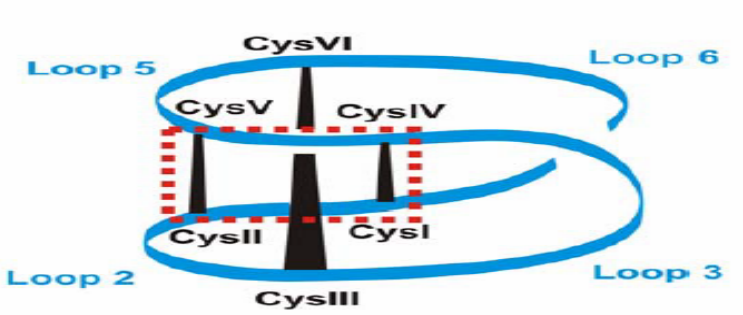

Fig.:2.6 Schematic representation of the cyclotide structure The ~30 aa cyclic backbone is stabilized by three disulfides arranged in a cystine knot, in which an embedded ring (shown by red dots) formed by two disulfides and their connecting backbone is connected by a third disulfide. The amino acids between each Cys residues form a loop**[53]**.

The disulfide of kalata b1 was basically distinguished but this idea was conflicted later **[54].** The knotted disulfide linking was reported in previous study but now reported as ladder like linking in NMR spectrum under high resolution **[55]**. The3D structural analysis and disulfide analysis OF kalata B1 reported that basically proposed disulfide linking was surely perfect.

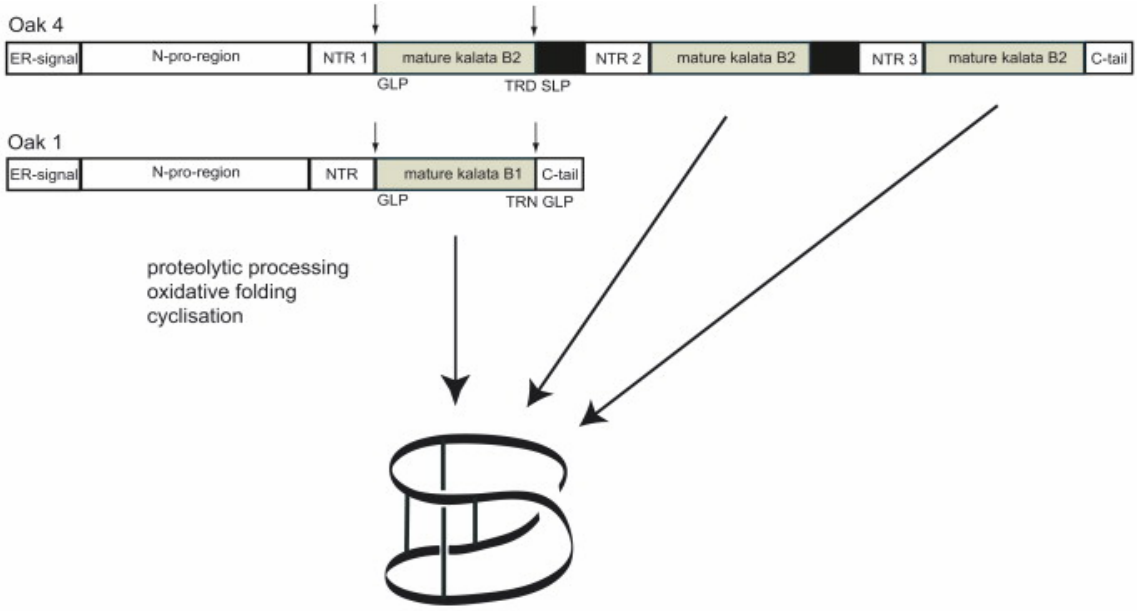

Fig.2.7 NMR structure of cyclotides Structure of cyclotides under NMR is showing that cylcotides have cyclic structure with three disulphide bonds that are interlink with six cysteine residues[56].

2.3.4. BIOACTIVITIES OF CYCLOTIDES

Many biological activities for example neurotensin binding, anti-HIV, antimicrobial anti-HIV, uteronic, insecticidal, ant hemolytic and anti HIV was shown by cyclotides. Kalata B1 had antimicrobial, hemolytic and antitumor activities. Cyclotides rendered the development and growth of insect and nematode larvae. The bioactivities of cyclotides suggested that it relied on their cooperation with the cell membrane. QSAR model mediated lipophilic nature and positively charge surface area of cyclotide that was necessary for its activity. The antimicrobial activity was reported in the following four cyclotide circulin A, circulin B, cyclopsychotride and Kalata. Cyclopsychotride and circulin A cyclotides were mediated its role only on Gram positive species, while circulin B and kalata B1 were mediated its role on both Gram positive and Gram negative species. The anti-fungal activities were also suggested in following four cyclotides. Kalata B1, circulin A, circulin B, cyclopsychotride revealed high activity against specific microbes, including *E. coli* and *Staphylococcus aureus* and *E. coli* **[57]**. Firstly, the cylcotides activity that is insecticidal was revealed in 2001. Kalata B1declined development and growth in helicoverpa larvae and enhanced death rate when larvae presented with artificial die comprising that cyclotide in same concentration as it was exhibited in natural leaf tissues. Further approaches towards insecticidal activity comprised interruption of mid-gut membrane of larvae**[58].**

CHAPTER 3

METHODOLOGY

3.1. TOXIN PROTEIN 3D STRUCTURE RETRIEVEL AND PURIFICATION

The three-dimensional (3D) structures of the toxin proteins NS5A and NS5B were obtained from the Protein Data Bank (PDB), a crucial repository providing detailed 3D structural data of various biological molecules, including DNA, RNA, and proteins. The retrieval process began by accessing the PDB website at http://www.rcsb.org.

The specific protein IDs for NS5A and NS5B were entered into the search bar, yielding structure summaries with comprehensive information on viral protein classification, the organism of origin, and any present mutations**[59]**.

The PDB format was selected from the available download options, and the files were opened using Biovia Discovery Studio Visualizer.It provides plot or graphical representation of protein data. Within Discovery Studio, water molecules and any ligands were removed to purify the protein structures, ensuring no interference from extraneous molecules during subsequent computational analyses. Purifying the protein structure is very important before docking. This purification step provided accurate and high-quality structural data essential for further studies**[60]**.

3.2. PHYSIOCHEMICAL PROPERTIES ANALYSIS

The physicochemical properties of the toxin proteins NS5A and NS5B and the selected cyclotides were predicted using ProtParam on the ExPASy server https://web.expasy.org/protparam/.ProtParam analyzes properties such as molecular weight, theoretical pI, amino acid composition, extinction coefficient, instability index, aliphatic index, half-life and GRAVY**[61].** By inputting the sequences of NS5A, NS5B, and the selected cyclotides, we obtained essential insights into their stability, solubility, and potential interactions, aiding in evaluating and optimizing cyclotides as potential drug candidates against HCV.

3.3. CYCLOTIDES RETRIEVAL

Cyclotides, known for their antibacterial and antiviral activities, were selected from Cybase (http://research.imb.uq.edu.au/cybase), a specialized database providing comprehensive information on cyclized proteins and their topological circular sequences. The selection process involved accessing the Cybase database and exploring over six different families of cyclotides. From these families, cyclotides with available 2D structures and sequences were chosen for further analysis, ensuring a diverse and representative sample for subsequent studies.

3.4. 3D STRUCTURE PREDICTION OF CYCLOTIDES

For the 3D structure prediction of cyclotides, SWISS-MODEL (https://swissmodel.expasy.org) was utilized. This bioinformatics tool facilitates the homology modelling of protein structures by providing a 3D model based on the amino acid sequence. Uploading the sequences of the selected cyclotides, templates with high coverage were identified and used to construct accurate 3D models, which were then downloaded in PDB format for subsequent analysis**[62]**.

3.5. MULTIPLE SEQUENCE ALIGNMENT OF CYCLOTIDES

For the multiple sequence alignment of cyclotides .We use CLUSTALW. It is a tool used to align amino acid and nucleotide sequences. It is highly use in molecular biology to make phylogenetic tree and give the information about amino acids.it align the higher similar sequence first than least similar one .With CLUSTALW we align sequences of

seven different families and get their results. We open this tool by using a link (https://www.genome.jp › tools-bin › clustalw).

3.6. DOCKING ANALYSIS & VISUALIZATION

For protein-protein docking, the ClusPro server (https://cluspro.org) was used, a web-based tool that facilitates protein docking by requiring only the ligand and receptor files in PDB format. A library of 44 cyclotides was created and docked against the NS5A and NS5B proteins to evaluate potential interactions by default parameters[63].

Docking visualization was performed using PyMOL (https://pymol.org), a bioinformatics software designed for molecular visualization tasks, including protein-protein and protein-ligand interactions and DNA studies **[64]**. This allowed for detailed examination and analysis of the docking results, providing insights into the interaction mechanisms between the cyclotides and the target proteins.

3.7. TOXICITY & ALLERGENICITY PREDICTION OF TOP CYCLOTIDES

The toxicity and allergenicity of the top cyclotides were evaluated using ToxinPred (https://webs.iiitd.edu.in/raghava/toxinpred/design.php) and AlgPred (https://webs.iiitd.edu.in/raghava/algpred/submission.html). ToxinPred analyzed the amino acid sequences to predict potential toxic effects, while AlgPred assessed the sequences for allergenic properties. These evaluations are essential to ensure the safety and suitability of cyclotides as therapeutic candidates.

3.8. MOLECULAR DYNAMIC SIMULATION

Desmond (https://www.schrodinger.com/platform/products/desmond/) is a highly efficient software used for MD simulations to analyze molecular behavior over time **[65]**. This study utilized Desmond to simulate ligand-receptor interactions, focusing on the drug candidate with the highest docking score to confirm its stability with the target receptor. Complexes were prepared and optimized using Maestro's Protein Preparation Wizard and System Builder module. Simulations used the TIP3P solvent model at 310K, 1 atm pressure, and the OPLS_2005 force field, with 0.15 M sodium chloride and a 20 Å exclusion region. The trajectory was recorded at 100,000 ps intervals and providing detailed insights into binding stability, conformational changes, and

interaction energies, thus evaluating the cyclotides antiviral potential **[66]**. The trajectory files were analyzed to evaluate the stability and dynamics of the protein-ligand complex. Key parameters, including Root Mean Square Deviation (RMSD), Root Mean Square Fluctuation (RMSF), and Radius of Gyration (Rg), were calculated. Hydrogen bonds, hydrophobic interactions, and other significant contacts between NS5A, NS5B and cyclotides were examined throughout the simulation. The MD simulation offered detailed insights into the stability and interactions of the protein protein complex, enhancing the understanding of their binding mechanism. The findings were crucial in confirming the potential of circulin E as an inhibitor of NS5B and PHYB L as an inhibitor of NS5A.

3.9. MM-GBSA ENERGY ANALYSIS

The MM-GBSA analysis was performed using the OPLS 2005 parameters in Prime (Schrödinger Suite). The binding energy, represented by ΔG_{bind}, was calculated by subtracting the Prime energy of the optimized complex from the free ligand and receptor **[67].** Their strain energies could be measured by comparing the receptor and ligand geometries in their free and optimized complex forms. The parameters had no missing side chains, and energy breakdown was enabled.

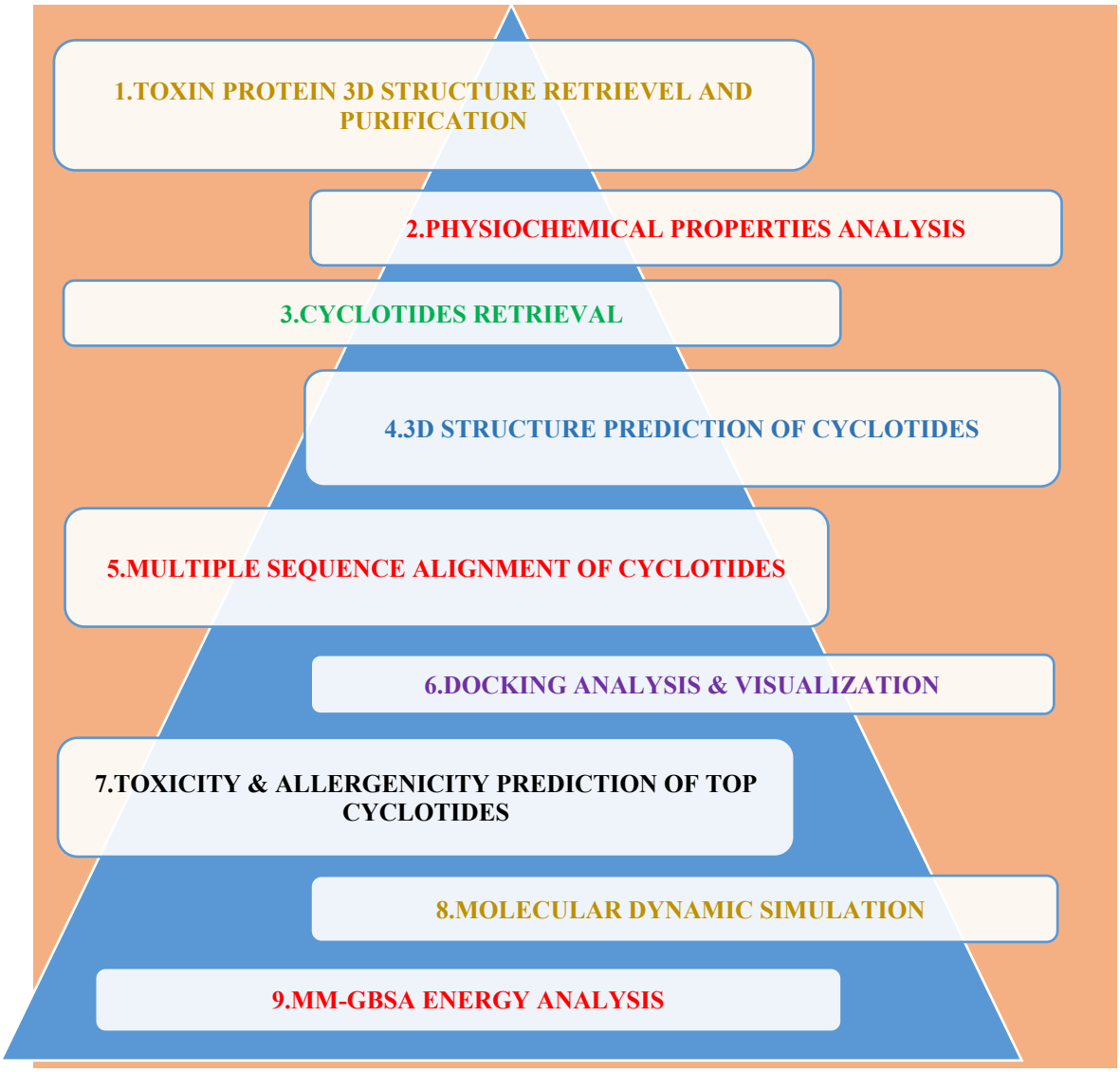

Fig 3.1 Methodology flow chart

CHAPTER 4

RESULTS

4.1. TOXIN PROTEINS RETRIEVAL AND PHYSIOCHEMICAL PROPERTIES ANALYSIS

The gravy values of the first protein, -0.364 and -0.272, indicate its hydrophilic nature. These negative values, which imply a strong attraction to water, also suggest that the protein is more soluble in an aqueous environment. This logical connection between the gravy values and protein solubility is key to understanding protein behavior. The theoretical pI (isoelectric point) values are 6.64 and 9.06, respectively, comparing the two proteins NS5A and NS5B. Hence, NS5A could be categorized under low pI proteins because the pi value of the NS5A protein is to be neutral at a slightly acidic to neutral pH. More specifically, a calculated pI value of 9.06 suggests that the NS5B protein will be neutral at a more alkaline pH. The behavior of these two proteins will differ in different pH environments. Table 1 indicates the physiochemical properties of both proteins. Figure 4.1 illustrates the 3D structure of toxin proteins NS5A and NS5B.

1 .NS5A

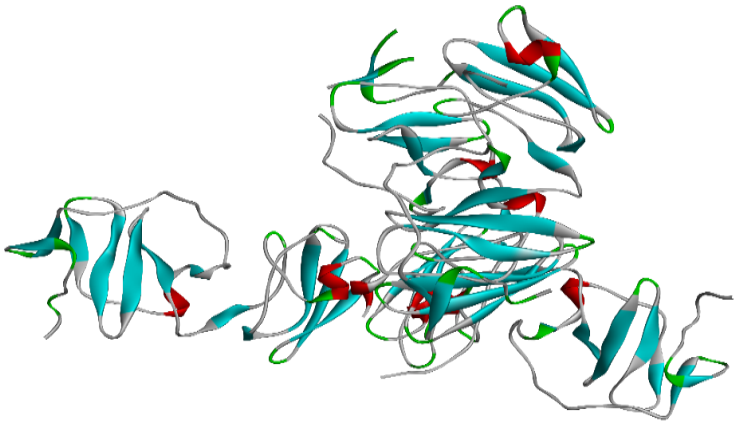

2. NS5B

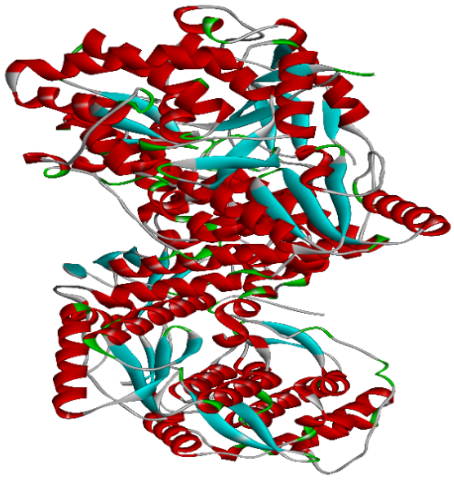

Figure 4.1: **3d structure visualization of toxin proteins (1): 3d structure of NS5A, and (2): 3d structure of NS5B**

Table: 4.1. Physiochemical Properties of NS5A & NS5B

Physiochemical Properties of NS5A & NS5B			
	Properties	**Values (NS5A)**	**Values (NS5B)**
Atomic and Amino-Acid Composition	Number of Amino Acids	177	576
	Total Number of Atoms	2729	8993
	Formula	C_{874} H_{1341} N_{247} O_{253} S_{14}	C_{2831} H_{4489} N_{809} O_{832} S_{32}
	Molecular Weight	19805.61	3420.03
State of Charge on Residues	Negatively Charged Residues (Asp + Glu)	20	54
	Positively Charged Residues (Arg + Lys)	19	71
Extinction Coefficients (M^{-1} cm^{-1} at 280 nm) Measured in Water	Assuming all pairs of Cys residues form cystines,	Ext. Coefficient: 25940 Abs 0.1% (=1 g/1): 1.310	Ext. Coefficient: 85020 Abs 0.1% (=1 g/1): 1.324
	Assuming all Cys residues are reduced	Ext. Coefficient: 25440 Abs 0.1% (=1 g/1): 1.284	Ext. Coefficient: 83770 Abs 0.1% (=1 g/1): 1.305
Estimated Half-Life	Mammalian reticulocytes, In-Vitro	30 hours	1.9 hours
	Yeast, In-Vivo	>20 hours	>20 hours
	Escherichia coli, In-Vivo	>10 hours	>10 hours
Protein Stability Indices	Aliphatic Index	64.35	81.68
	Instability Index	38.89 (Stable Protein)	46.27 (Unstable Protein)
Protein Hydrophobicity & Isoelectric Parameters	GRAVY (Grand Average of Hydropathicity)	-0.364	-0.272
	Theoretical pI	6.64	9.06

4.2 SELECTED CYCLOTIDES

We choose 6 different families of cyclotides from the Cybase database. The sequences and structures of all these families are available in CYABASE database. For multiple sequence alignment of single family we use CLUSTAL W software. Following steps have been done

1. Open **CLUSTAL W** in Google chrome by using the link (https://www.genome.jp › tools-bin › clustal w).
2. The multiple sequences of same family member selected and paste in clustal w.
3. Click on Execute Multiple alignment.
4. The CLUSTALW give results.
5. Took screenshot of all the sequences alignment results.

4.2.1 CYCLOTIDE FAMILIES SELECTED FROM CYBASE

- **Circulin**
- **CYL**
- **HYFL**
- **Kalata**
- **Phyb**
- **Vian family**

4.2.2 CIRCULIN FAMILY

Table 4.2 Amino acid number and sequences of circulin (A, B, C, D, E,)

NAME	SEQUENCE	A.A
Circulin A	GIPCGESCVWIPCISAALGCSCKNKVCYRN	30
Circulin B	GVIPCGESCVFIPCISTLLGCSCKNKVCYRN	31
Circulin C	GIPCGESCVFIPCITSVAGCSCKSKVCYRN	30
Circulin D	KIPCGESCVWIPCVTSIFNCKCENKVCYHD	30
Circulin E	KIPCGESCVWIPCLTSVFNCKCENKVCYHD	30

4.2.3. CYI FAMILY

Table 4.3 Amino acid sequence of CYI (1, 2, 3, 4, 5, 6) family

NAME	SEQUENCE	AMINO ACIDS
CYL 1	GTFPCGESCVYIPCISSVVGCSCKSKVCYKN	**31**
CYL 2	GTFPCGESCVWIPCISSVVGCSCKSKVCYKN	**31**
CYL 3	GNPGACGETCIWGKCYSASIGCSCSKYKVCTLN	**33**
CYL 4	GNPGACGETCVWGKCYSASIGCSCNKYKVCTLN	**33**
CYL 5	GNPGACGETCIWGKCYSASIGCSCSRYKVCTLN	**33**
CYL 6	GNPGACGETCIWGKCYSAKIGCSCSKYKICTLN	**33**

4.2.4. Hyfl FAMILY

Table 4.4 Amino acid sequence of HYFL (A, B, C, D, F, I, K, L,) family

NAME	SEQUENCE	AMINO ACIDS
Hyfl A	SISCGESCVYIPCTVTALVGCTCKDKVCYLN	**31**
Hyfl B	GSPIQCAETCFIGKCYTEELGCTCTAFLCMKN	**32**
Hyfl C	GSPRQCAETCFIGKCYTEELGCTCTAFLCMKN	**32**
Hyfl D	GSVPCGESCVYIPCFTGIAGCSCKSKVCYYN	**31**
Hyfl F	SISCGETCTTFNCWIPNCKCNHHDKVCYWN	**30**
Hyfl I	GIPCGESCVFIPCISGVIGCSCKSKVCYRN	**30**
Hyfl K	GTPCGESCVYIPCFTAVVGCTCKDKVCYLN	**30**
Hyfl L	GTPCAESCVYLPCFTGVIGCTCKDKVCYLN	**30**

4.2.5. KALATA FAMILY

Table 4.5 Amino acid sequence of kalata family

NAME	SEQUENCE	A.A
Kalata B9	GSVFNCGETCVLGTCYTPGCTCNTYRVCTKD	**31**
Kalata B10	GLPTCGETCFGGTCNTPGCSCSSWPICTRD	**30**
Kalata B13	GLPVCGETCFGGTCNTPGCACDPWPVCTRD	**30**
Kalata B14	GLPVCGESCFGGTCNTPGCACDPWPVCTRD	**30**
Kalata B16	GIPCAESCVYIPCTITALLGCKCQDKVCYD	**30**
Kalata B17	GIPCAESCVYIPCTITALLGCKCKDQVCYN	**30**
Kalata B18	GVPCAESCVYIPCISTVLGCSCSNQVCYRN	**30**

4.2.6. PHYB FAMILY

Table 4.6 Amino acid sequence of Phyb family

Name	Sequence	Amino acid no
Phyb A	GIGCGESCVWIPCVSAAIGCSCSNKICYRN	**30**
Phyb D	GIPCGESCMWIPCISAAIGCSCTNHVCYKN	**30**
Phyb E	GIPCGESCVWIPCISGVQGCSCSNKICYRN	**30**
Phyb F	GIPCGGSCVWIPCISGVQGCSCSNKICYRN	**30**
Phyb G	GIPCGESCAWIPCISAVQGCSCRNKICYRN	**30**
Phyb H	GLPCGESCIWIECISGAIGCSCRNKVCYRN	**30**
Phyb I	GIPCGESCIWIPCTTTALLGCSCSNKVCYKN	**31**
Phyb J	SYTCGESCLWIPCTVTAAFGCYCSNKVCVKD	**31**
Phyb L	QSISCAETCVWIPCATSLIGCSCVNSICTYTN	**32**
Phyb B	GVPCGESCVWMYCISAAMGCSCRNKVCYRN	**30**
Phyb C	GIPCGESCVWMYCITATMGCSCRNKVCYKN	**30**

4.2.7. VIAN FAMILY

Table 4.6 Amino acid sequence of Vian family using cybase database.

Name	Sequence	Amino acid no
Vian 3	GSIFNCGETCIMGTCYTPGCSCVYGACSKN	**30**
Vian 5	GIPCGESCVYIPCISAVIGCSCSSKVCYRN	**30**
Vian 6	GAFPCGESCVYIGCITSIAGCSCSDNVCYKN	**31**
Vian 7	LPLCGGETCTFGTCDTPGCTCGYWPFCTKD	**30**
Vian 9	SDTGYCNESCGTNECTTLGCICRKKVCVID	**30**
Vian 10	SLPCGESCVYIPCISGLLGCSCKNKVCYYN	**30**
Vian 11	GLNCGETCWGFHCDSPGCSCGLTWPYCSKN	**30**

4.3 MULTIPLE SEQUENCE ALLIGNMENT OF CYCLOTIDES

4.3.1 CIRCULIN FAMILY MULTIPLE SEQUENCE ALIGNMENT

```
 CLUSTAL 2.1 Multiple Sequence Alignments


Sequence type explicitly set to Protein
Sequence format is Pearson
Sequence 1: circulinA     30 aa
Sequence 2: circulinB     31 aa
Sequence 3: circulinC     30 aa
Sequence 4: circulinD     30 aa
Sequence 5: circulinE     30 aa
Start of Pairwise alignments
Aligning...
```

```
clustalw.aln

CLUSTAL 2.1 multiple sequence alignment


circulinA       -GIPCGESCVWIPCISAALGCSCKNKVCYRN
circulinB       GVIPCGESCVFIPCISTLLGCSCKNKVCYRN
circulinC       -GIPCGESCVFIPCITSVAGCSCKSKVCYRN
circulinD       -KIPCGESCVWIPCVTSIFNCKCENKVCYHD
circulinE       -KIPCGESCVWIPCLTSVFNCKCENKVCYHD
                 ********:***:::  .*.*:.****::
```

Fig 4.2 Multiple sequence alignment of circulin (A, B, C, D, and E) by CLUSTAL W bioinformatics software.

Interpretation of results

This is the circulin family sequence alignment result predicted through clustal w .It shows the amino acids number of every member of Circulin family circulin (A, B, C, D and E). The signs describe following things. . In alignment steric is showing similar sequences, double dots are showing any functional grop similarity and single dot means that there is biological similarity where gaps showing dissimilarities between amino acid in each cyclotide.

"*"This mean the amino acids in that sequence are all identical to each other.

":" This Dot mean conserved regions in all sequences.

"." This sign mean semi conserved regions observed in the amino acids having same shape.

4.3.2. CYI FAMILY

```
  CLUSTAL 2.1 Multiple Sequence Alignments

Sequence type explicitly set to Protein
Sequence format is Pearson
Sequence 1: cyI1            31 aa
Sequence 2: cyI2            31 aa
Sequence 3: cyI3            33 aa
Sequence 4: cyI4            33 aa
Sequence 5: cyI5            33 aa
Sequence 6: cyI6            33 aa
Start of Pairwise alignments
Aligning...
```

```
clustalw.aln

CLUSTAL 2.1 multiple sequence alignment


cyI3            GNPGACGETCIWGKCYSASIGCSCSKYKVCTLN
cyI5            GNPGACGETCIWGKCYSASIGCSCSRYKVCTLN
cyI6            GNPGACGETCIWGKCYSAKIGCSCSKYKICTLN
cyI4            GNPGACGETCVWGKCYSASIGCSCNKYKVCTLN
cyI1            -GTFPCGESCVYIPCISSVVGCSC-KSKVCYKN
cyI2            -GTFPCGESCVWIPCISSVVGCSC-KSKVCYKN
                 .. .***:*::  * *: :**** : *:*  *
```

Fig 4.3 Multiple sequence alignment of CYI family by CLUSTAL W bioinformatics software

Interpretation of results

This is the CYI family sequence alignment result predicted through clustal w .It shows the amino acids number of every member of CYI family (1, 2, 3, 4,5and 6) the signs describe the following things. . In alignment steric is showing similar sequences, double dots are showing any functional grop similarity and single dot means that there is biological similarity where gaps showing dissimilarities between amino acid in each cyclotide.

"*"

This mean the amino acids in CYI family sequences are all identical to each other.

":"

This Dot mean conserved regions in all family member sequences.

"."

This sign mean semi conserved regions observed in the amino acids having same shape.

4.3.3 HYFL FAMILY

```
 CLUSTAL 2.1 Multiple Sequence Alignments

Sequence type explicitly set to Protein
Sequence format is Pearson
Sequence 1: HyflA           31 aa
Sequence 2: HyflB           32 aa
Sequence 3: HyflC           32 aa
Sequence 4: HyflD           31 aa
Sequence 5: HyflF           30 aa
Sequence 6: HyflI           30 aa
Sequence 7: HyflK           30 aa
Sequence 8: HyflL           30 aa
Start of Pairwise alignments
Aligning...
```

```
clustalw.aln

CLUSTAL 2.1 multiple sequence alignment


HyflK             --GTPCGESCVYIPC-FTAVVGCTCKDKVCYLN
HyflL             --GTPCAESCVYLPC-FTGVIGCTCKDKVCYLN
HyflD             -GSVPCGESCVYIPC-FTGIAGCSCKSKVCYYN
HyflI             --GIPCGESCVFIPC-ISGVIGCSCKSKVCYRN
HyflA             --SISCGESCVYIPCTVTALVGCTCKDKVCYLN
HyflF             --SISCGETCTTFNCWIPNCK-CNHHDKVCYWN
HyflB            GSPIQCAETCFIGKC-YTEELGCTCTAFLCMKN
HyflC            GSPRQCAETCFIGKC-YTEELGCTCTAFLCMKN
                       *.*:*    *  .    *.    :*  *
```

Fig 4.4 Multiple sequence alignment of HYFL family by CLUSTAL W bioinformatics software**.**

Interpretation of results

This is the Hyfl family sequence alignment result predicted through clustal w .It shows the amino acids number of every member of Hyfl family. Hyfl (A, B, C, D, F, I, K and L) the signs below the alignment describes the following things. . In alignment steric is showing similar sequences, double dots are showing any functional grop similarity and single dot means that there is biological similarity where gaps showing dissimilarities between amino acid in each cyclotide.

"*"

This sign mean the amino acids in Hyfl family sequences are all identical to each other.

":"

This Dot mean conserved regions in all family member sequences.

"."

This sign mean semi conserved regions observed in the amino acids having same shape

4.3.4. KALATA FAMILY

```
 CLUSTAL 2.1 Multiple Sequence Alignments


Sequence type explicitly set to Protein
Sequence format is Pearson
Sequence 1: KalataB9      31 aa
Sequence 2: KalataB10     30 aa
Sequence 3: KalataB13     30 aa
Sequence 4: KalataB14     30 aa
Sequence 5: KalataB16     30 aa
Sequence 6: KalataB17     30 aa
Sequence 7: KalataB18     30 aa
Start of Pairwise alignments
Aligning...
```

```
clustalw.aln

CLUSTAL 2.1 multiple sequence alignment


KalataB13       -GLPVCGETCFGGTC---NTPGCACDPWPVCTRD
KalataB14       -GLPVCGESCFGGTC---NTPGCACDPWPVCTRD
KalataB10       -GLPTCGETCFGGTC---NTPGCSCSSWPICTRD
KalataB9        GSVFNCGETCVLGTC---YTPGCTCNTYRVCTKD
KalataB16       -GIP-CAESCVYIPCTITALLGCKCQDK-VCYD-
KalataB17       -GIP-CAESCVYIPCTITALLGCKCKDQ-VCYN-
KalataB18       -GVP-CAESCVYIPC-ISTVLGCSCSNQ-VCYRN
                 .:  *.*:*.  .*      ** *.   :*
```

Fig 4.5 Multiple sequence alignment of KALATA family by using CLUSTAL W bioinformatics software.

Interpretation of results

This is the Kalata family sequence alignment result predicted through clustal w .It shows the amino acids number of every member of Kalata family. Kalata (B9, B10, B13, B14, B16, B17 and B18) the signs below the alignment describes the following things. . In alignment steric is showing similar sequences, double dots are showing any functional grop similarity and single dot means that there is biological similarity where gaps showing dissimilarities between amino acid in each cyclotide.

"*"

This mean the amino acids in Kalata family sequences are all identical to each other.

":"

This Dot mean conserved regions in all family member sequences.

"."

This sign mean semi conserved regions observed in the amino acids having same shape.

4.3.5. PHYB FAMILY

```
  CLUSTAL 2.1 Multiple Sequence Alignments

Sequence type explicitly set to Protein
Sequence format is Pearson
Sequence 1: A-Phyb          30 aa
Sequence 2: D-Phyb          30 aa
Sequence 3: E-Phyb          30 aa
Sequence 4: F-Phyb          30 aa
Sequence 5: G-Phyb          30 aa
Sequence 6: H-Phyb          30 aa
Sequence 7: I-Phyb          31 aa
Sequence 8: J-Phyb          31 aa
Sequence 9: L-Phyb          32 aa
Sequence 10: B-Phyb          30 aa
Sequence 11: C-Phyb          30 aa
Start of Pairwise alignments
Aligning...
```

```
clustalw.aln

CLUSTAL 2.1 multiple sequence alignment


B-Phyb            -GVPCGESCVWMYCIS-AAMGCSCRNKVCYRN-
C-Phyb            -GIPCGESCVWMYCIT-ATMGCSCRNKVCYKN-
H-Phyb            -GLPCGESCIWIECIS-GAIGCSCRNKVCYRN-
D-Phyb            -GIPCGESCMWIPCIS-AAIGCSCTNHVCYKN-
E-Phyb            -GIPCGESCVWIPCIS-GVQGCSCSNKICYRN-
F-Phyb            -GIPCGGSCVWIPCIS-GVQGCSCSNKICYRN-
G-Phyb            -GIPCGESCAWIPCIS-AVQGCSCRNKICYRN-
A-Phyb            -GIGCGESCVWIPCVS-AAIGCSCSNKICYRN-
L-Phyb            QSISCAETCVWIPCAT-SLIGCSCVNSICTYTN
I-Phyb            -GIPCGESCIWIPCTTTALLGCSCSNKVCYKN-
J-Phyb            -SYTCGESCLWIPCTVTAAFGCYCSNKVCVKD-
                   .  *. :* *: *   .  ** * * :*
```

Fig 4.6 Multiple sequence alignment of PHYB family by using CLUSTAL W bioinformatics software.

Interpretation of results

This is the Phyb family sequence alignment result predicted through clustal w. It shows the amino acids number of every member of Phyb family. Phyb (A, B, C, D, E, F, G, H, I, J, and L) the signs below the alignment describes the following things. . In alignment steric is showing similar sequences, double dots are showing any functional grop similarity and single dot means that there is biological similarity where gaps showing dissimilarities between amino acid in each cyclotide.

"*"

This mean the amino acids in Phyb family sequences are all identical to each other.

":"

This Dot mean conserved regions in all family member sequences.

"."

This sign mean semi conserved regions observed in the amino acids having same shape

4.3.6. VIAN FAMILY

```
  CLUSTAL 2.1 Multiple Sequence Alignments


Sequence type explicitly set to Protein
Sequence format is Pearson
Sequence 1: Vian3          30 aa
Sequence 2: Vian5          30 aa
Sequence 3: Vian6          31 aa
Sequence 4: Vian7          30 aa
Sequence 5: Vian9          30 aa
Sequence 6: Vian10         30 aa
Sequence 7: Vian11         30 aa
Start of Pairwise alignments
Aligning...
```

```
clustalw.aln

CLUSTAL 2.1 multiple sequence alignment


Vian5           --GIPCGESCVYIPCISAVIGCSCSSKVCYRN
Vian10          --SLPCGESCVYIPCISGLLGCSCKNKVCYYN
Vian6           -GAFPCGESCVYIGCITSIAGCSCSDNVCYKN
Vian7           -LPLCGGETCTFGTCDTPGCTCG-YWPFCTKD
Vian11          --GLNCGETCWGFHCDSPGCSCGLTWPYCSKN
Vian3           GSIFNCGETCIMGTCYTPGCSCV--YGACSKN
Vian9           SDTGYCNESCGTNECTTLGCICR--KKVCVID
                      .*:*    * :    *      *  :
```

Fig 4.7 Multiple sequence alignment VIAN family by using CLUSTAL W bioinformatics software.

Interpretation of results

This is the Vian family sequence alignment result predicted through clustal w .It shows the amino acids number of every member of Vian family. Vian (3, 5, 6, 7, 9, 10 and 11) the signs below the alignment describes the following things.

"*"

This mean the amino acids in Vian family sequences are all identical to each other.

":"

This Dot mean conserved regions in all family member sequences.

"."

This sign mean semi conserved regions observed in the amino acids having same shape

4.4. 2D AND 3D STRUCTURAL MODELS OF CYCLOPEPTIDES

Cyclotides constitute a remarkable family of plant-derived peptides characterized by their cyclic structure and a wide array of biological activities. Among these, circulin, hyfusin, kalata, phyb, and vianin are prominent members, each with distinct properties and potential applications. Circulins have garnered attention for their potent insecticidal properties, presenting a sustainable alternative for pest control in agriculture while minimizing environmental impact. Hyfusins have emerged as intriguing candidates for anti-inflammatory therapeutics, holding potential for managing inflammatory conditions such as arthritis and autoimmune diseases. Kalata peptides, notably kalata B1, have long been recognized for their uterotonic effects, sparking interest in their application as oxytocic agents during childbirth. Phytochelatins, known as phyb, are notable for their ability to chelate heavy metals, offering avenues for environmental remediation in contaminated sites and industrial settings. Vianins, conversely, have demonstrated potent cytotoxic activity against cancer cells, prompting exploration into their potential as anticancer agents in chemotherapy regimens. The cyclotide family presents a rich source of bioactive compounds with diverse applications spanning medicine, agriculture, and environmental science, underscoring their significance in addressing various societal challenges and advancing scientific knowledge.

4.4.1. CIRCULIN FAMILY

The family of **CIRCULIN (A, B C, D and E)** belongs to a class of cyclotide which have antibacterial hemolytic properties. Cyclic structure wild type protein and with monoisotopic mass.

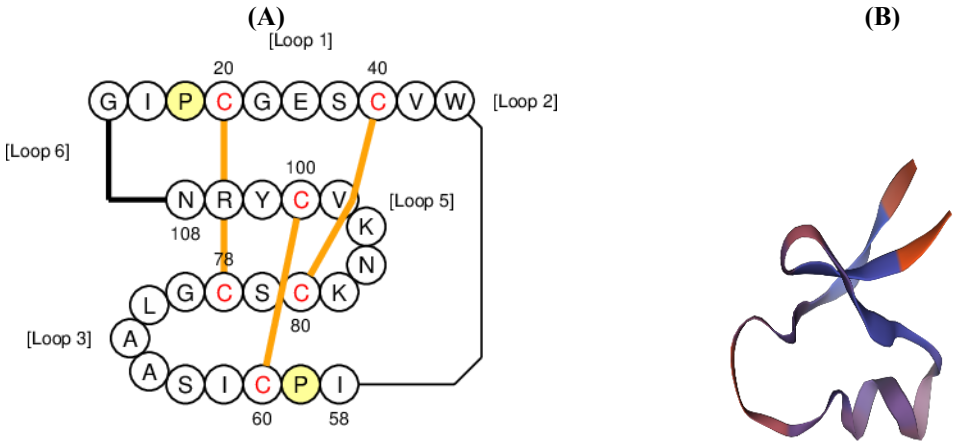

fig 4.8 (A) circulin A 2d structure using cybase database **(B)** circulin A 3d structure by using Swiss model.

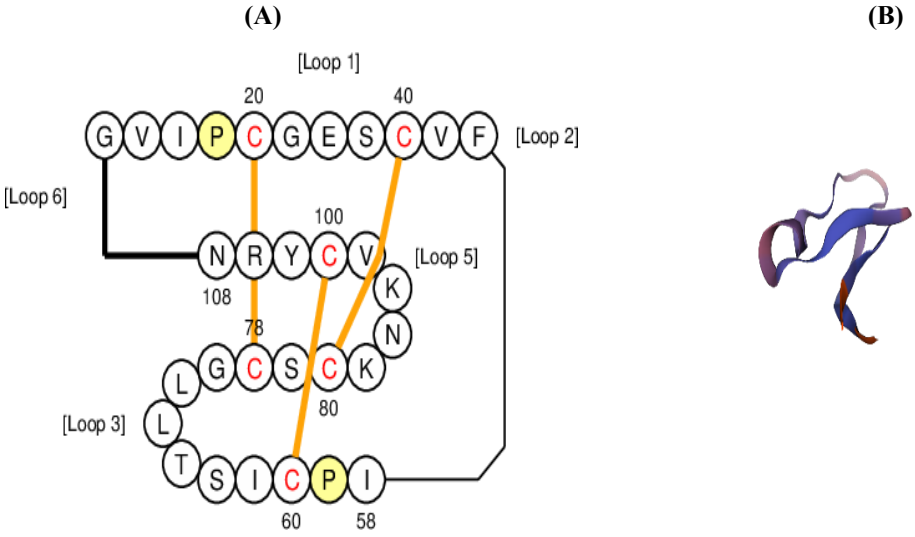

Fig 4.9 (A) circulin B 2D structure using cybase database **(B)** circulin B 3D structure by using Swiss model.

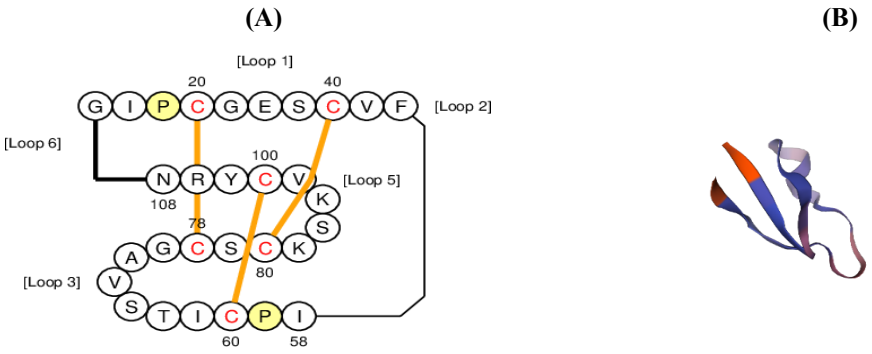

Fig 4.10 (A) circulin C 2D structure using cybase database **(B)** circulin C 3D structure by using Swiss model.

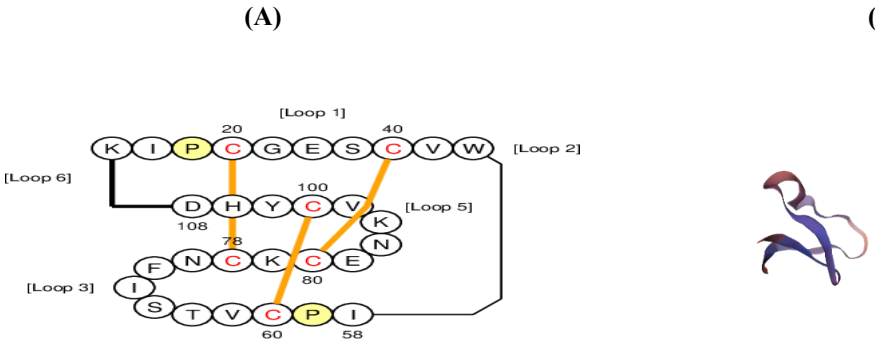

Fig 4.11 (A) circulin D 2D structure using cybase database **(B)** circulin D 3D structure by using Swiss model.

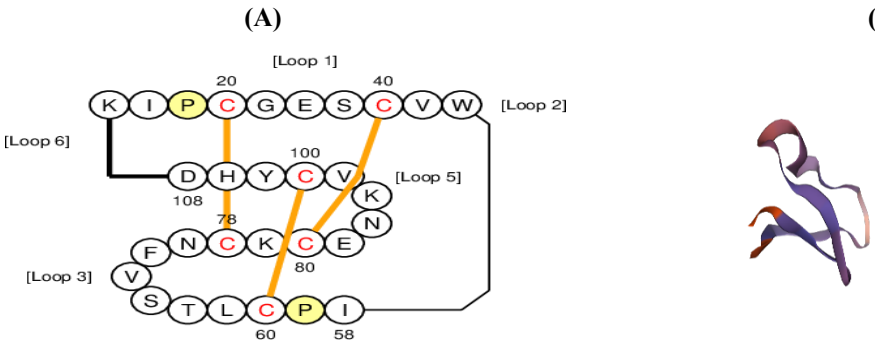

Fig 4.12 (A) circulin E 2D structure using cybase database **(B)** circulin E 3D structure by using Swiss model.

4.4.2. CYL FAMILY

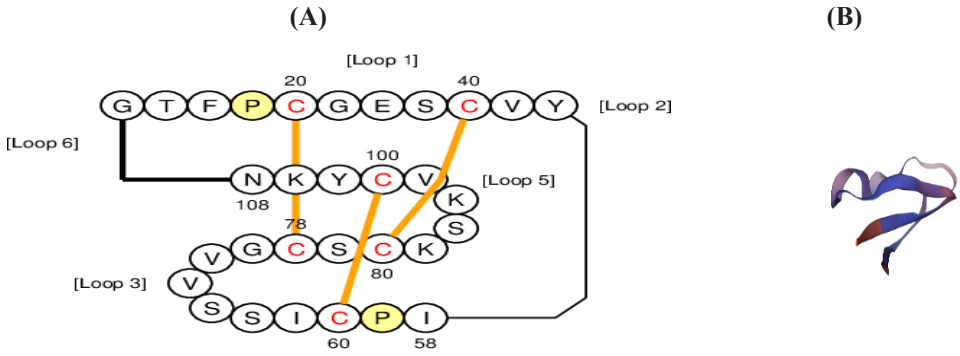

Fig 4.13 (A) CYI 1 2D structure using cybase database (B) CYI 1 3D structure by using Swiss model.

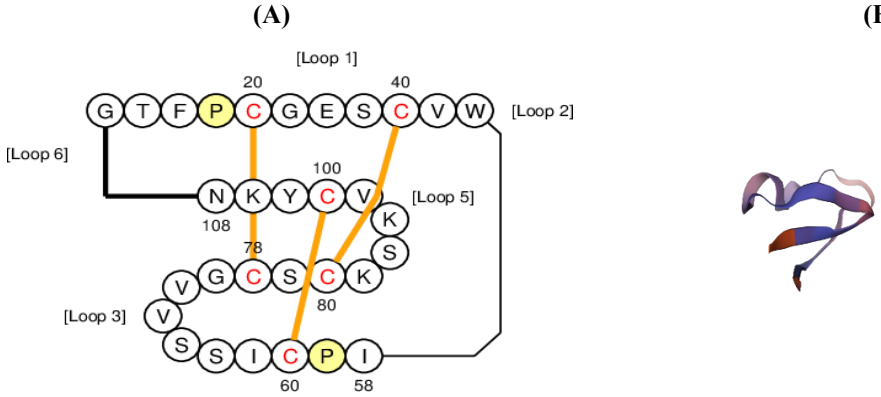

Fig 4.14 (A) CYI 2 2D structure using cybase database (B) CYI 2 3D structure by using Swiss model.

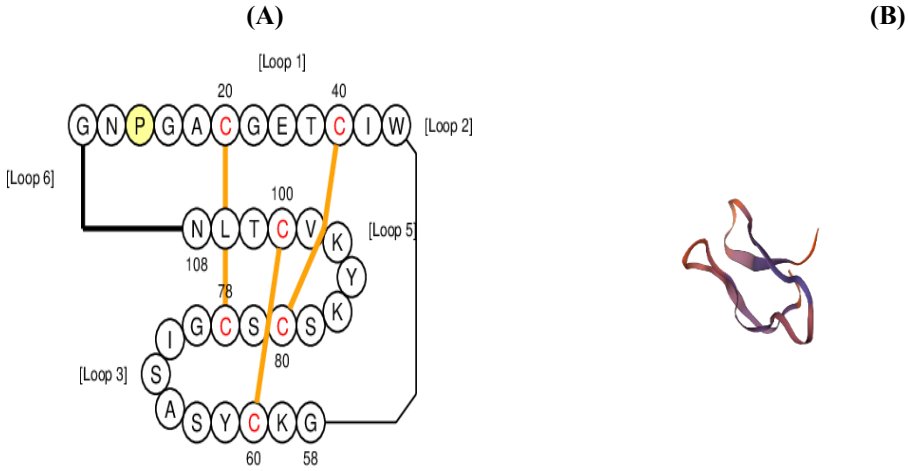

Fig 4.15 (A) CYI 3 2D structure using cybase database (B) CYI 3 3D structure by using Swiss model.

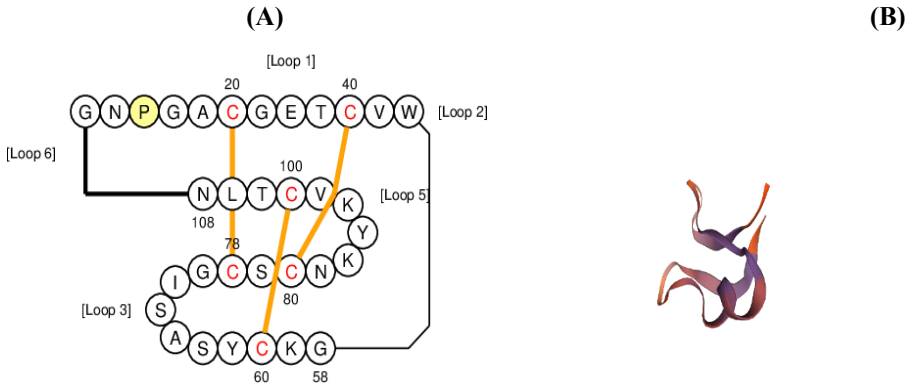

Fig 4.16 (A) CYI 4 2D structure using cybase database (B) CYI 4 3D structure by using Swiss model.

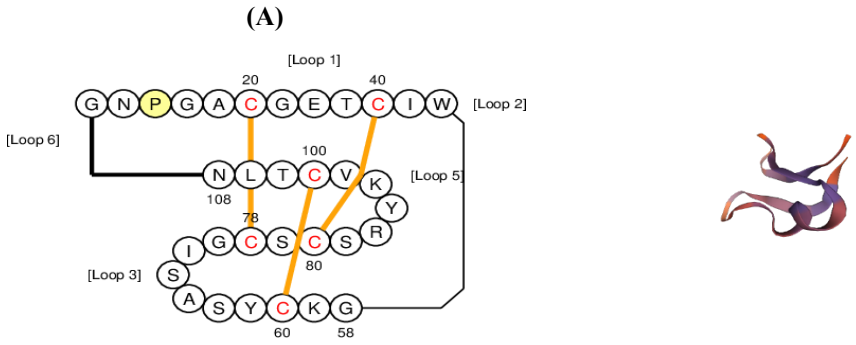

Fig 4.17 (A) CYI 5 2D structure using cybase database (B) CYI 5 3D structure by using Swiss model**.**

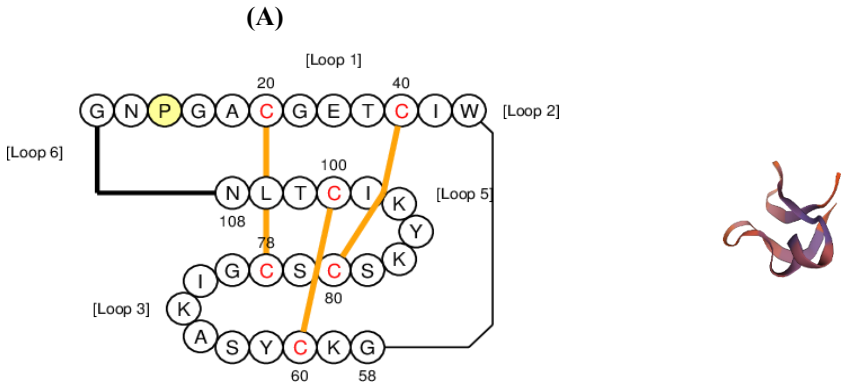

Fig 4.18 (A) CYI 6 2D structure using cybase database (B) CYI 6 3D structure by using Swiss model.

4.4.3. Hyfl FAMILY"2D AND 3D STRUCTURAL IMAGES

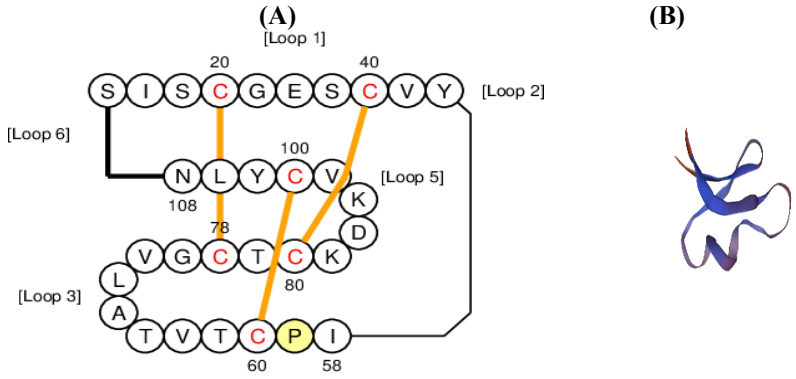

Fig 4.19 (A) HYFL A 2D structure using cybase database (B) HYFL A 3D structure by using Swiss model

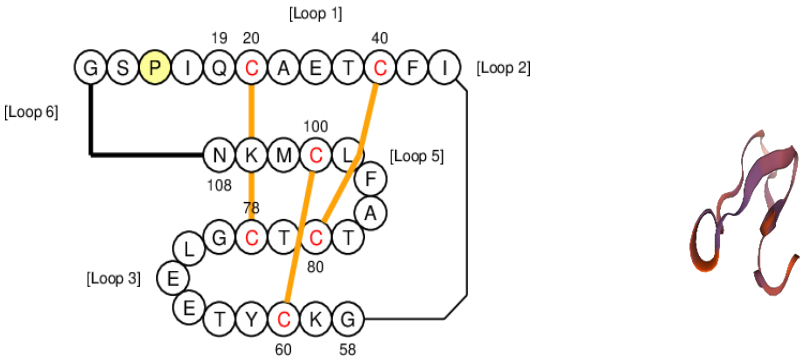

Fig 4.20 (A) HYFL B 2D structure using cybase database (B) HYFL B 3D structure by using Swiss model.

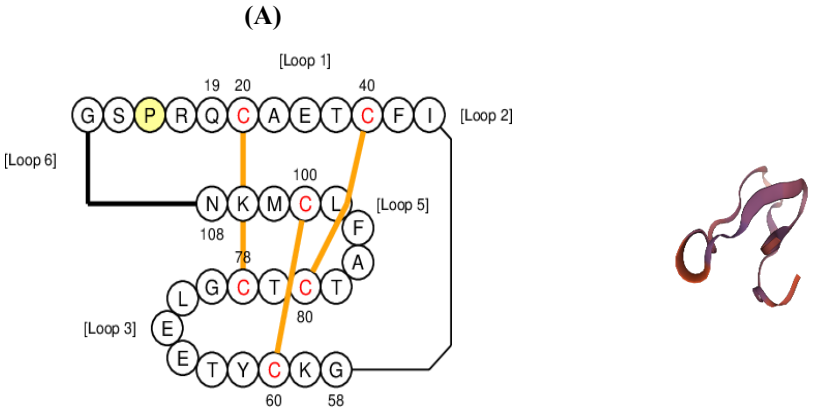

Fig 4.21 (A) HYFL C 2D structure using cybase database (B) HYFL C 3D structure by using Swiss model.

(A) (B)

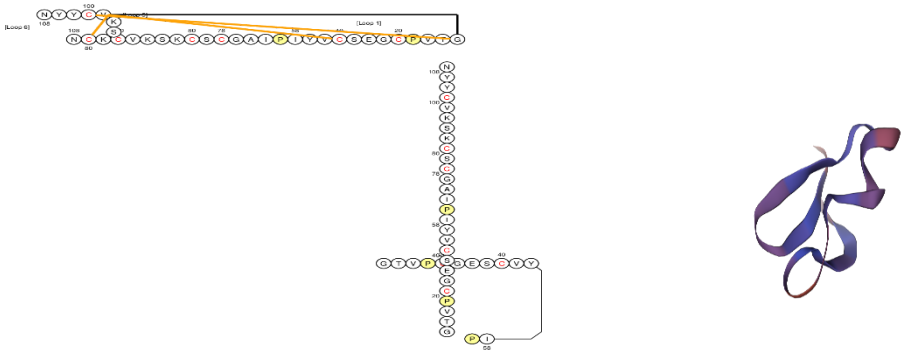

Fig 4.22 (A) HYFL D 2D structure using cybase database (B) HYFL D 3D structure by using Swiss model

(A) **(B)**

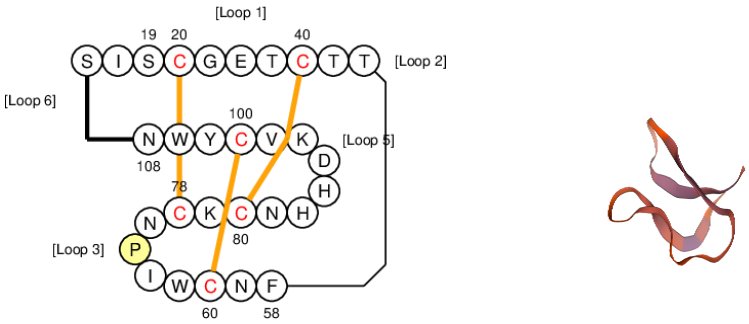

Fig 4.23 (A) HYFL F 2D structure using cybase database (B) HYFL F 3D structure by using Swiss model

(A) **(B)**

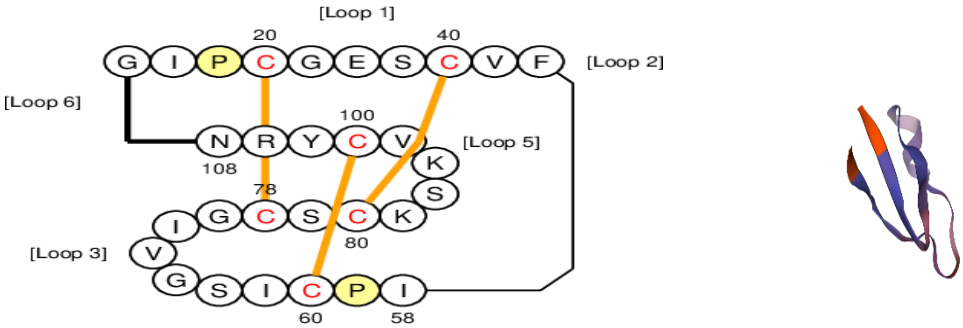

Fig 4.24 (A) HYFL I 2D structure using cybase database (B) HYFL I 3D structure by using Swiss model.

(A) **(B)**

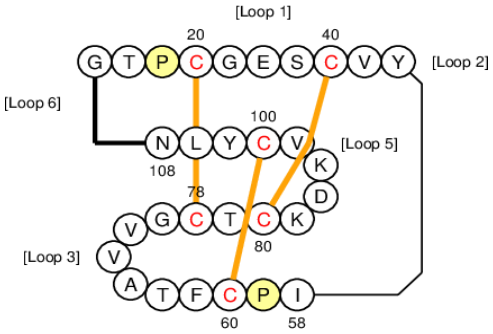

Fig 4.25 (A) HYFL K 2D structure using cybase database (B) HYFL K 3D structure by using Swiss model.

(A) **(B)**

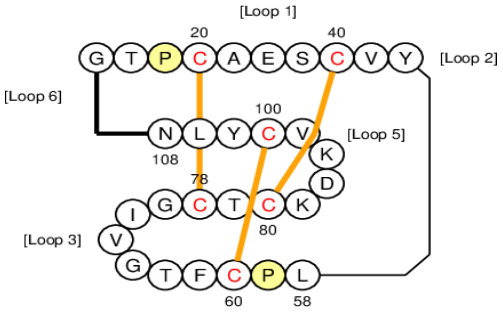

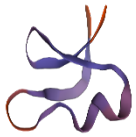

Fig 4.26 (A) HYFL L 2D structure using cybase database (B) HYFL L 3D structure by using Swiss model.

4.4.5 "KALATA FAMILY

(A) (B)

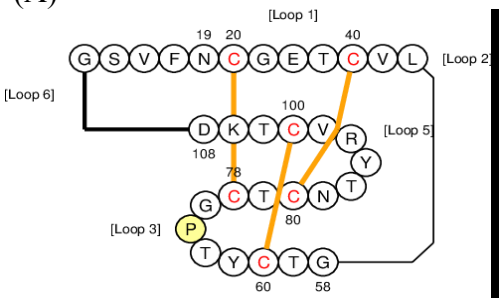

Fig 4.27 (A) KALATA B9 2D structure using cybase database (B) KALATA B9 3D structure by using Swiss model.

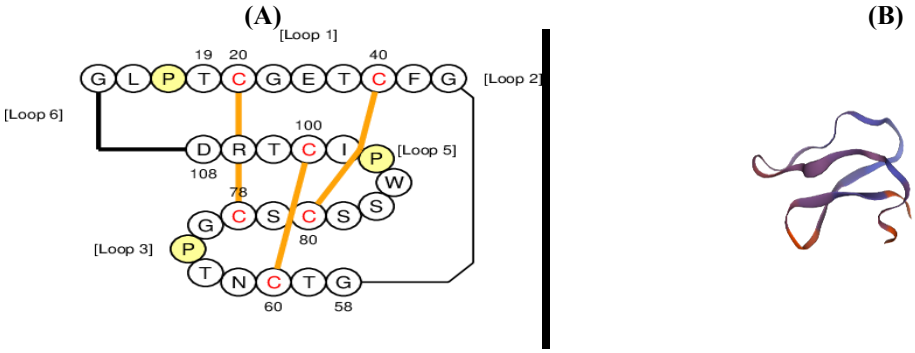

Fig 4.28 (A) KALATA B10 2D structure using cybase database (B) KALATA B10 3D structure by using Swiss model.

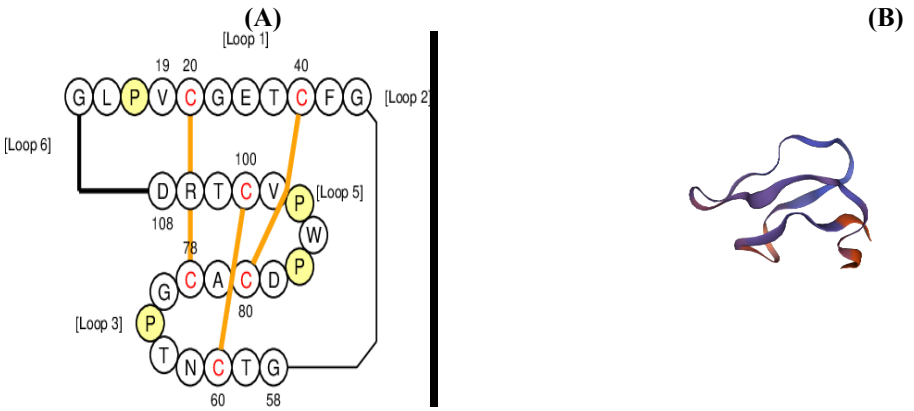

Fig 4.29 (A) KALATA B13 2D structure using cybase database (B) KALATA B13 3D structure by using Swiss model.

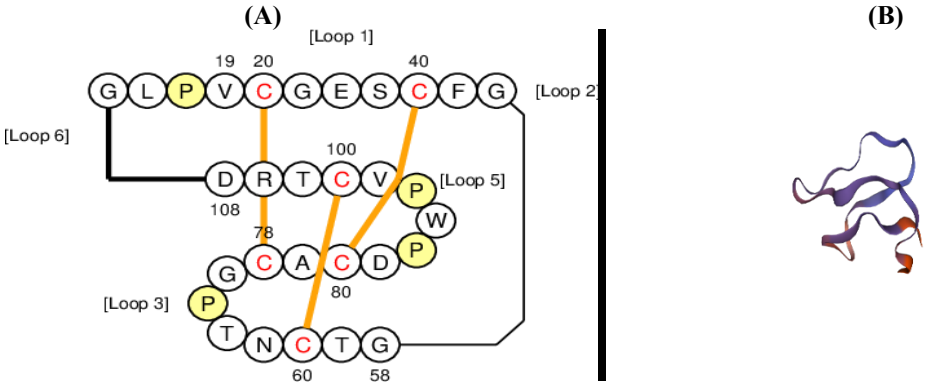

Fig 4.30 (A) KALATA B14 2D structure using cybase database (B) KALATA B14 3D structure by using Swiss model.

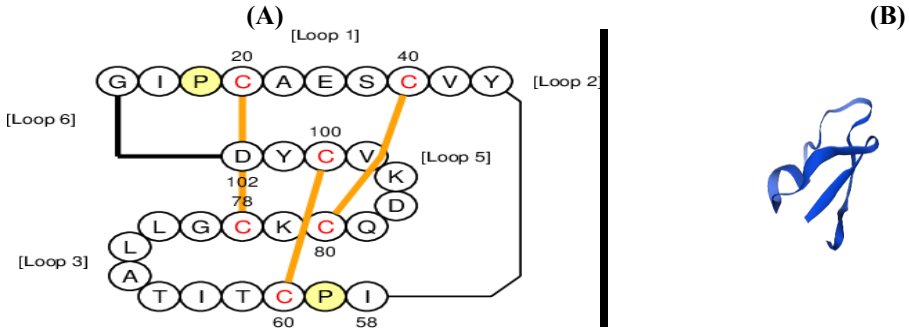

Fig 4.31 (A) KALATA B16 2D structure using cybase database (B) KALATA B16 3D structure by using Swiss model.

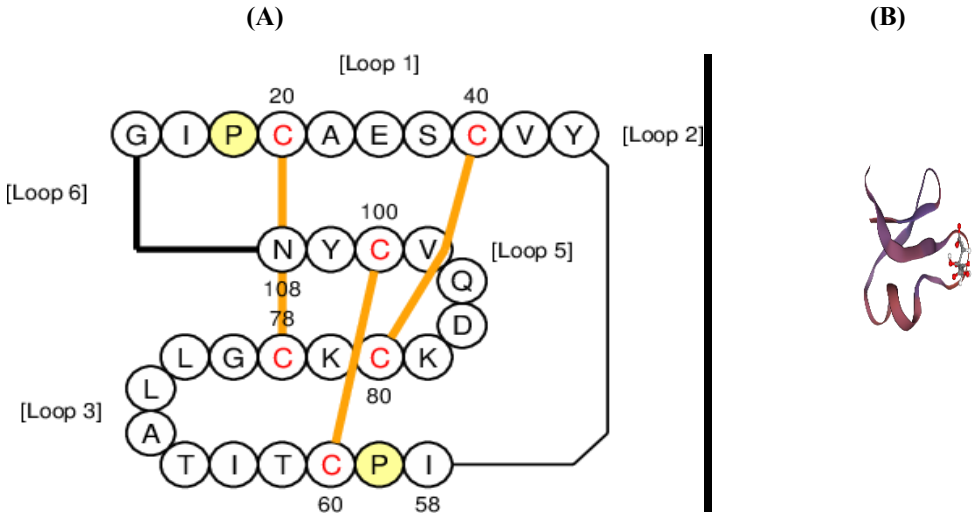

Fig 4.32 (A) KALATA B17 2D structure using cybase database (B) KALATA B17 3D structure by using Swiss model.

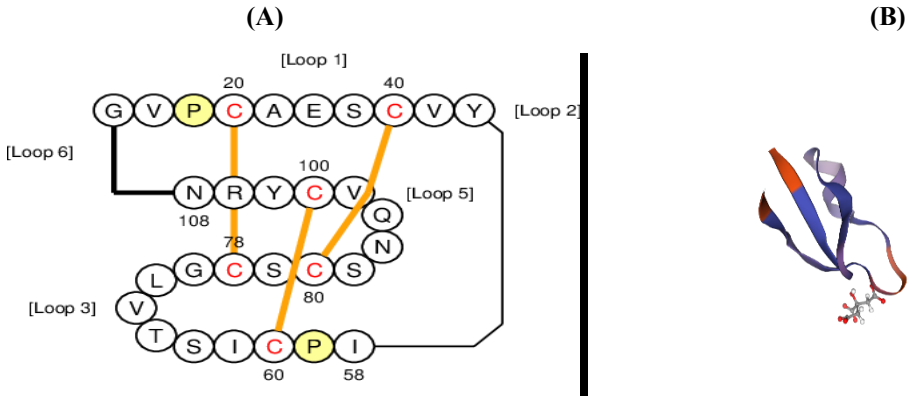

Fig 4.33 (A) KALATA B18 2D structure using cybase database (B) KALATA B18 3D structure by using Swiss model.

4.4.6"PHYB FAMILY" 2D 3D STRUCTURE

(A) **(B)**

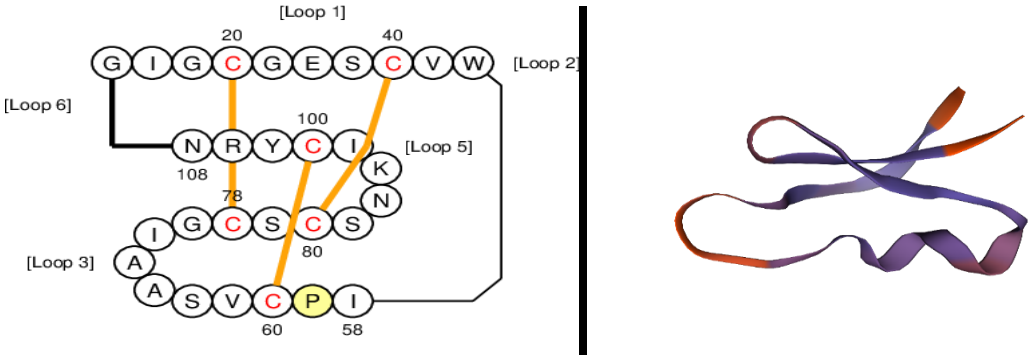

Fig 4.34 (A) PHYB A 2D structure using cybase database (B) PHYB A 3D structure by using Swiss model.

(A) **(B)**

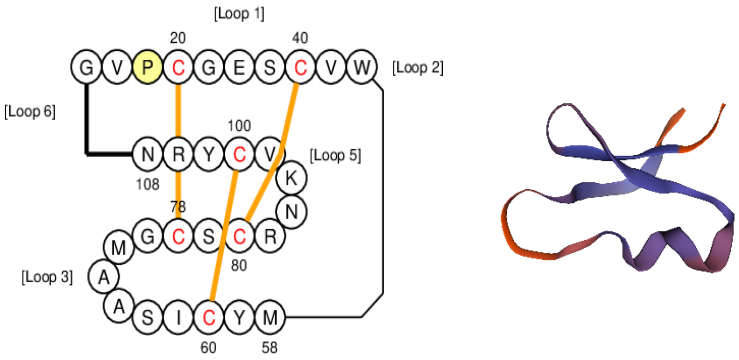

Fig 4.35 (A) PHYB B 2D structure using cybase database (B) PHYB B 3D structure by using Swiss model.

(A) **(B)**

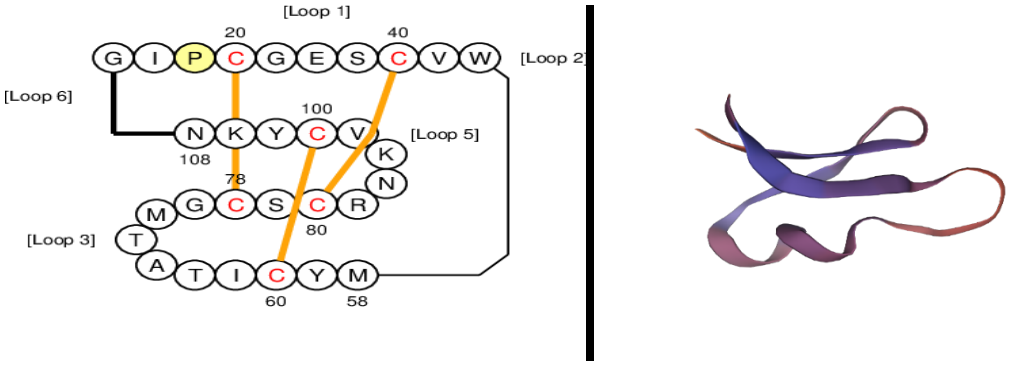

Fig 4.36 (A) PHYB C 2D structure using cybase database (B) PHYB C 3D structure by using Swiss model.

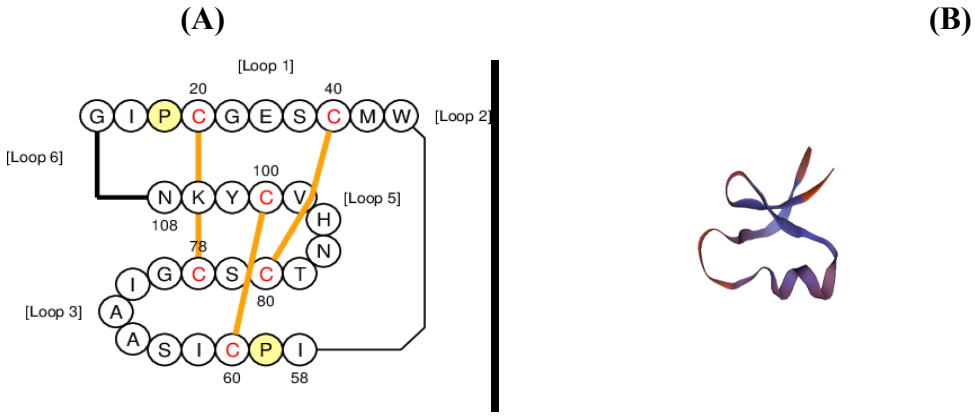

Fig 4.37(A) PHYB D 2D structure using cybase database (B) PHYB D 3D structure by using Swiss model.

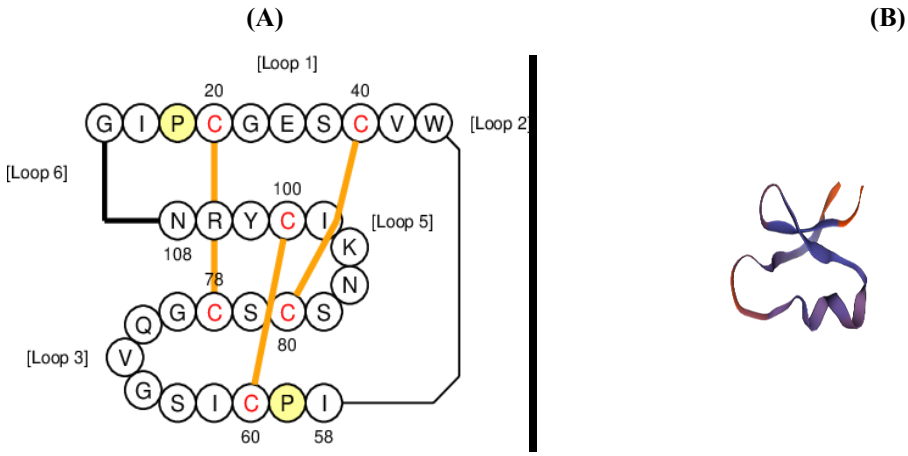

Fig 4.38 (A) PHYB E 2D structure using cybase database (B) PHYB E 3D structure by using Swiss model.

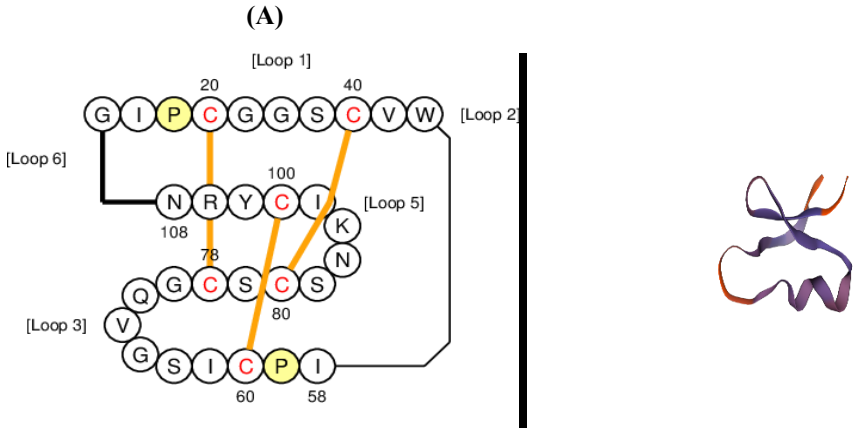

Fig 4.39 (A) PHYB F 2D structure using cybase database (B) PHYB F 3D structure by using Swiss model.

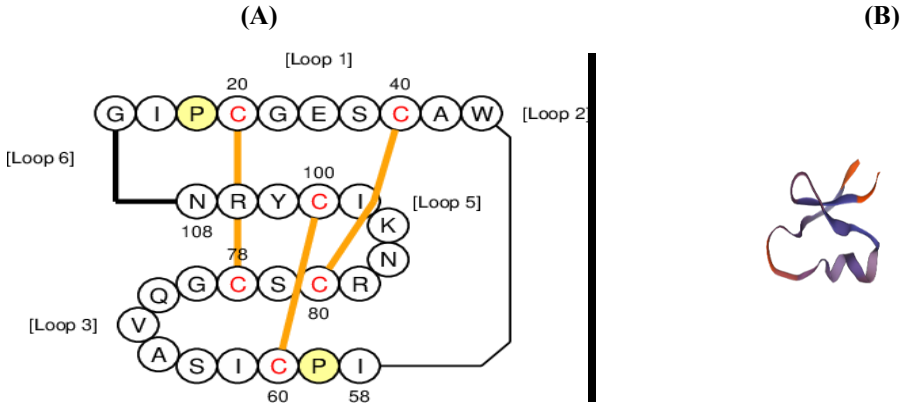

Fig 4.40 (A) PHYB G 2D structure using cybase database (B) PHYB G 3D structure by using Swiss model.

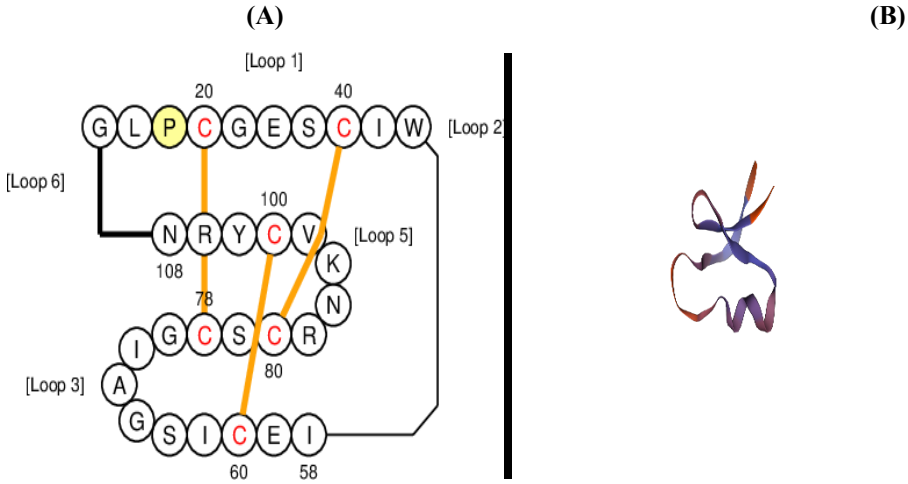

Fig 4.41 (A) PHYB h 2D structure using cybase database (B) PHYB h 3D structure by using Swiss model.

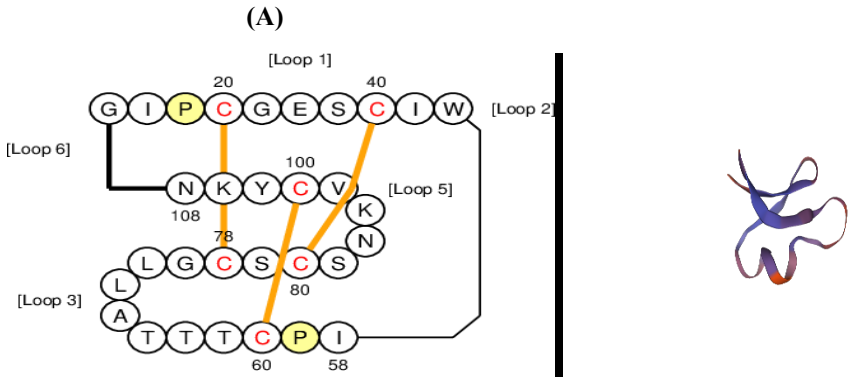

Fig 4.42 (A) PHYB I 2D structure using cybase database (B) PHYB I 3D structure by using Swiss model.

(A) **(B)**

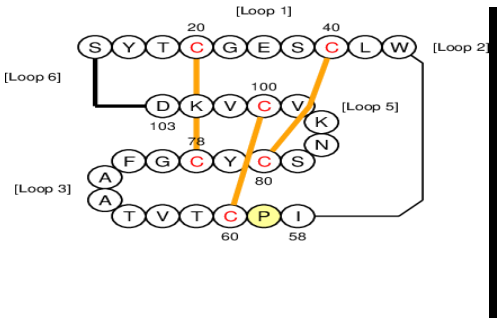

Fig 4.43 (A) PHYB J 2D structure using cybase database (B) PHYB J 3D structure by using Swiss model.

(A) **(B)**

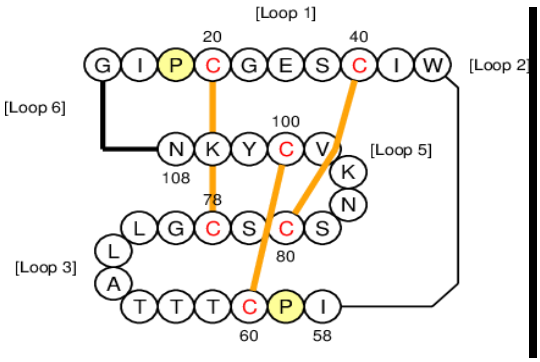

Fig 4.44 (A) PHYB L 2D structure using cybase database (B) PHYB L 3D structure by using Swiss model.

4.4.6. VIAN FAMILY 2D AND 3D STRUCTURES

(A) **(B)**

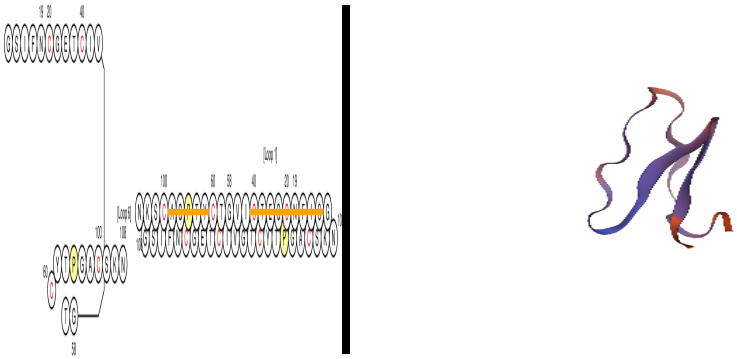

Fig 4.45 (A) vian 3 2D structure using cybase database (B) vian 3 3D structure by using Swiss model.

(A) **(B)**

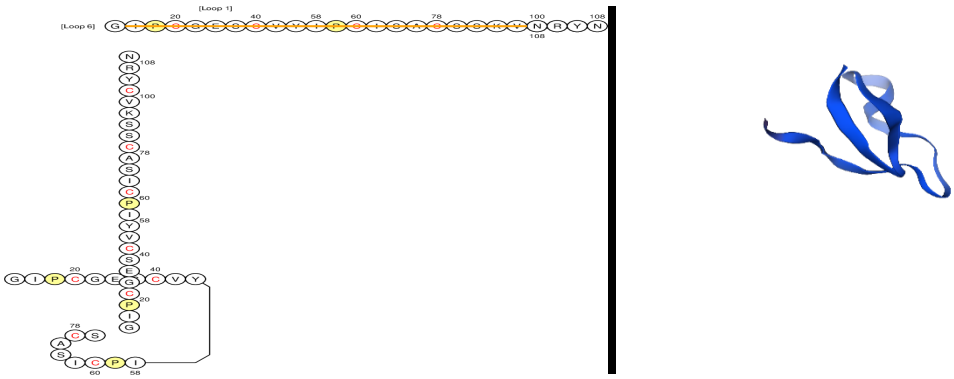

Fig 4.46 (A) vian 5 2D structure using cybase database (B) vian 5 3D structure by using Swiss model.

(A) **(B)**

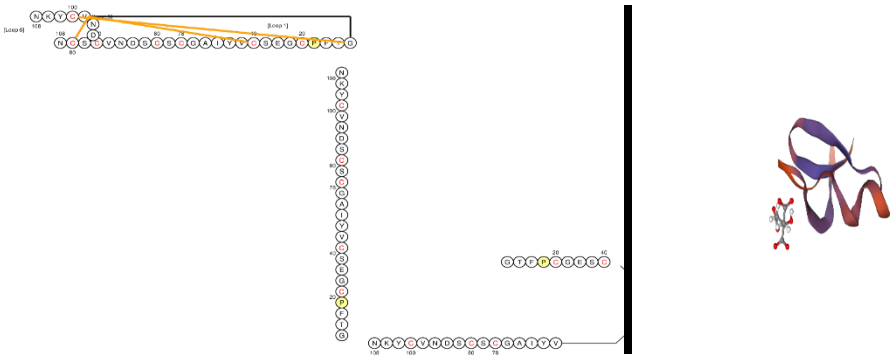

Fig 4.47 (A) vian 6 2D structure using cybase database (B) vian 6 3D structure by using Swiss model.

(A) **(B)**

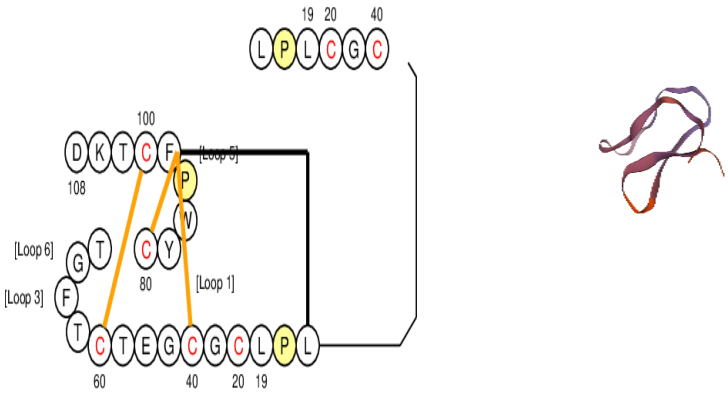

Fig 4.48 (A) vian 7 2D structure using cybase database (B) vian 7 3D structure by using Swiss model.

(A) **(B)**

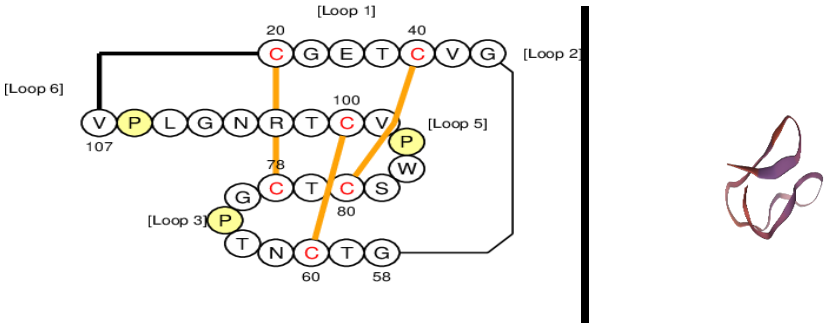

Fig 4.49 (A) vian 9 2D structure using cybase database (B) vian 9 3D structure by using Swiss model.

(A) **(B)**

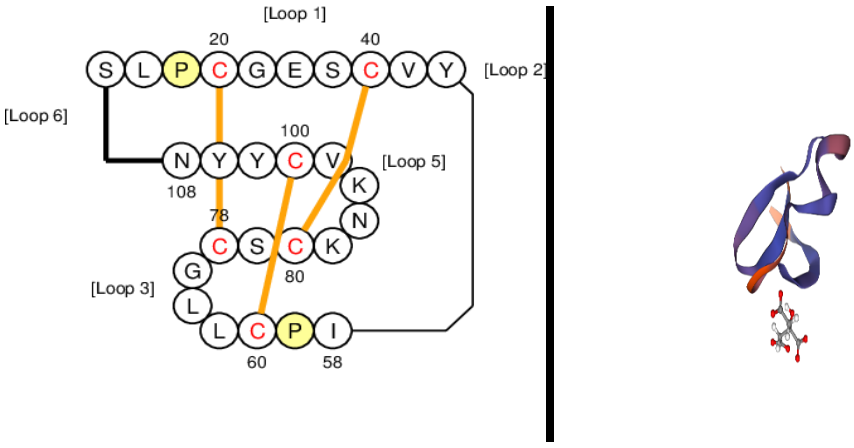

Fig 4.50 (A) vian 10 2D structure using cybase database (B) vian 10 3D structure by using Swiss model.

(A) **(B)**

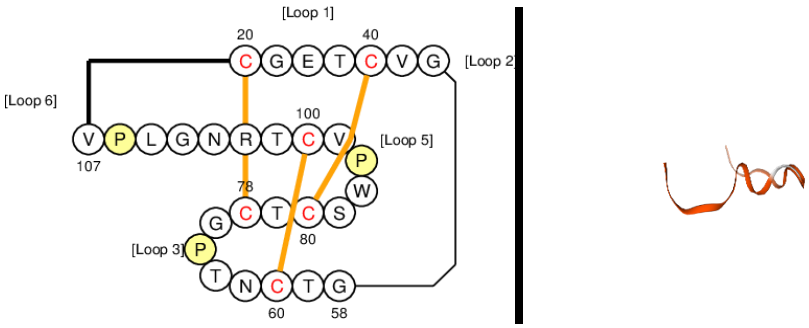

Fig 4.51 (A) vian 11 2D structure using cybase database (B) vian 11 3D structure by using Swiss model.

4.5 DOCKING RESULTS

ClusPro docking results were retrieved and are listed in Table 4.7. The results are obtained by calculating the lowest energy and the center of the energy distribution. These conformations are important as they identify the protein-ligand complex most stable and probable conformations. The center of energy conformation gives the best estimate of the interaction between the structures within the cluster. In contrast, the lower energy conformation corresponds to the pose with the least energy, a favorable thermodynamic interaction.

Table 4.7 NS5A CHAIN A DOCKING RESULTS WITH CYCLOTIDES

CYCLOTIDE	CLUSTER	MEMBER	REPRESENTATIVE	WEIGHTED SCORE
Phyb A	0	362	Center	-743.6
			Lowest Energy	-878.9
Phyb D	0	304	Center	-738.1
			Lowest Energy	-986.4
Phyb E	0	317	Center	-744.2
			Lowest Energy	-924.7
Phyb F	0	196	Center	-743.0
			Lowest Energy	-971.3

Phyb G	0	261	Center	-717.6
			Lowest Energy	-872.6
Phyb H	0	321	Center	-745.2
			Lowest Energy	-886.8
Phyb I	0	344	Center	-695.5
			Lowest Energy	-903.7
Phyb J	0	307	Center	-716.5
			Lowest Energy	-874.4
Phyb L	0	163	Center	-747.5
			Lowest Energy	-1037.8
Phyb B	0	304	Center	-738.1
			Lowest Energy	-986.4
Phyb C	0	314	Center	-747.3
			Lowest Energy	-878.2
Circulin A	0	264	Center	-705.9
			Lowest Energy	-962.9
Circulin B	0	198	Center	-721.9
			Lowest Energy	-944.6
Circulin C	0	452	Center	-692.9
			Lowest Energy	-833.1
Circulin D	0	260	Center	-805.2
			Lowest Energy	-933.6
Circulin E	0	218	Center	-717.5
			Lowest Energy	-924.2
Hyfl A	0	271	Center	-647.2
			Lowest Energy	-811.8

Hyfl B	0	307	Center	-812.1
			Lowest Energy	-828.1
Hyfl C	0	296	Center	-701.1
			Lowest Energy	-792.8
Hyfl D	0	159	Center	-743.0
			Lowest Energy	-962.7
Hyfl F	0	259	Center	-761.0
			Lowest Energy	-875.8
Hyfl I	0	200	Center	-700.0
			Lowest Energy	-870.3
Hyfl K	0	343	Center	-746.6
			Lowest Energy	-839.2
Hyfl L	0	220	Center	-746.5
			Lowest Energy	-864.9
CYI 1	0	234	Center	-667.8
			Lowest Energy	-911.5
CYI 2	0	286	Center	-696.2
			Lowest Energy	-903.2
CYI 3	0	165	Center	-621.6
			Lowest Energy	-738.9
CYI 4	0	302	Center	-689.1
			Lowest Energy	-862.8
CYI 5	0	202	Center	-702.6
			Lowest Energy	-830.1
CYI 6	0	204	Center	-623.2
			Lowest Energy	-783.5

Kalata B9	0	220	Center	-674.2
			Lowest Energy	-732.6
Kalata B10	0	262	Center	-837.9
			Lowest Energy	-837.9
Kalata B13	0	295	Center	-807.8
			Lowest Energy	-807.8
Kalata B14	0	280	Center	-787.9
			Lowest Energy	-787.9
Kalata B16	0	209	Center	-739.4
			Lowest Energy	-878.5
Kalata B17	0	244	Center	-726.1
			Lowest Energy	-841.1
Kalata B18	0	234	Center	-766.7
			Lowest Energy	-952.9
Vian 3	0	282	Center	-699.1
			Lowest Energy	-787.8
Vian 5	0	279	Center	-736.9
			Lowest Energy	-915.5
Vian 6	**0**	**288**	Center	-676.1
			Lowest Energy	-880.3
Vian 7	0	351	Center	-736.4
			Lowest Energy	-901.5
Vian 9	0	204	Center	-588.6
			Lowest Energy	-740.7
Vian 10	0	291	Center	-751.2
			Lowest Energy	-980.2
Vian 11	0	272	Center	-704.3
			Lowest Energy	-801.6

4.6. PYMOL DOCKING VISUALIZATION RESULTS OF NS5A PROTEIN WITH CYCLOTIDES

CIRCULIN A

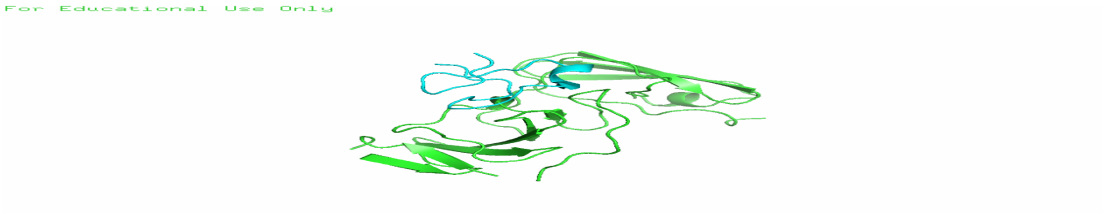

Fig 4.52 3d docking visualization of pathogenic proteins (NS5A CHAIN A) with cyclotide circulin A. Pathogenic proteins are presented in green color and cyclotides are shown in blue colour

Table 4.8 circulin a docking score with NS5A chain A

CYCLOTIDE	CLUSTER	MEMBERS	REPRESENTATIVE	WEIGHTED SCORE
Circulin A	0	264	Center	-705.9
			Lowest Energy	-962.9

CIRCULIN B

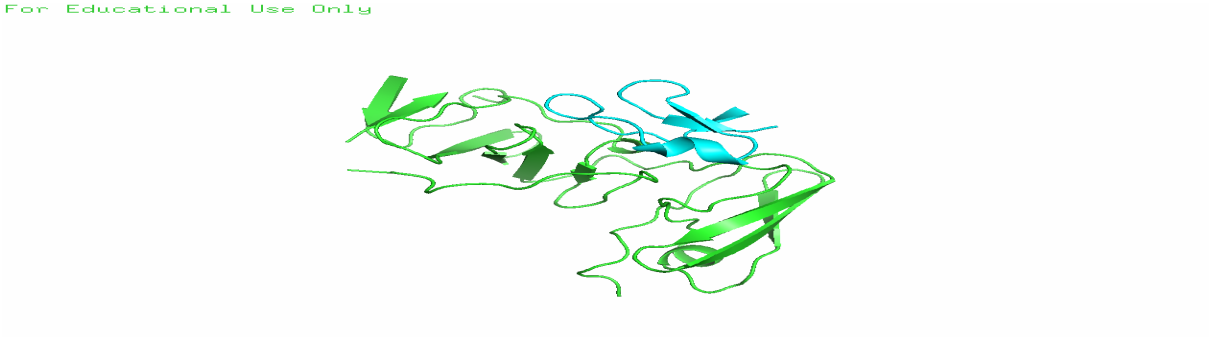

Fig 4.53 3d docking visualization of pathogenic proteins (NS5A CHAIN A) with cyclotide circulin B. Pathogenic proteins are presented in green color and cyclotides are shown in blue color

Table 4.9 circulin B Docking score with NS5A chain A

CYCLOTIDE	CLUSTER	MEMBER	REPRESENTATIVE	WEIGHTED SCORE
Circulin B	0	198	Center	-721.9
			Lowest Energy	-944.6

CIRCULIN C

Fig 4.54 3d docking visualization of pathogenic proteins (NS5A CHAIN A) with cyclotide circulin C. Pathogenic proteins are presented in green color and cyclotides are shown in blue color

Table 4.10 circulin C docking score with NS5A chain A

CYCLOTIDE	CLUSTER	MEMBER	REPRESENTATIVE	WEIGHTED SCORE
Circulin C	0	452	Center	-692.9
			Lowest Energy	-833.1

CIRCULIN D

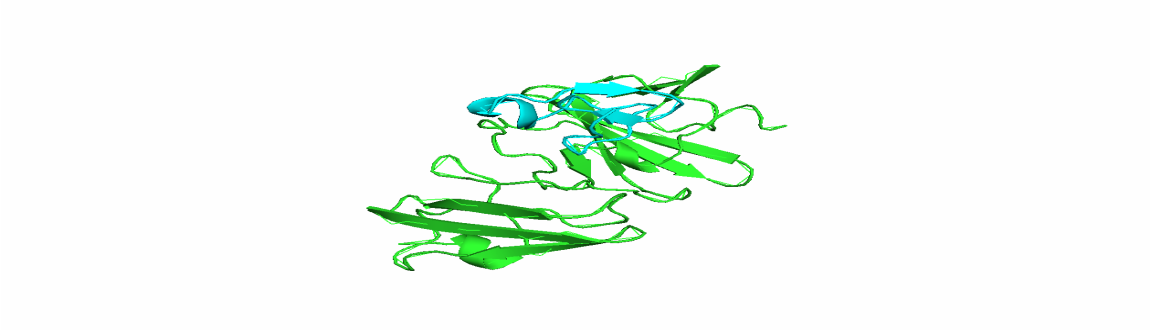

Fig 4.55 3d docking visualization of pathogenic proteins (NS5A CHAIN A) with cyclotide circulin D. Pathogenic proteins are presented in green color and cyclotides are shown in blue color

Table 4.11 circulin D docking score with NS5A chain A

CYCLOTIDE	CLUSTER	MEMBERS	REPRESENTATIVE	WEIGHTED SCORE
Circulin D	0	260	Center	-805.2
			Lowest Energy	-933.6

CIRCULIN E

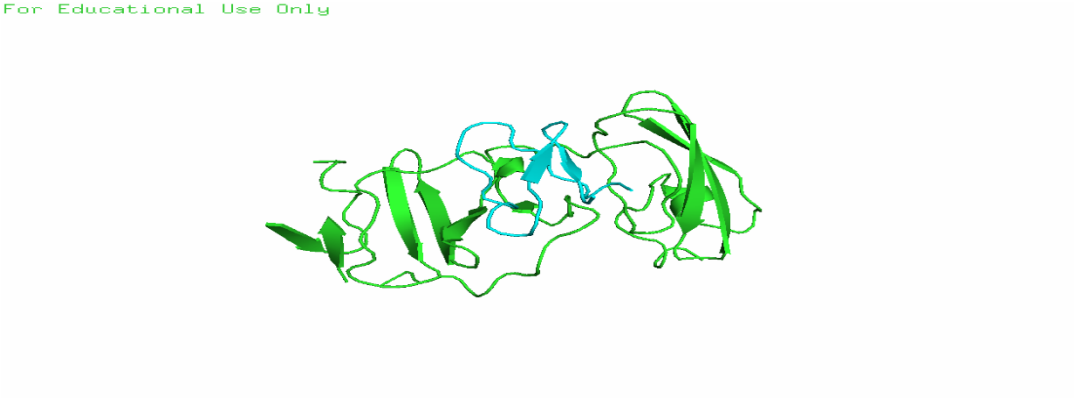

Fig 4.56 3d docking visualization of pathogenic proteins (NS5A CHAIN A) with cyclotide circulin E. Pathogenic proteins are presented in green color and cyclotides are shown in blue color

Table 4.12 circulin E docking score with NS5A chain A

CYCLOTIDE	CLUSTER	MEMBER	REPRESENTATIVE	WEIGHTED SCORE
Circulin E	0	218	Center	-717.5
			Lowest Energy	-924.2

CYI 1

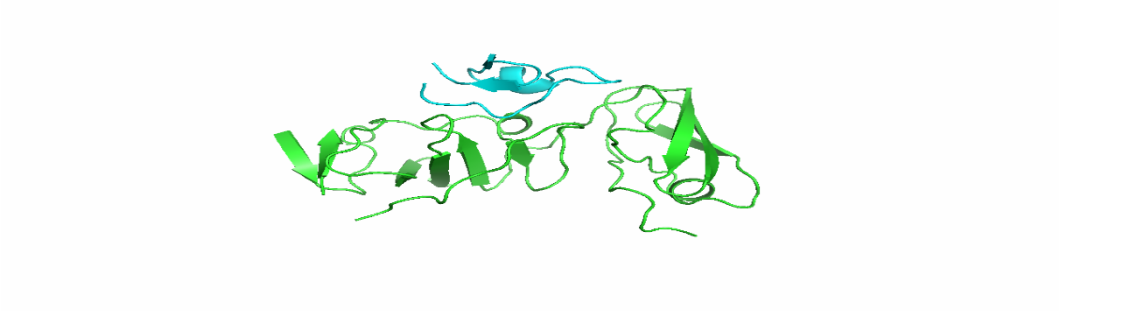

Fig 4.57 3d docking visualization of pathogenic proteins (NS5A CHAIN A) with cyclotide CYI 1. Pathogenic proteins are presented in green color and cyclotides are shown in blue color

Table 4.13 CYI 1 docking score with NS5A chain A

CYCLOTIDE	CLUSTER	MEMBER	REPRESENTATIVE	WEIGHTED SCORE
CYI 1	0	234	Center	-667.8
			Lowest Energy	-911.5

CYI 2

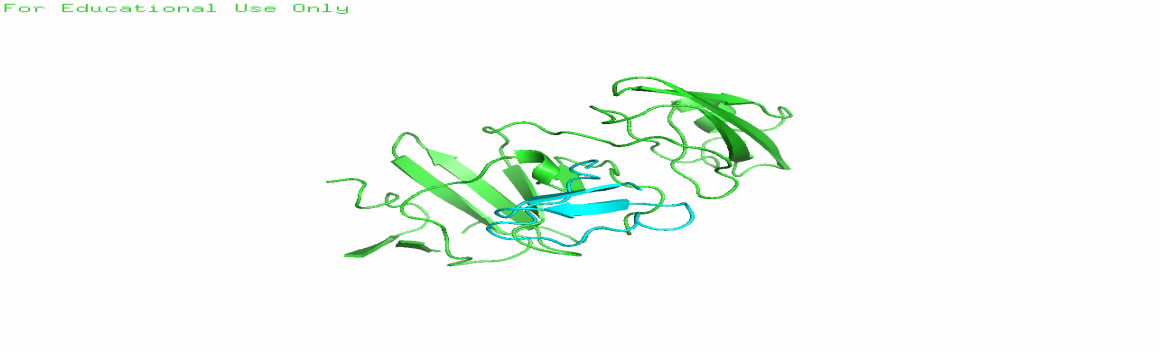

Fig 4.58 3d docking visualization of pathogenic proteins (NS5A CHAIN A) with cyclotide CYI 2. Pathogenic proteins are presented in green color and cyclotides are shown in blue color

Table 4.14 CYI 2 docking score with NS5A chain A

CYCLOTIDE	CLUSTER	MEMBERS	REPRESENTATIVE	WEIGHTED SCORE
CYI 2	0	286	Center	-696.2
			Lowest Energy	-903.2

CYI 3

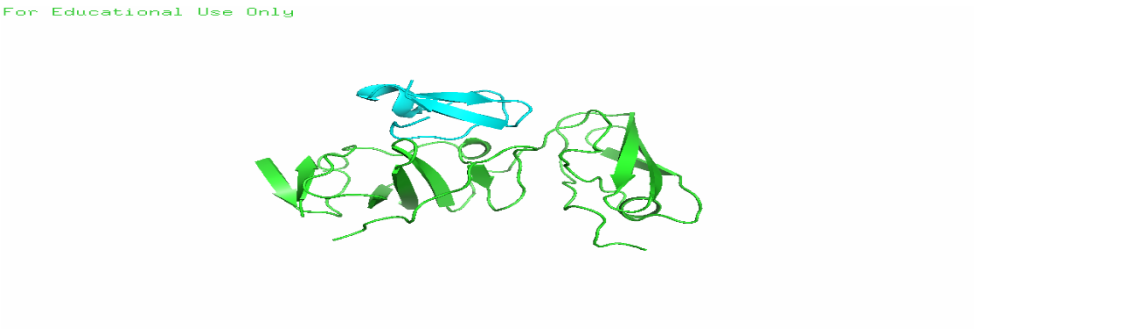

Fig 4.59 3d docking visualization of pathogenic proteins (NS5A CHAIN A) with cyclotide CYI 3

Pathogenic proteins are presented in green color and cyclotides are shown in blue color

Table 4.15 CYI 3 docking score with NS5A chain A

CYCLOTIDE	CLUSTER	MEMBERS	REPRESENTATIVE	WEIGHTED SCORE
CYI 3	0	165	Center	-621.6
			Lowest Energy	-738.9

CYI4

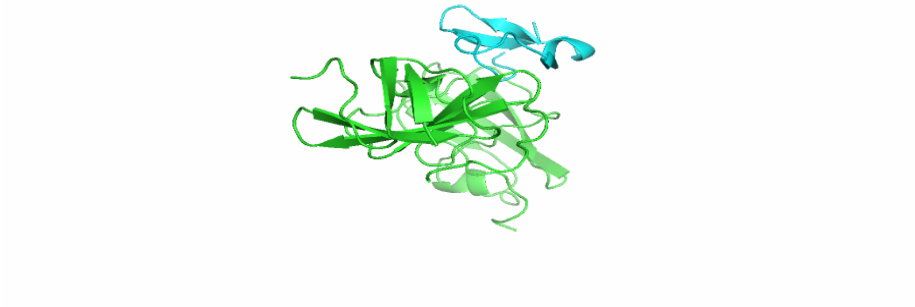

Fig 4.60 3d docking visualization of pathogenic proteins (NS5A CHAIN A) with cyclotide CYI 4
Pathogenic proteins are presented in green color and cyclotides are shown in blue color

Table 4.16 CYI 4 docking score with NS5A chain A

CYCLOTIDE	CLUSTER	MEMBERS	REPRESENTATIVE	WEIGHTED SCORE
CYI 4	0	302	Center	-689.1
			Lowest Energy	-862.8

CYI5

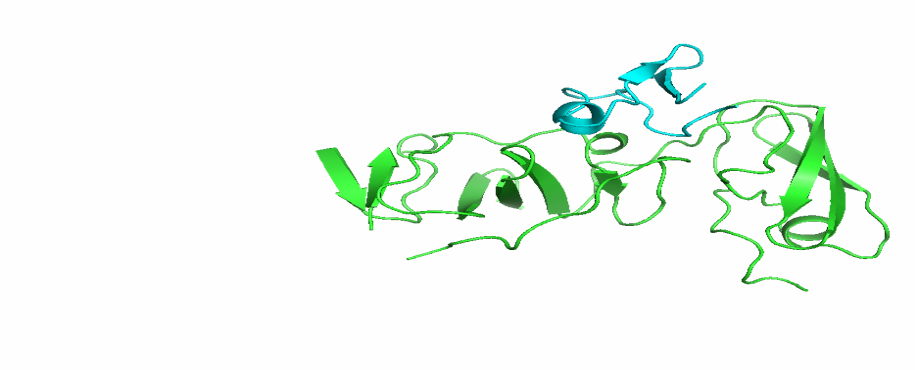

Fig 4.61 3d docking visualization of pathogenic proteins (NS5A CHAIN A) with cyclotide CYI 5
Pathogenic proteins are presented in green color and cyclotides are shown in blue color

Table 4.17 CYI 5 docking score with NS5A chain A

CYCLOTIDE	CLUSTER	MEMBERS	REPRESENTATIVE	WEIGHTED SCORE
CYI 5	0	202	Center	-702.6
			Lowest Energy	-830.1

CYI 6

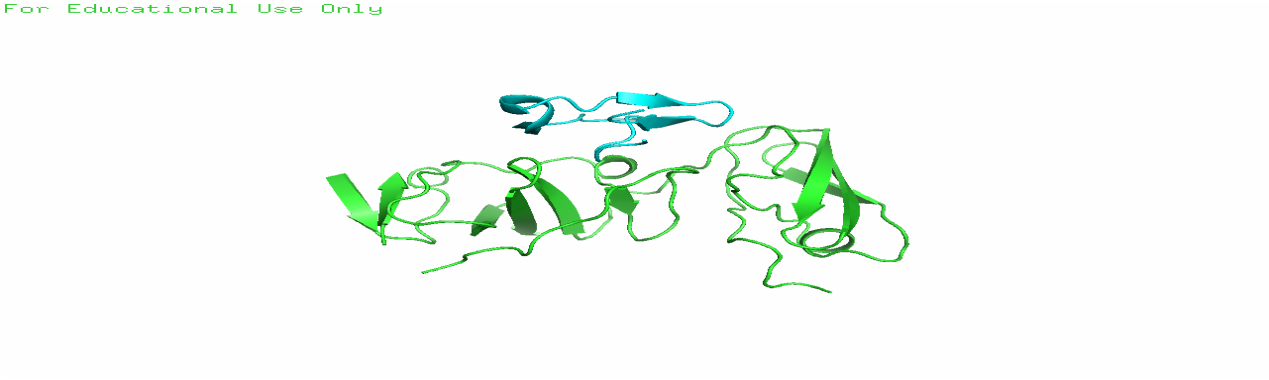

Fig 4.62 3d docking visualization of pathogenic proteins (NS5A CHAIN A) with cyclotide CYI 6
Pathogenic proteins are presented in green color and cyclotides are shown in blue color

Table 4.18 CYI 6 docking score with NS5A chain A

CYCLOTIDE	CLUSTER	MEMBERS	REPRESENTATIVE	WEIGHTED SCORE
CYI 6	0	204	Center	-623.2
			Lowest Energy	-783.5

HYFL A

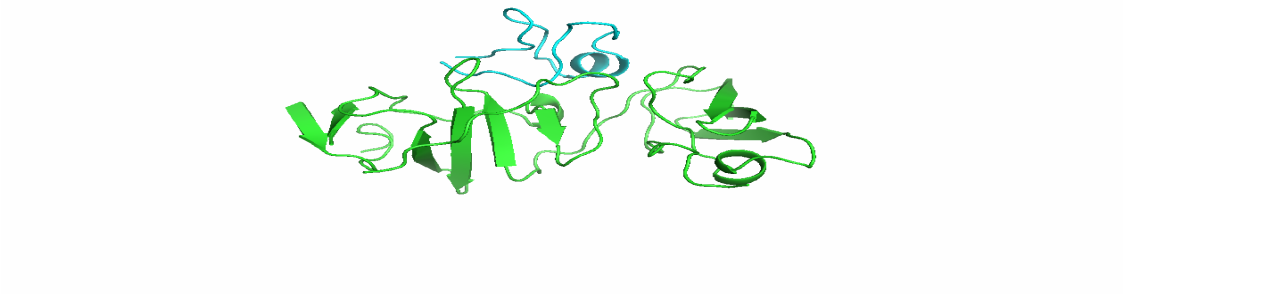

Fig 4.63 3d docking visualization of pathogenic proteins (NS5A CHAIN A) with cyclotide HYFL A
Pathogenic proteins are presented in green color and cyclotides are shown in blue color

Table 4.19 HYFL A docking score with NS5A chain A

CYCLOTIDE	CLUSTER	MEMBERS	REPRESENTATIVE	WEIGHTED SCORE
Hyfl A	0	271	Center	-647.2
			Lowest Energy	-811.8

HYFL B

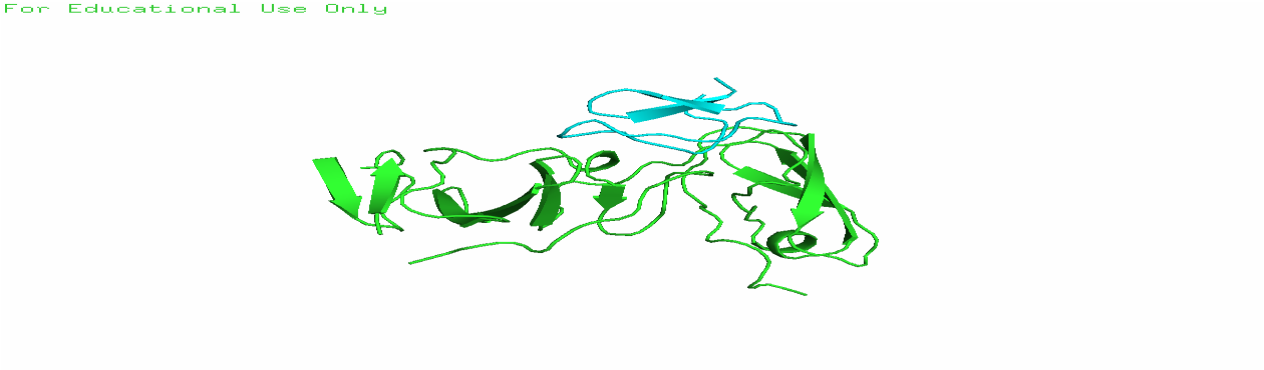

Fig 4.64 3d docking visualization of pathogenic proteins (NS5A CHAIN A) with cyclotide Hyfl B Pathogenic proteins are presented in green color and cyclotides are shown in blue color

Table 4.20 HYFL B docking score with NS5A chain A

CYCLOTIDE	CLUSTER	MEMBERS	REPRESENTATIVE	WEIGHTED SCORE
Hyfl B	0	307	Center	-812.1
			Lowest Energy	-828.1

HYFL C

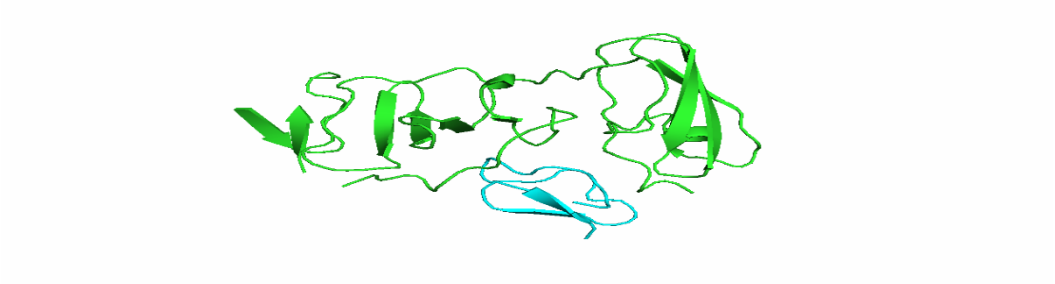

Fig 4.65 3d docking visualization of pathogenic proteins (NS5A CHAIN A) with cyclotide Hyfl C Pathogenic proteins are presented in green color and cyclotides are shown in blue color

Table 4.21 HYFL C docking score with NS5A chain A

CYCLOTIDE	CLUSTER	MEMBERS	REPRESENTATIVE	WEIGHTED SCORE
Hyfl C	0	296	Center	-701.1
			Lowest Energy	-792.8

HYFL D

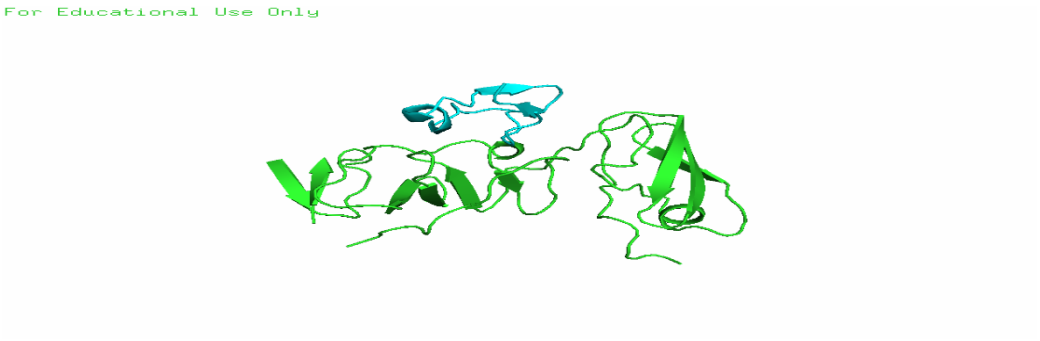

Fig 4.66 3d docking visualization of pathogenic proteins (NS5A CHAIN A) with cyclotide Hyfl D Pathogenic proteins are presented in green color and cyclotides are shown in blue color

Table 4.22 HYFL D docking score with NS5A chain A

CYCLOTIDE	CLUSTER	MEMBERS	REPRESENTATIVE	WEIGHTED SCORE
Hyfl D	0	159	Center	-743.0
			Lowest Energy	-962.7

HYFL F

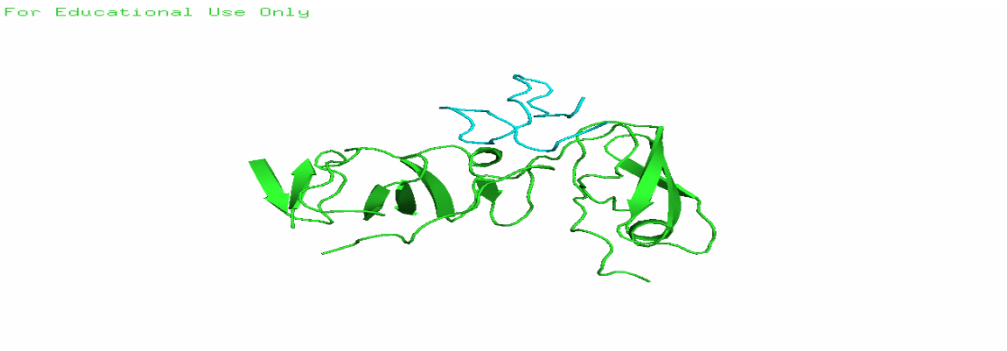

Fig 4.67 3d docking visualization of pathogenic proteins (NS5A CHAIN A) with cyclotide Hyfl F Pathogenic proteins are presented in green color and cyclotides are shown in blue color

Table 4.23 HYFL F docking score with NS5A chain A

CYCLOTIDE	CLUSTER	MEMBERS	REPRESENTATIVE	WEIGHTED SCORE
Hyfl F	0	259	Center	-761.0
			Lowest Energy	-875.8

HYFL I

Fig 4.68 3d docking visualization of pathogenic proteins (NS5A CHAIN A) with cyclotide Hyfl D I Pathogenic proteins are presented in green color and cyclotides are shown in blue color

Table 4.24 HYFL I docking score with NS5A chain A

CYCLOTIDE	CLUSTER	MEMBERS	REPRESENTATIVE	WEIGHTED SCORE
Hyfl I	0	200	Center	-700.0
			Lowest Energy	-870.3

HYFL K

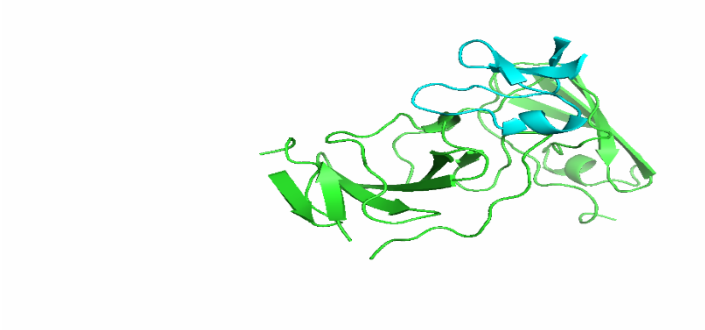

Fig 4.69 3d docking visualization of pathogenic proteins (NS5A CHAIN A) with cyclotide Hyfl K Pathogenic proteins are presented in green color and cyclotides are shown in blue color

Table 4.25 HYFL K docking score with NS5A chain A

CYCLOTIDE	CLUSTER	MEMBERS	REPRESENTATIVE	WEIGHTED SCORE
Hyfl K	0	343	Center	-746.6
			Lowest Energy	-839.2

HYFL L

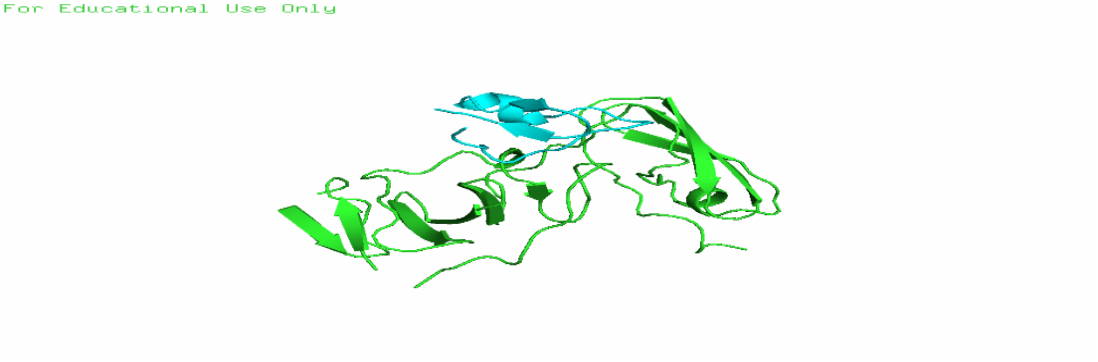

Fig 4.70 3d docking visualization of pathogenic proteins (NS5A CHAIN A) with cyclotide Hyfl L
Pathogenic proteins are presented in green color and cyclotides are shown in blue color

Table 4.26 HYFL L docking score with NS5A chain A

CYCLOTIDE	CLUSTER	MEMBERS	REPRESENTATIVE	W EIGHTED SCORE
Hyfl L	0	220	Center	-746.5
			Lowest Energy	-864.9

KALATA B9

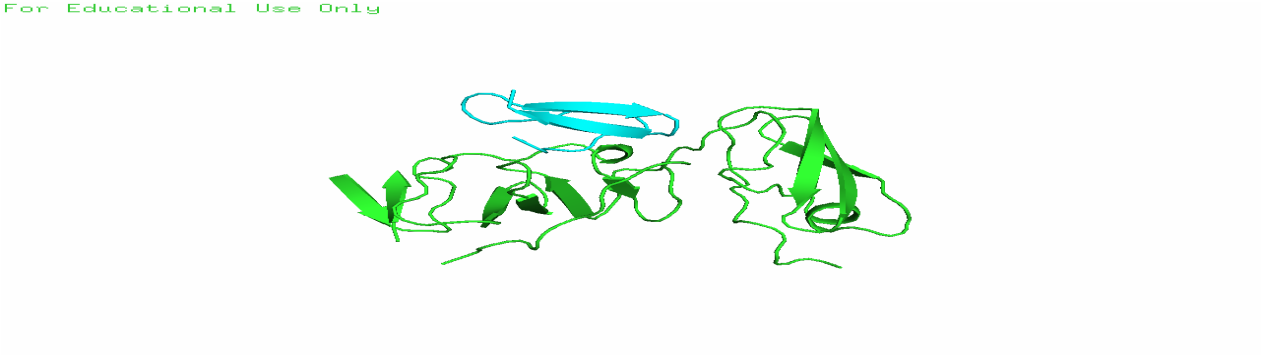

Fig 4.71 3d docking visualization of pathogenic proteins (NS5A CHAIN A) with cyclotide KALATAB9
Pathogenic proteins are presented in green color and cyclotides are shown in blue color

Table 4.27 kalata b9 docking score with NS5A chain A

CYCLOTIDE	CLUSTER	MEMBERS	REPRESENTATIVE	WEIGHTED SCORE
Kalata B9	0	220	Center	-674.2
			Lowest Energy	-732.6

KALATA B10

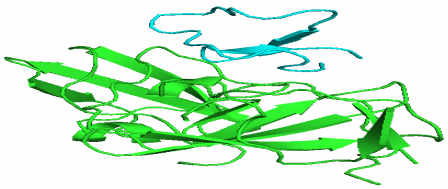

Fig 4.72 3d docking visualization of pathogenic proteins (NS5A CHAIN A) with cyclotide kalata B10 Pathogenic proteins are presented in green color and cyclotides are shown in blue color

Table 4.28 KALATA B10 docking score with NS5A chain A

CYCLOTIDE	CLUSTER	MEMBER	REPRESENTATIVE	WEIGHTED SCORE
Kalata B10	0	262	Center	-837.9
			Lowest Energy	-837.9

KALATA B13

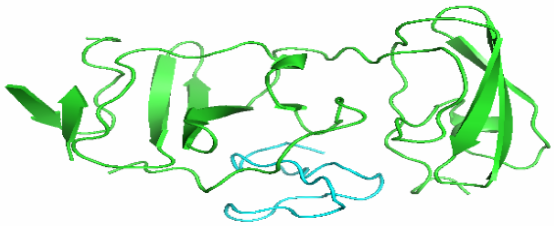

Fig 4.73 3d docking visualization of pathogenic proteins (NS5A CHAIN A) with cyclotide kalata B13 Pathogenic proteins are presented in green color and cyclotides are shown in blue color

Table 4.29 KALATA B13 docking score with NS5A chain A

CYCLOTIDE	CLUSTER	MEMBER	REPRESENTATIVE	WEIGHTED SCORE
Kalata B13	0	295	Center	-807.8
			Lowest Energy	-807.8

KALATA B14

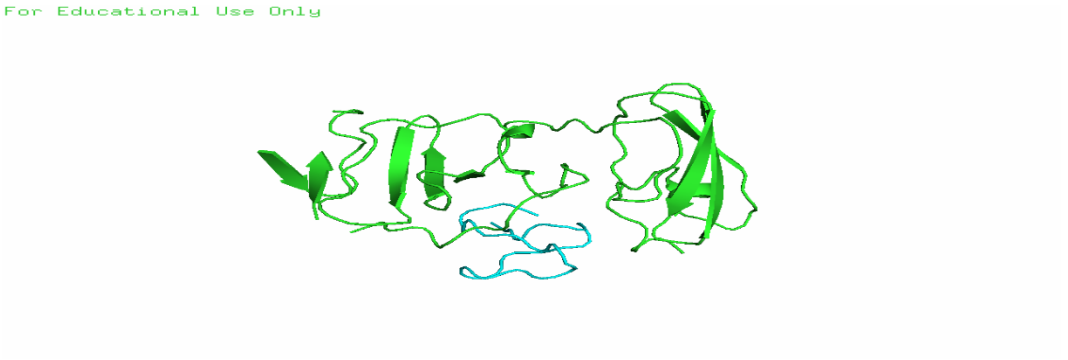

Fig 4.74 3d docking visualization of pathogenic proteins (NS5A CHAIN A) with cyclotide kalata B14 Pathogenic proteins are presented in green color and cyclotides are shown in blue color

Table 4.30 KALATA B14 docking score with NS5A chain A

CYCLOTIDE	CLUSTER	MEMBERS	REPRESENTATIVE	WEIGHTED SCORE
Kalata B14	0	280	Center	-787.9
			Lowest Energy	-787.9

KAALATA B16

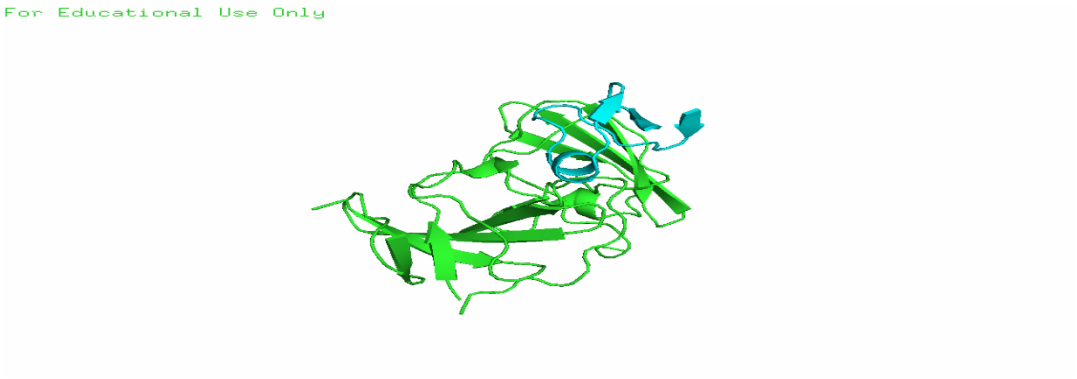

Fig 4.75 3d docking visualization of pathogenic proteins (NS5A CHAIN A) with cyclotide kalata B16 Pathogenic proteins are presented in green color and cyclotides are shown in blue color

Table 4.31 KALATA B16 docking score with NS5A chain A

CYCLOTIDE	CLUSTER	MEMBER	REPRESENTATIVE	WEIGHTED SCORE
Kalata B16	0	209	Center	-739.4
			Lowest Energy	-878.5

KALATA B17

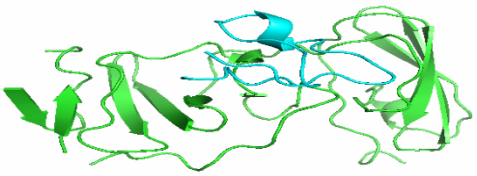

Fig 4.76 3d docking visualization of pathogenic proteins (NS5A CHAIN A) with cyclotide kalata B17 Pathogenic proteins are presented in green color and cyclotides are shown in blue color

Table 4.32 KALATA B17 docking score with NS5A chain A

CYCLOTIDE	CLUSTER	MEMBER	REPRESENTATIVE	WEIGHTED SCORE
Kalata B17	0	244	Center	-726.1
			Lowest Energy	-841.1

KALATA B18

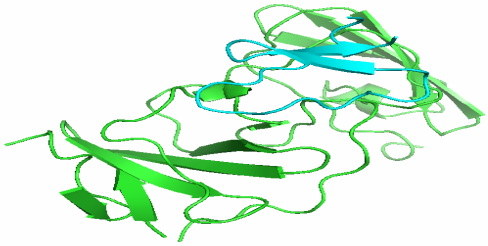

Fig 4.77 3d docking visualization of pathogenic proteins (NS5A CHAIN A) with cyclotide kalata B18 Pathogenic proteins are presented in green color and cyclotides are shown in blue color

Table 4.33 KALATA B18 docking score with NS5A chain A

CYCLOTIDE	CLUSTER	MEMBER	REPRESENTATIVE	WEIGHTED SCORE
Kalata B18	0	234	Center	-766.7
			Lowest Energy	-952.9

PHYB A

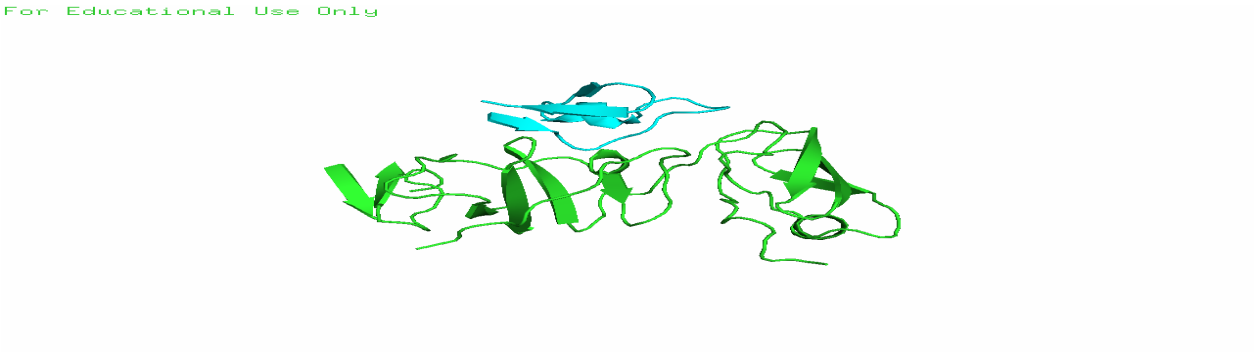

Fig 4.78 3d docking visualization of pathogenic proteins (NS5A CHAIN A) with cyclotide Phyb A Pathogenic proteins are presented in green color and cyclotides are shown in blue color

Table 4.34 Phyb A docking score with NS5A chain A

CYCLOTIDE	CLUSTER	MEMBERS	REPRESENTATIVE	WEIGHTED SCORE
Phyb A	0	362	Center	-743.6
			Lowest Energy	-878.9

PHYB B

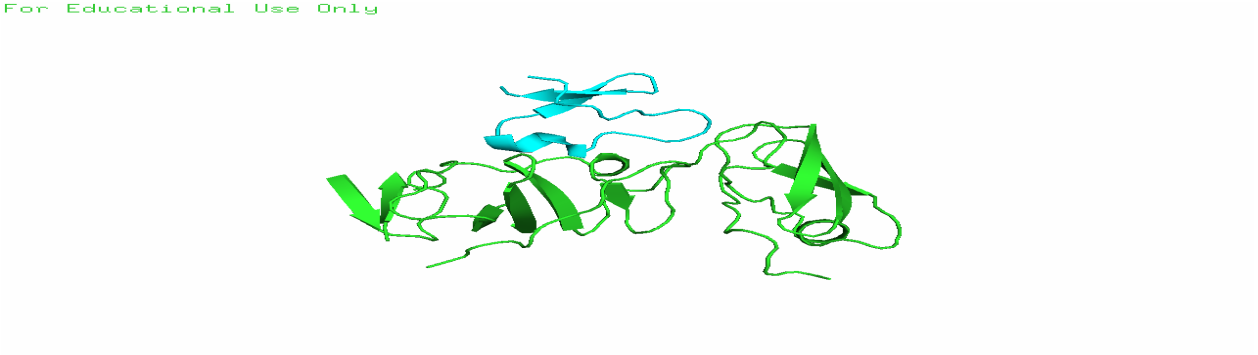

Fig 4.79 3d docking visualization of pathogenic proteins (NS5A CHAIN A) with cyclotide Phyb B Pathogenic proteins are presented in green color and cyclotides are shown in blue color

Table 4.35 Phyb B docking score with NS5A chain A

CYCLOTIDE	CLUSTER	MEMBERS	REPRESENTATIVE	WEIGHTED SCORE
Phyb B	0	304	Center	-738.1
			Lowest Energy	-986.4

PHYB

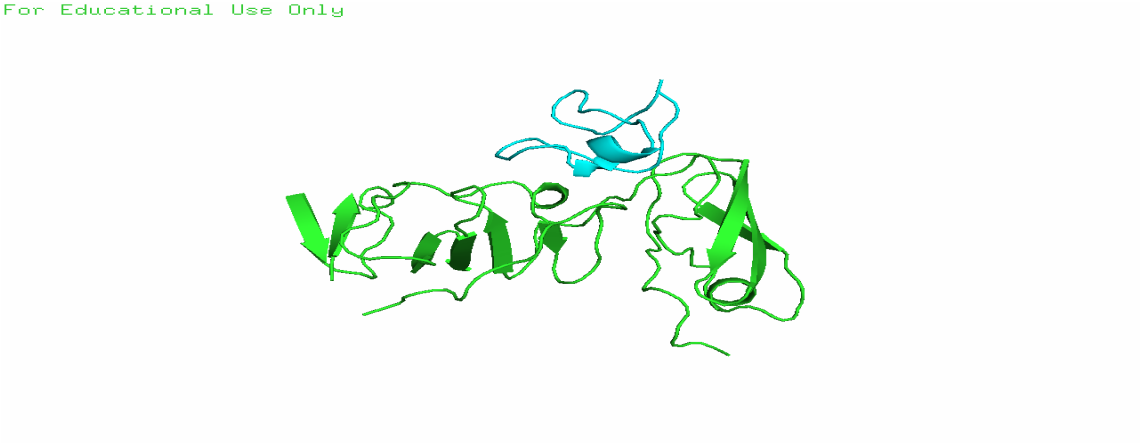

Fig 4.80 3d docking visualization of pathogenic proteins (NS5A CHAIN A) with cyclotide Phyb C Pathogenic proteins are presented in green color and cyclotides are shown in blue color

Table 4.36 Phyb C docking score with NS5A chain A

CYCLOTIDE	CLUSTER	MEMBERS	REPRESENTATIVE	WEIGHTED SCORE
Phyb C	0	314	Center	-747.3
			Lowest Energy	-878.2

PHYB D

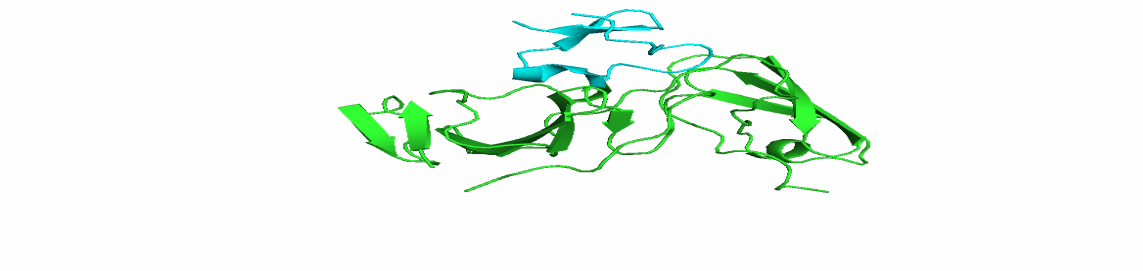

Fig 4.81 3d docking visualization of pathogenic proteins (NS5A CHAIN A) with cyclotide Phyb D Pathogenic proteins are presented in green color and cyclotides are shown in blue color

Table 4.37 Phyb D docking score with NS5A chain A

CYCLOTIDE	CLUSTER	MEMBERS	REPRESENTATIVE	WEIGHTED SCORE
Phyb D	0	304	Center	-738.1
			Lowest Energy	-986.4

PHYB E

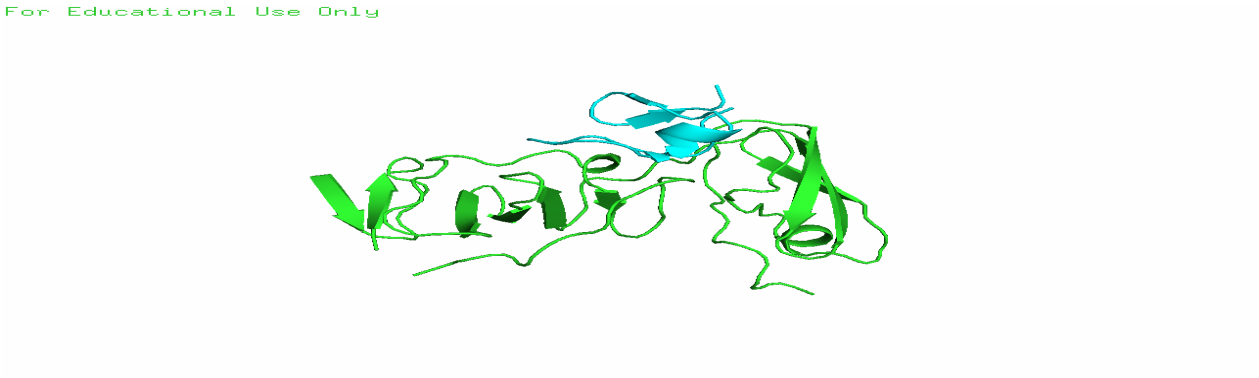

Fig 4.82 3d docking visualization of pathogenic proteins (NS5A CHAIN A) with cyclotide Phyb E
Pathogenic proteins are presented in green color and cyclotides are shown in blue color

Table 4.38 Phyb E docking score with NS5A chain A

CYCLOTIDE	CLUSTER	MEMBERS	REPRESENTATIVE	WEIGHTED SCORE
Phyb E	0	317	Center	-744.2
			Lowest Energy	-924.7

PHYB F

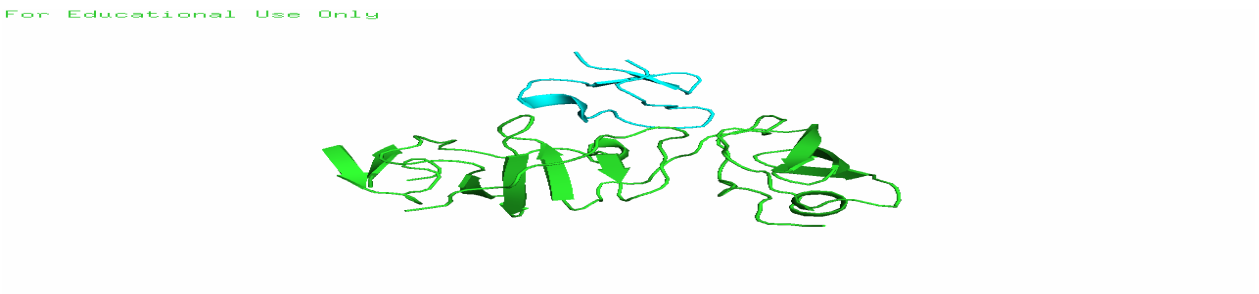

Fig 4.83 3d docking visualization of pathogenic proteins (NS5A CHAIN A) with cyclotide Phyb F
Pathogenic proteins are presented in green color and cyclotides are shown in blue color

Table 4.39 Phyb F docking score with NS5A chain A

CYCLOTIDE	CLUSTER	MEMBERS	REPRESENTATIVE	WEIGHTED SCORE
Phyb f	0	261	Center	-717.6
			Lowest Energy	-872.6

PHYB G

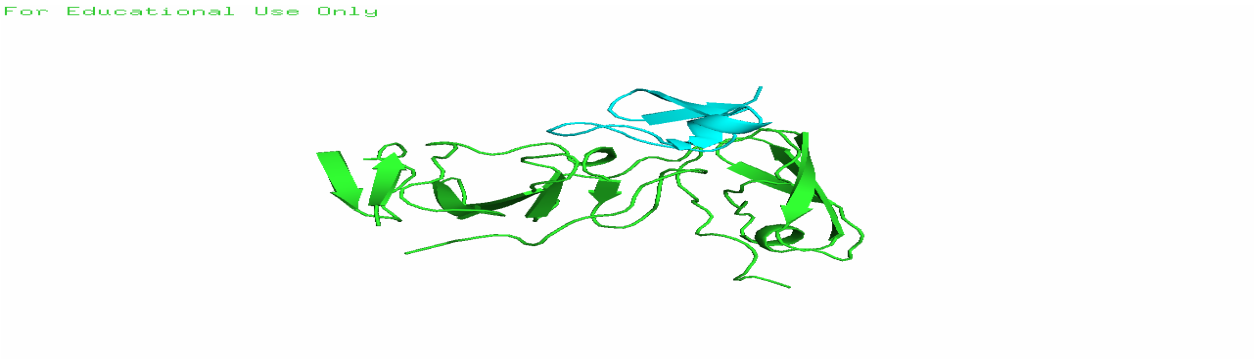

Fig 4.84 3d docking visualization of pathogenic proteins (NS5A CHAIN A) with cyclotide Phyb G Pathogenic proteins are presented in green color and cyclotides are shown in blue color

Table 4.40 Phyb G docking score with NS5A chain A

CYCLOTIDE	CLUSTER	MEMBERS	REPRESENTATIVE	WEIGHTED SCORE
Phyb G	0	261	Center	-717.6
			Lowest Energy	-872.6

PHYB H

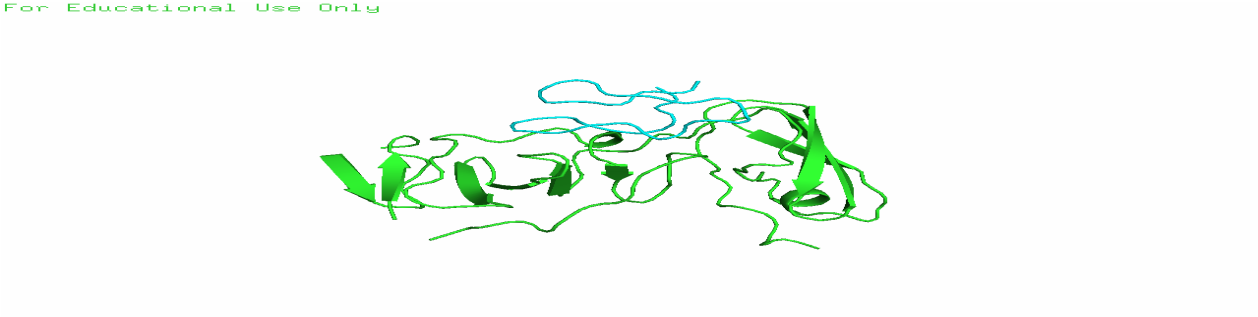

Fig 4.85 3d docking visualization of pathogenic proteins (NS5A CHAIN A) with cyclotide Phyb h Pathogenic proteins are presented in green color and cyclotides are shown in blue color

Table 4.41 Phyb H docking score with NS5A chain A

CYCLOTIDE	CLUSTER	MEMBERS	REPRESENTATIVE	WEIGHTED SCORE
phyb H	0	321	Center	-745.2
			Lowest Energy	-886.8

PHYB I

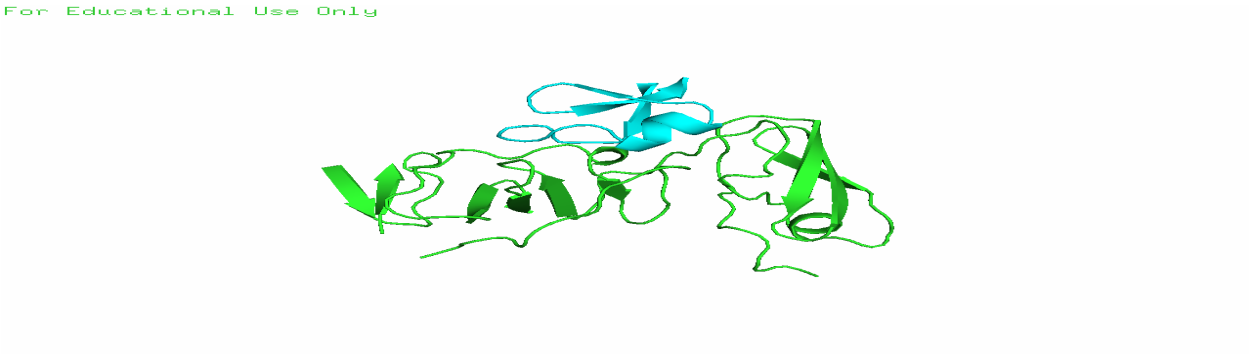

Fig 4.86 3d docking visualization of pathogenic proteins (NS5A CHAIN A) with cyclotide Phyb I
Pathogenic proteins are presented in green color and cyclotides are shown in blue color

Table 4.42 Phyb I docking score with NS5A chain A

CYCLOTIDE	CLUSTER	MEMBERS	REPRESENTATIVE	WEIGHTED SCORE
Phyb I	0	344	Center	-695.5
			Lowest Energy	-903.7

PHYB J

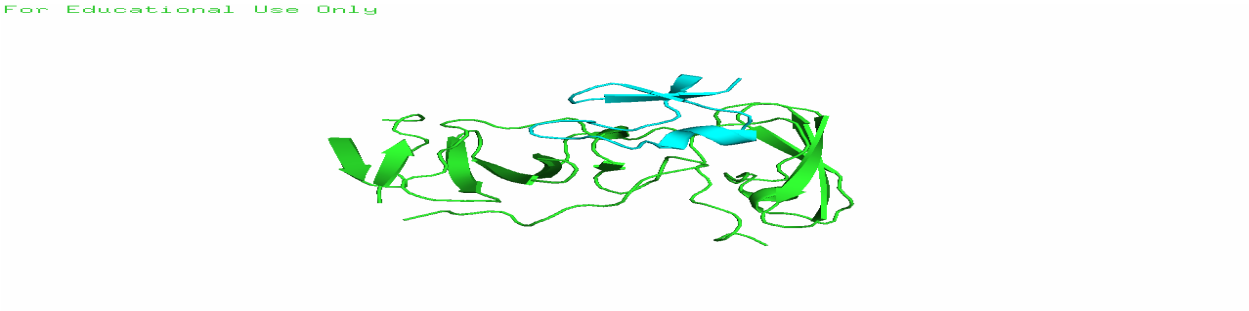

Fig 4.87 3d docking visualization of pathogenic proteins (NS5A CHAIN A) with cyclotide Phyb J
Pathogenic proteins are presented in green color and cyclotides are shown in blue color

Table 4.43 Phyb J docking score with NS5A chain A

CYCLOTIDE	CLUSTER	MEMBER	REPRESENTATIVE	WEIGHTED SCORE
Phyb J	0	307	Center	-716.5
			Lowest Energy	-874.4

PHYB L

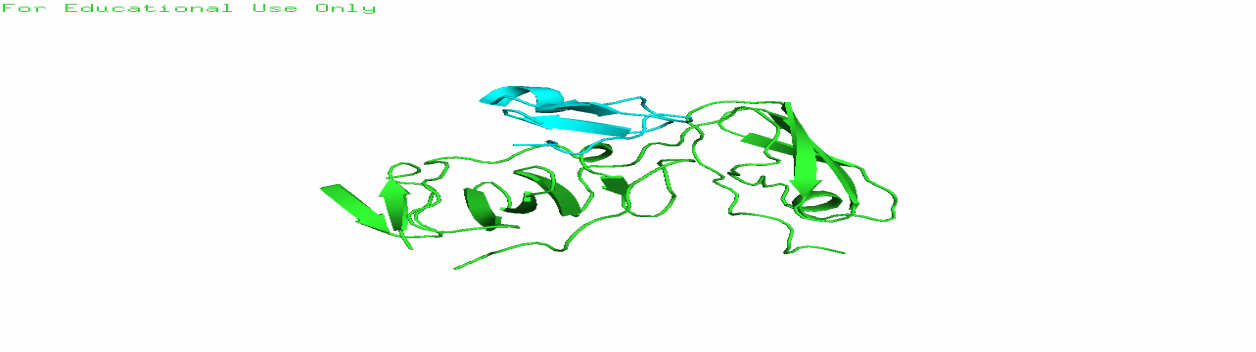

Fig 4.88 3d docking visualization of pathogenic proteins (NS5A CHAIN A) with cyclotide Phyb L
Pathogenic proteins are presented in green color and cyclotides are shown in blue color

Table 4.44 Phyb L docking score with NS5A chain A

CYCLOTIDE	CLUSTER	MEMBERS	REPRESENTATIVE	WEIGHTED SCORE
Phyb L	0	163	Center	-747.5
			Lowest Energy	-1037.8

VIAN 3

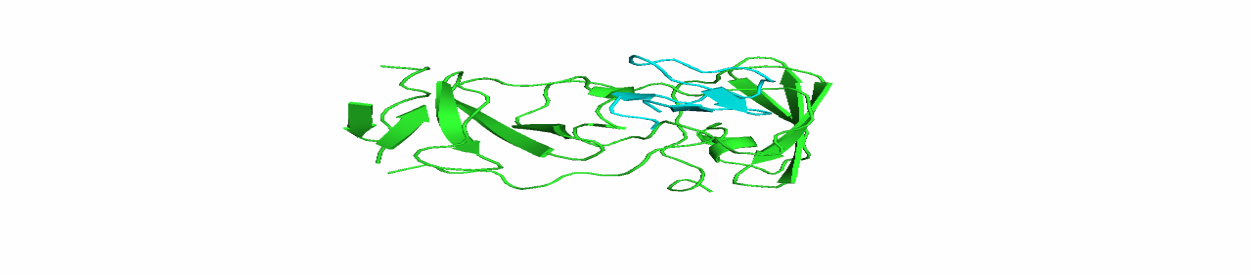

Fig 4.89 3d docking visualization of pathogenic proteins (NS5A CHAIN A) with cyclotide Vian 3
Pathogenic proteins are presented in green color and cyclotides are shown in blue color

Table 4.45 vian 3 docking score with NS5A chain A

CYCLOTIDE	CLUSTER	MEMBERS	REPRESENTATIVE	WEIGHTED SCORE
Vian 3	0	282	Center	-699.1
			Lowest Energy	-787.8

VIAN 5

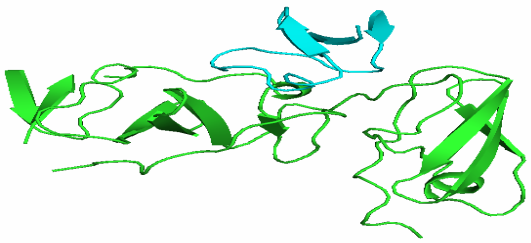

Fig 4.90 3d docking visualization of pathogenic proteins (NS5A CHAIN A) with cyclotide vian 5 Pathogenic proteins are presented in green color and cyclotides are shown in blue color

Table 4.46 vian 5 docking score with NS5A chain A

CYCLOTIDE	CLUSTER	MEMBERS	REPRESENTATIVE	WEIGHTED SCORE
Vian 5	0	279	Center	-736.9
			Lowest Energy	-915.5

VIAN 6

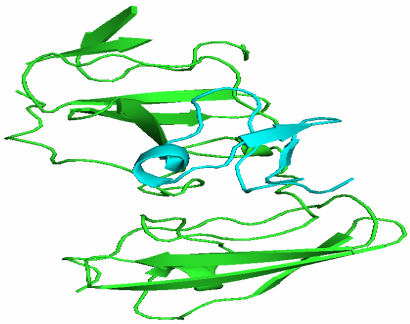

Fig 4.913d docking visualization of pathogenic proteins (NS5A CHAIN A) with cyclotide vian 6 Pathogenic proteins are presented in green color and cyclotides are shown in blue color

Table 4.47 vian 6 docking score with NS5A chain A

CYCLOTIDE	CLUSTER	MEMBERS	REPRESENTATIVE	WEIGHTED SCORE
Vian 6	**0**	**288**	**Center**	**-676.1**
			Lowest Energy	**-880.3**

VIAN 7

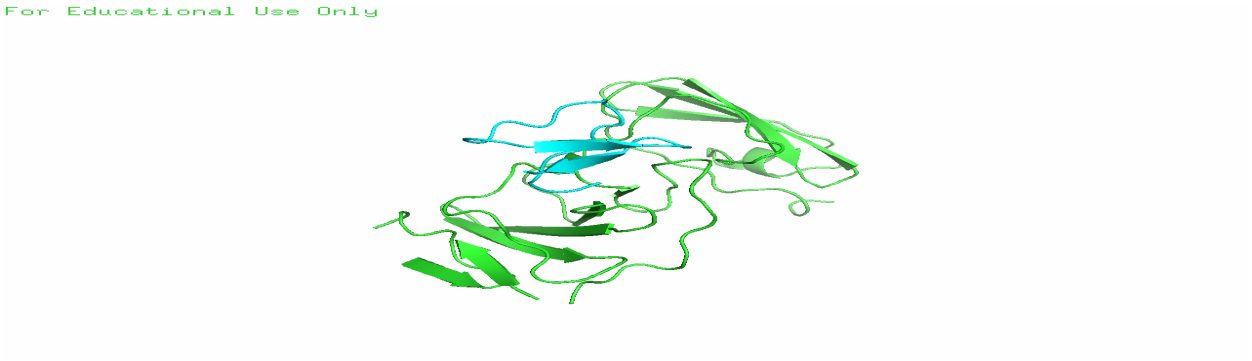

Fig 4.92 3d docking visualization of pathogenic proteins (NS5A CHAIN A) with cyclotide vian 7
Pathogenic proteins are presented in green color and cyclotides are shown in blue color

Table 4.48 vian 7 docking score with NS5A chain A

CYCLOTIDE	CLUSTER	MEMBERS	REPRESENTATIVE	WEIGHTED SCORE
Vian 7	0	351	Center	-736.4
			Lowest Energy	-901.5

VIAN 9

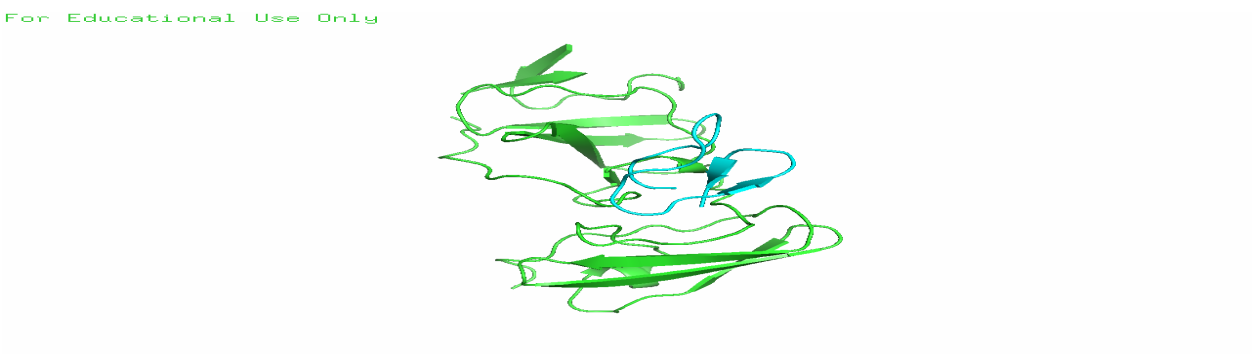

Fig 4.93 3d docking visualization of pathogenic proteins (NS5A CHAIN A) with cyclotide vian 9
Pathogenic proteins are presented in green color and cyclotides are shown in blue color

Table 4.49 vian 9 docking score with NS5A chain A

CYCLOTIDE	CLUSTER	MEMBERS	REPRESENTATIVE	WEIGHTED SCORE
Vian 9	0	204	Center	-588.6
			Lowest Energy	-740.7

VIAN 10

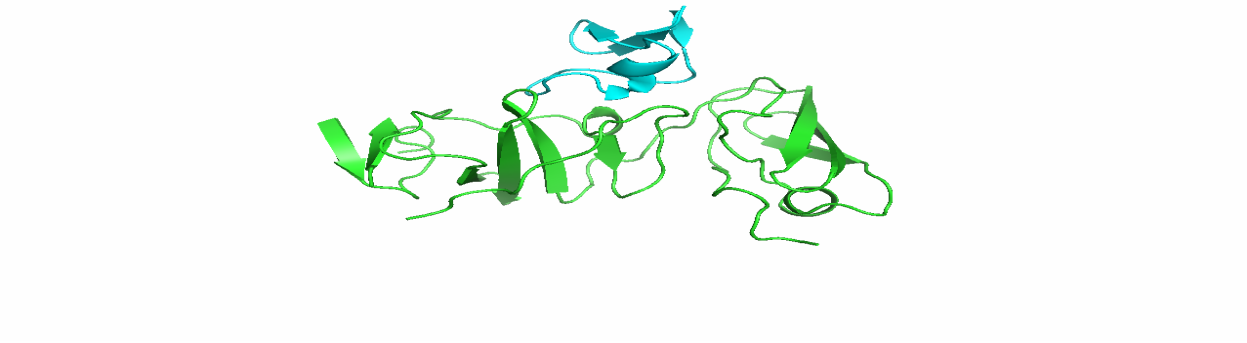

Fig 4.94 3d docking visualization of pathogenic proteins (NS5A CHAIN A) with cyclotide vian 10 Pathogenic proteins are presented in green color and cyclotides are shown in blue color

Table 4.50 vian 10 docking score with NS5A chain A

CYCLOTIDE	CLUSTER	MEMBERS	REPRESENTATIVE	WEIGHTED SCORE
Vian 10	0	291	Center	-751.2
			Lowest Energy	-980.2

VIAN 11

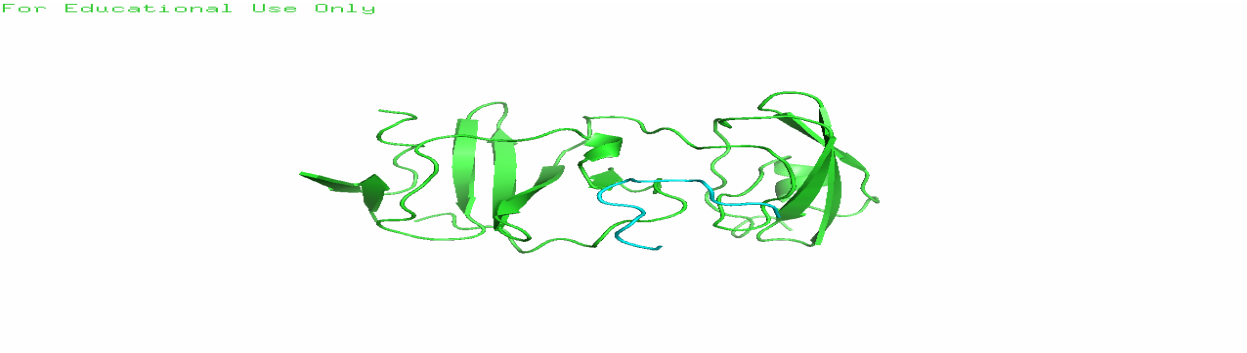

Fig 4.95 3d docking visualization of pathogenic proteins (NS5A CHAIN A) with cyclotide vian 11 Pathogenic proteins are presented in green color and cyclotides are shown in blue color

Table 4.51 vian 11 docking score with NS5A chain A

CYCLOTIDE	CLUSTER	MEMBERS	REPRESENTATIVE	WEIGHTED SCORE
Vian 11	0	272	Center	-704.3
			Lowest Energy	-801.6

4.7. NS5B CHAIN A DOCKING RESULTS WITH CYCLOTIDES

Table 4.53 NS5B CHAIN A DOCKING RESULTS WITH CYCLOTIDES

CYCLOTIDES	Cluster	Members	Representative	Weighted Score
PHYB A	0	209	Center	-744.5
			Lowest Energy	-826.7
PHYB D	0	208	Center	-717.9
			Lowest Energy	-815.9
PHYB E	0	285	Center	-842.2
			Lowest Energy	-990.2
PHYB F	0	261	Center	-764.4
			Lowest Energy	-995.7
PHYB G	0	231	Center	-777.2
			Lowest Energy	-901.1
PHYB H	0	240	Center	-656.3
			Lowest Energy	-760.8
PHYB I	0	175	Center	-713.6
			Lowest Energy	-754.5
PHYB J	0	222	Center	-661.3
			Lowest Energy	-801.9
PHYB L	0	277	Center	-831.5
			Lowest Energy	-1015.7
PHYB B	0	253	Center	-779.4
			Lowest Energy	-1011.2
PHYB C	0	194	Center	-728.7
			Lowest Energy	-903.8
CIRCULIN A	0	202	Center	-726.5
			Lowest Energy	-764.1

CIRCULIN B	0	130	Center	-709.0
			Lowest Energy	-826.6
CIRCULIN C	0	272	Center	-658.8
			Lowest Energy	-787.4
CIRCULIN D	0	260	Center	-814.1
			Lowest Energy	-964.8
CIRCULIN E	0	249	Center	-734.1
			Lowest Energy	-1059.7
HYFL A	0	160	Center	-661.1
			Lowest Energy	-730.0
HYFL B	0	313	Center	-708.2
			Lowest Energy	-790.1
HYFL C	0	183	Center	-610.7
			Lowest Energy	-761.3
HYFL D	0	415	Center	-876.5
			Lowest Energy	-979.8
HYFL F	0	287	Center	-684.3
			Lowest Energy	-873.3
HYFL I	0	295	Center	-684.6
			Lowest Energy	-849.9
HYFL K	0	333	Center	-740.1
			Lowest Energy	-851.8
HYFL L	0	224	Center	-711.5
			Lowest Energy	-936.3
CYI 1	0	221	Center	-659.6
			Lowest Energy	-698.7

CYI 2	0	238	Center	-777.9
			Lowest Energy	-777.9
CYI 3	0	195	Center	-614.9
			Lowest Energy	-717.4
CYI 4	0	274	Center	-711.7
			Lowest Energy	-946.6
CYI 5	0	317	Center	-821.4
			Lowest Energy	-973.8
CYI 6	0	261	Center	-605.1
			Lowest Energy	-816.7
KALATA B9	0	214	Center	-651.3
			Lowest Energy	-988.6
KALATA B10	0	178	Center	-726.7
			Lowest Energy	-864.2
KALATA B13	0	320	Center	-677.4
			Lowest Energy	-811.4
KALATA B14	0	331	Center	-674.5
			Lowest Energy	-787.7
KALATA B16	0	399	Center	-945.1
			Lowest Energy	-954.2
KALATA B17	0	190	Center	-738.4
			Lowest Energy	-829.1
KALATA B18	0	299	Center	-739.3
			Lowest Energy	-957.8
VIAN 3	0	418	Center	-668.8
			Lowest Energy	-865.7

VIAN 5	0	244	Center	-713.5
			Lowest Energy	-956.4
VIAN 6	0	273	Center	-749.8
			Lowest Energy	-798.6
VIAN 7	0	345	Center	-802.6
			Lowest Energy	-999.9
VIAN 9	0	213	Center	-587.4
			Lowest Energy	-758.7
VIAN 10	0	296	Center	-751.0
			Lowest Energy	-929.6
VIAN 11	0	216	Center	-789.5
			Lowest Energy	-953.9

4.8. PYMOL DOCKING VISUALIZATION RESULTS OF NS5B PROTEIN WITH CYCLOTIDES

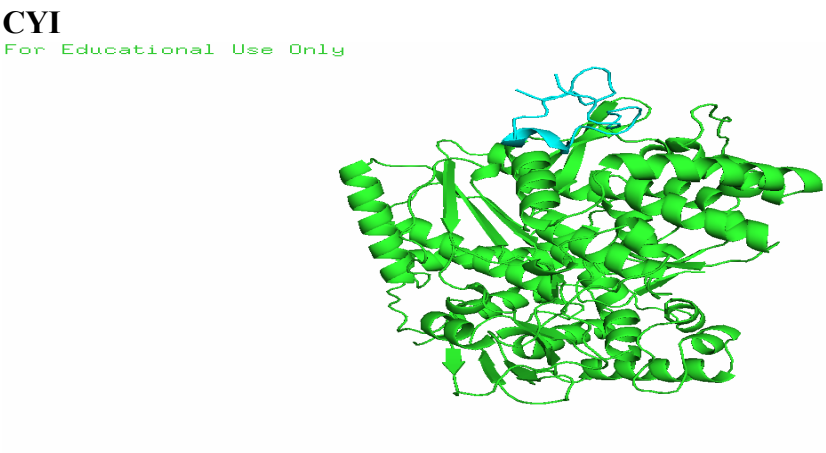

FIG 4.96 3d docking visualization of pathogenic proteins (NS5B CHAIN A) with cyclotide CYI 1 Pathogenic proteins are presented in green color and cyclotides are shown in blue color

Table 4.53 CYI 1 docking score with NS5B chain A

				WEIGHTED

CYCLOTIDE	CLUSTER	MEMBERS	REPRESENTATIVE	SCORE
CYI 1	0	221	Center	-659.6
			Lowest Energy	-698.7

CYI 2

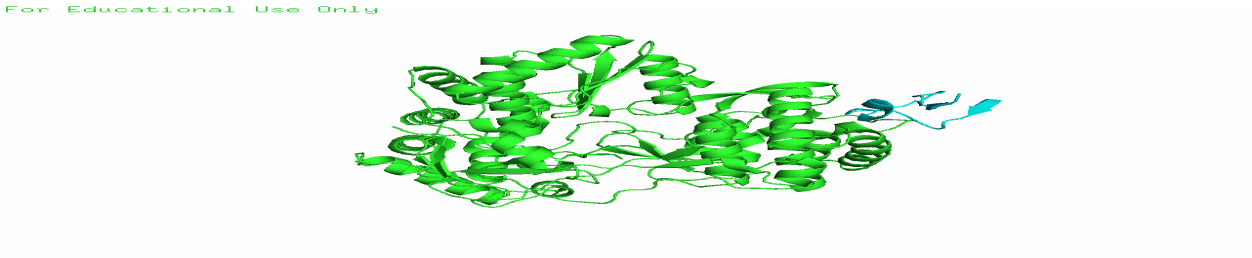

FIG 4.97 3d docking visualization of pathogenic proteins (NS5B CHAIN A) with cyclotide CYI 2 Pathogenic proteins are presented in green color and cyclotides are shown in blue color

Table 4.54 CYI 2 docking score with NS5B chain A

CYCLOTIDE	CLUSTER	MEMBERS	REPRESENTATIVE	WEIGHTED SCORE
CYI 2	0	238	Center	-777.9
			Lowest Energy	-777.9

CYI 3

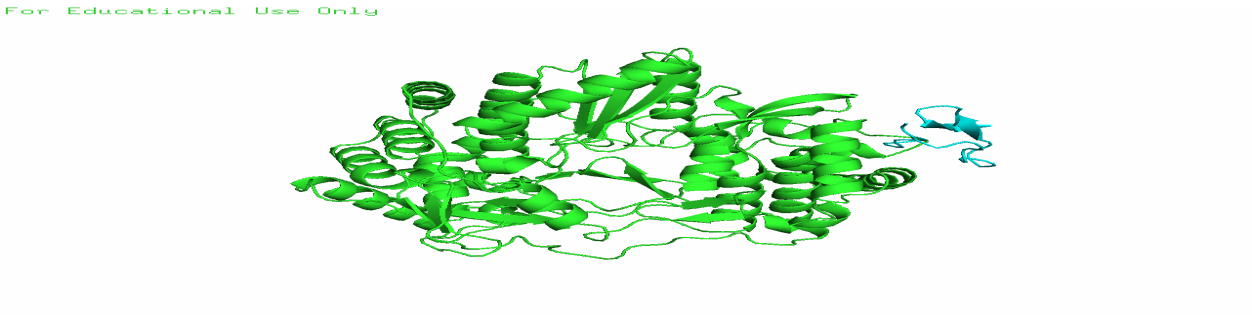

FIG 4.98 3d docking visualization of pathogenic proteins (NS5B CHAIN A) with cyclotide CYI 3 Pathogenic proteins are presented in green color and cyclotides are shown in blue color

Table 4.55 CYI 3 docking score with NS5B chain A

CYCLOTIDE	CLUSTER	MEMBERS	REPRESENTATIVE	WEIGHTED SCORE
CYI 3	0	195	Center	-614.9
			Lowest Energy	-717.4

CYI 4

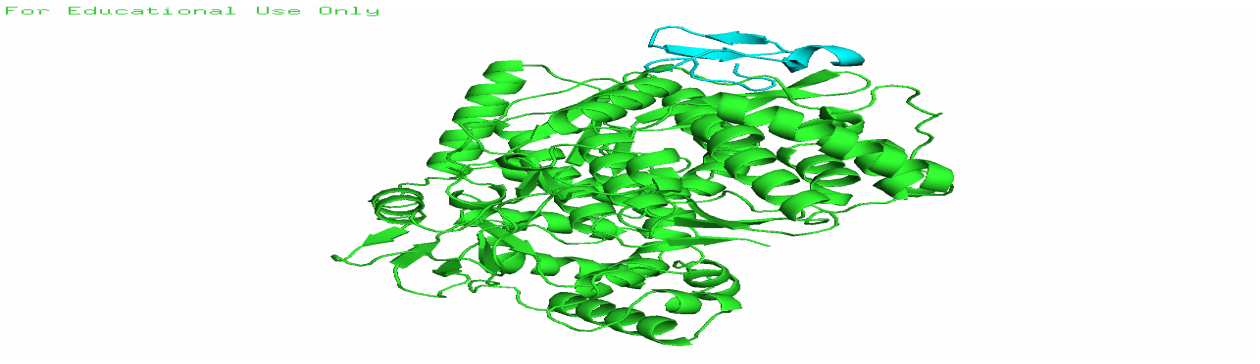

FIG 4.99 3d docking visualization of pathogenic proteins (NS5B CHAIN A) with cyclotide CYI 4
Pathogenic proteins are presented in green color and cyclotides are shown in blue color

Table 4.56 CYI 4 docking score with NS5B chain A

CYCLOTIDE	CLUSTER	MEMBERS	REPRESENTATIVE	WEIGHTED SCORE
CYI 4	0	274	Center	-711.7
			Lowest Energy	-946.6

CYI 5

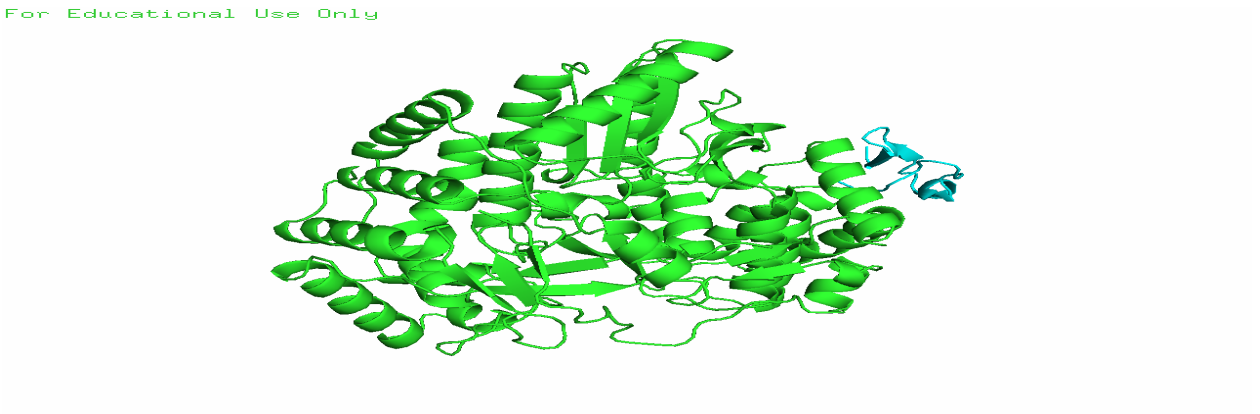

FIG 4.100 3d docking visualization of pathogenic proteins (NS5B CHAIN A) with cyclotide CYI 5
Pathogenic proteins are presented in green color and cyclotides are shown in blue color

Table 4.57 CYI 5 docking score with NS5B chain A

CYCLOTIDE	CLUSTER	MEMBERS	REPRESENTATIVE	WEIGHTED SCORE
CYI 5	0	317	Center	-821.4
			Lowest Energy	-973.8

CYI 6

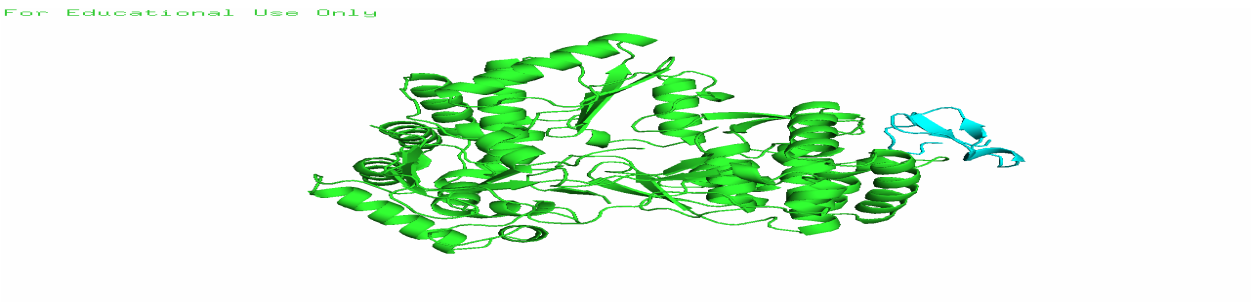

FIG 4.101 3d docking visualization of pathogenic proteins (NS5B CHAIN A) with cyclotide CYI 6 Pathogenic proteins are presented in green color and cyclotides are shown in blue color

Table 4.58 CYI 6 docking score with NS5B chain A

CYCLOTIDE	CLUSTER	MEMBERS	REPRESENTATIVE	WEIGHTED SCORE
CYI 6	0	261	Center	-605.1
			Lowest Energy	-816.7

CIRCULIN A

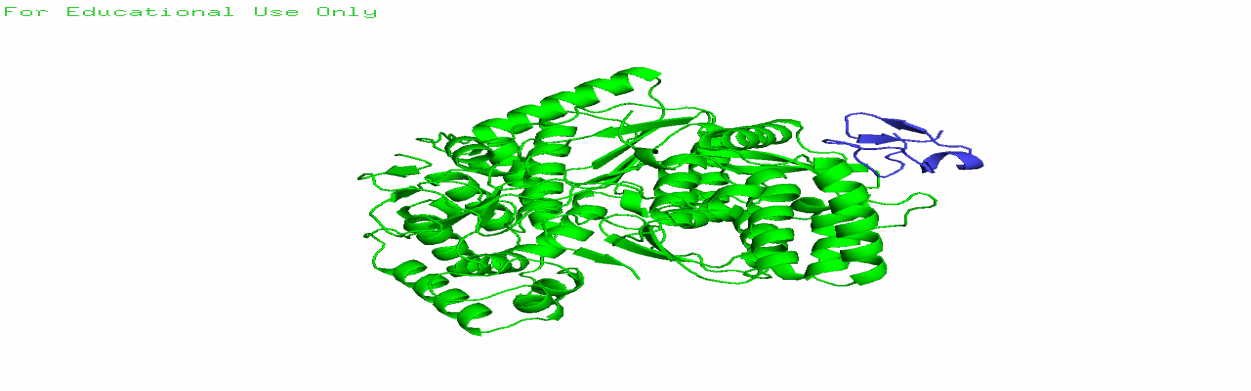

FIG 4.102 3d docking visualization of pathogenic proteins (NS5B CHAIN A) with cyclotide Circulin A Pathogenic proteins are presented in green color and cyclotides are shown in blue color

Table 4.59 Circulin A docking score with NS5B chain A

CYCLOTIDE	CLUSTER	MEMBERS	REPRESENTATIVE	WEIGHTED SCORE
CIRCULIN A	0	202	Center	-726.5
			Lowest Energy	-764.1

CIRCULIN B

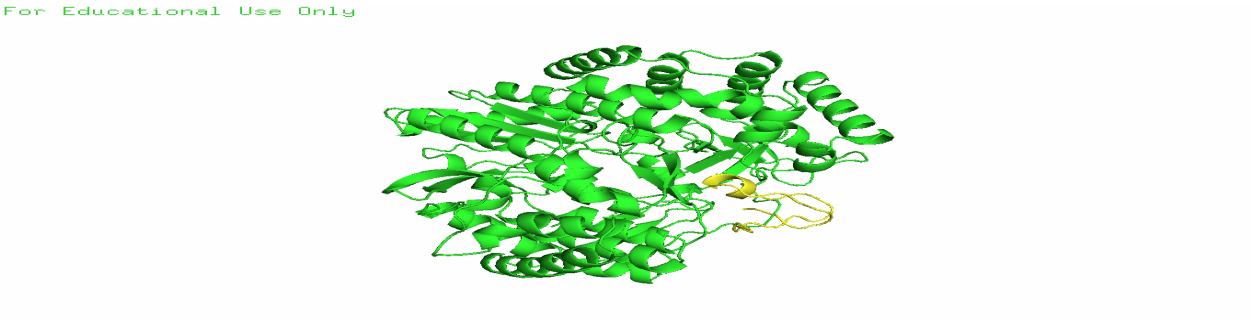

FIG 4.103 3d docking visualization of pathogenic proteins (NS5B CHAIN A) with Circulin B Pathogenic proteins are presented in green color and cyclotides are shown in golden color

Table 4.60 Circulin B docking score with NS5B chain A

CYCLOTIDE	CLUSTER	MEMBERS	REPRESENTATIVE	WEIGHTED SCORE
CIRCULIN B	0	130	Center	-709.0
			Lowest Energy	-826.6

CIRCULIN C

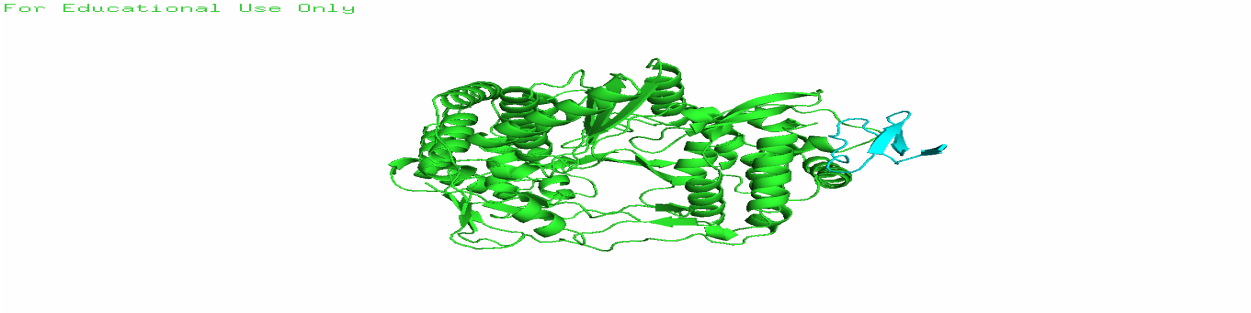

FIG 4.104 3d docking visualization of pathogenic proteins (NS5B CHAIN A) with Circulin C Pathogenic proteins are presented in green color and cyclotides are shown in blue color

Table 4.61 Circulin C docking score with NS5B chain A

CYCLOTIDE	CLUSTER	MEMBERS	REPRESENTATIVE	WEIGHTED SCORE
CIRCULIN C	0	272	Center	-658.8
			Lowest Energy	-787.4

CIRCULIN D

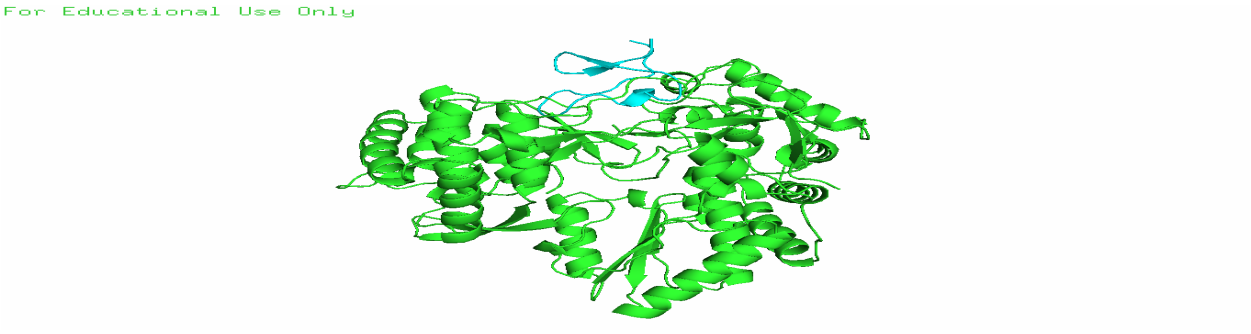

FIG 4.105 3d docking visualization of pathogenic proteins (NS5B CHAIN A) with Circulin D Pathogenic proteins are presented in green color and cyclotides are shown in blue color

Table 4.62 Circulin D docking score with NS5B chain A

CYCLOTIDE	CLUSTER	MEMBERS	REPRESENTATIVE	WEIGHTED SCORE
CIRCULIN D	0	260	Center	-814.1
			Lowest Energy	-964.8

CIRCULIN E

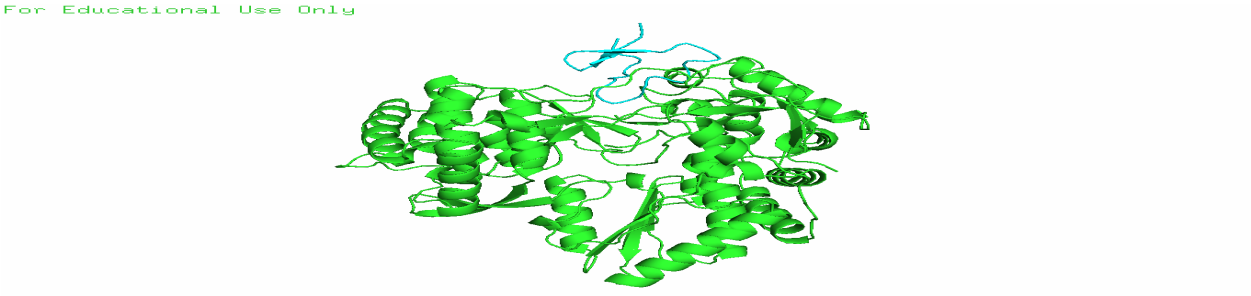

FIG 4.106 3d docking visualization of pathogenic proteins (NS5B CHAIN A) with Circulin E Pathogenic proteins are presented in green color and cyclotides are shown in blue color

Table 4.63 Circulin E docking score with NS5B chain A

CYCLOTIDE	CLUSTER	MEMBERS	REPRESENTATIVE	WEIGHTED SCORE
CIRCULIN E	0	249	Center	-734.1
			Lowest Energy	-1059.7

HYFL A

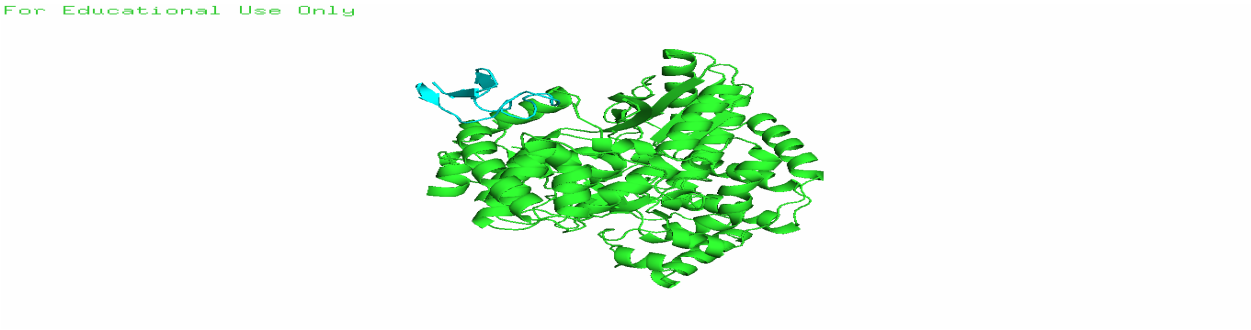

FIG 4.107 3d docking visualization of pathogenic proteins (NS5B CHAIN A) with Hyfl A Pathogenic proteins are presented in green color and cyclotides are shown in blue color

Table 4.64 Hyfl A docking score with NS5B chain A

CYCLOTIDE	CLUSTER	MEMBERS	REPRESENTATIVE	WEIGHTED SCORE
HYFL A	0	160	Center	-661.1
			Lowest Energy	-730.0

HYFL B

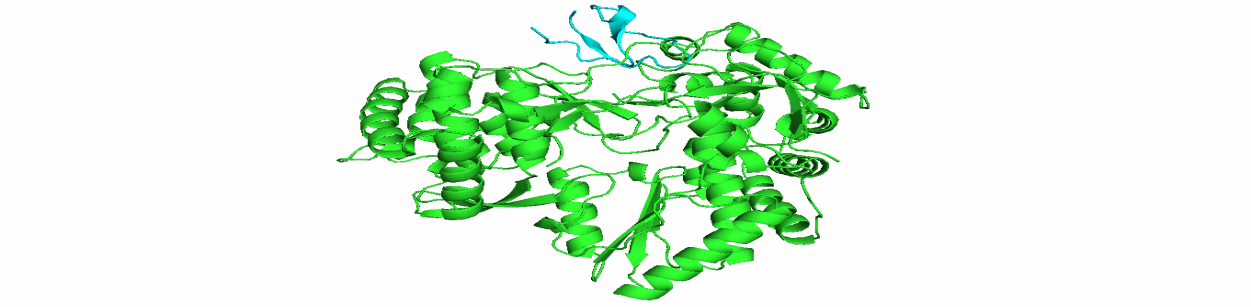

FIG 4.108 3d docking visualization of pathogenic proteins (NS5B CHAIN A) with Hyfl B Pathogenic proteins are presented in green color and cyclotides are shown in blue color

Table 4.65 Hyfl B docking score with NS5B chain A

CYCLOTIDE	CLUSTER	MEMBERS	REPRESENTATIVE	WEIGHTED SCORE
HYFL B	0	313	Center	-708.2
			Lowest Energy	-790.1

HYFL C

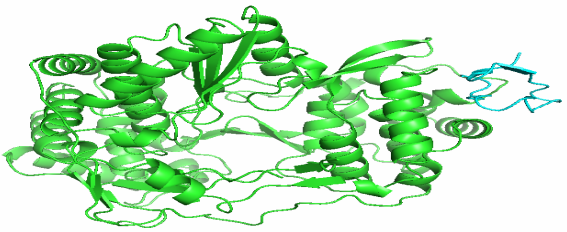

FIG 4.109 3d docking visualization of pathogenic proteins (NS5B CHAIN A) with Hyfl C Pathogenic proteins are presented in green color and cyclotides are shown in blue color

Table 4.66 Hyfl C docking score with NS5B chain A

CYCLOTIDE	CLUSTER	MEMBERS	REPRESENTATIVE	WEIGHTED SCORE
HYFL C	0	183	Center	-610.7
			Lowest Energy	-761.3

HYFL D

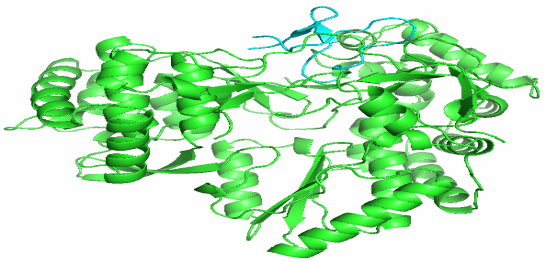

FIG 4.110 3d docking visualization of pathogenic proteins (NS5B CHAIN A) with Hyfl D Pathogenic proteins are presented in green color and cyclotides are shown in blue color

Table 4.67 Hyfl D docking score with NS5B chain A

CYCLOTIDE	CLUSTER	MEMBERS	REPRESENTATIVE	WEIGHTED SCORE
HYFL D	0	415	Center	-876.5
			Lowest Energy	-979.8

HYFL F

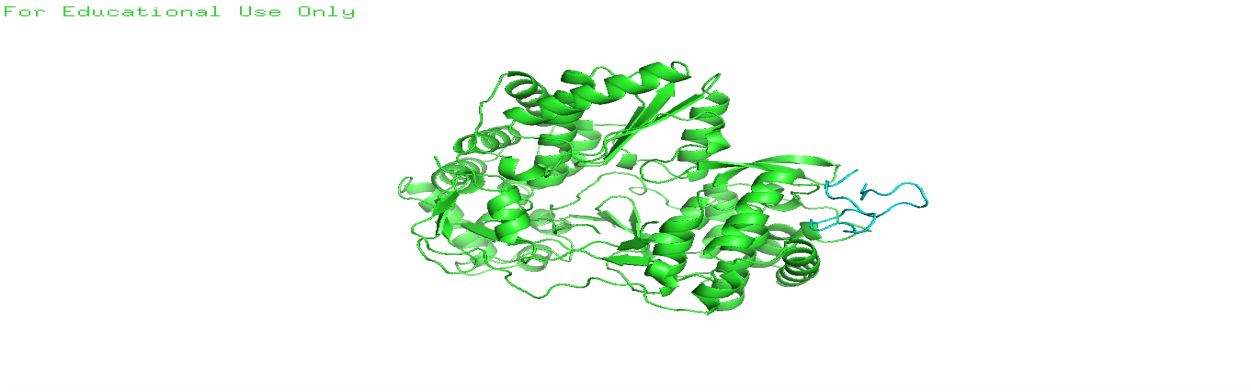

FIG 4.111 3d docking visualization of pathogenic proteins (NS5B CHAIN A) with Hyfl F Pathogenic proteins are presented in green color and cyclotides are shown in blue color

Table 4.68 Hyfl F docking score with NS5B chain A

CYCLOTIDE	CLUSTER	MEMBERS	REPRESENTATIVE	WEIGHTED SCORE
HYFL F	0	287	Center	-684.3
			Lowest Energy	-873.3

HYFL I

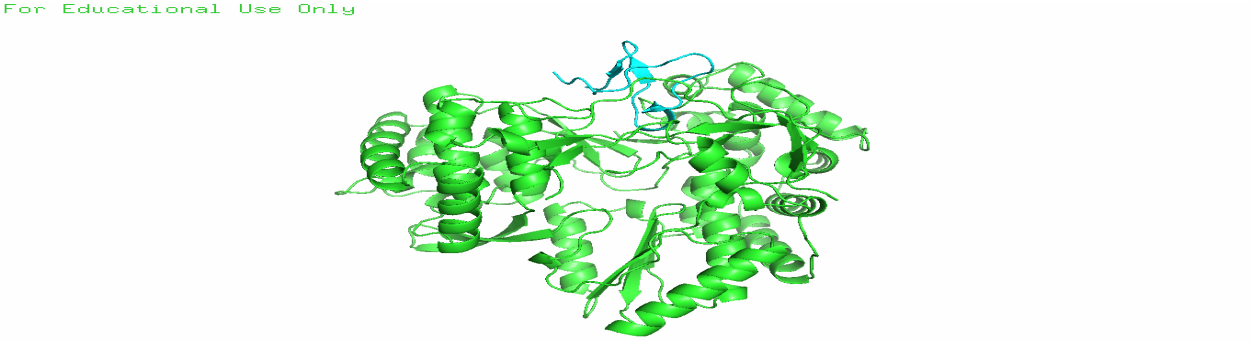

FIG 4.112 3d docking visualization of pathogenic proteins (NS5B CHAIN A) with Hyfl I Pathogenic proteins are presented in green color and cyclotides are shown in blue color

Table 469 Hyfl I docking score with NS5B chain A

CYCLOTIDE	CLUSTER	MEMBERS	REPRESENTATIVE	W EIGHTED SCORE
HYFL I	0	295	Center	-684.6
			Lowest Energy	-849.9

HYFL K

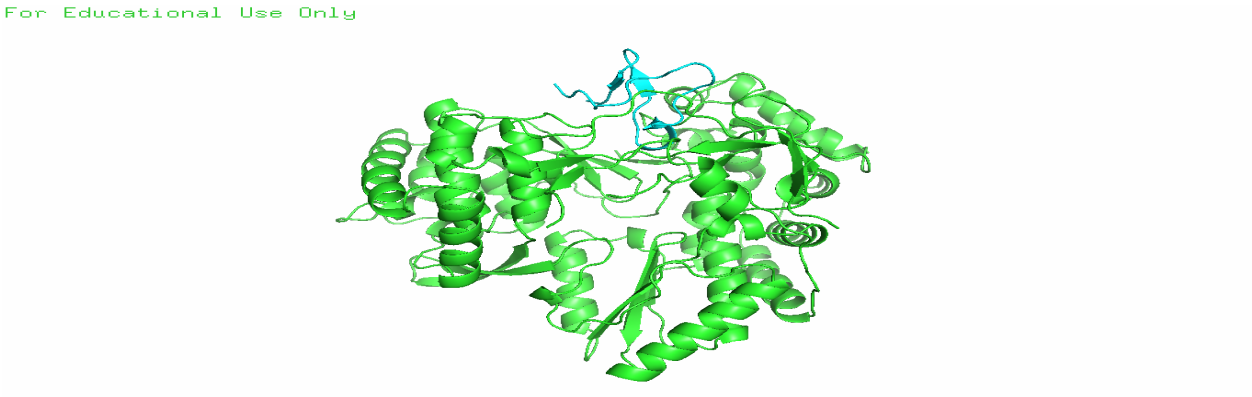

FIG 4.113 3d docking visualization of pathogenic proteins (NS5B CHAIN A) with Hyfl K Pathogenic proteins are presented in green color and cyclotides are shown in blue color

Table 4.70 Hyfl K docking score with NS5B chain A

CYCLOTIDE	CLUSTER	MEMBERS	REPRESENTATIVE	WEIGHTED SCORE
HYFL K	0	333	Center	-740.1
			Lowest Energy	-851.8

HYFL L

FIG 4.114 3d docking visualization of pathogenic proteins (NS5B CHAIN A) with Hyfl L Pathogenic proteins are presented in green color and cyclotides are shown in golden color

Table 4.71 Hyfl L docking score with NS5B chain A

CYCLOTIDE	CLUSTER	MEMBERS	REPRESENTATIVE	WEIGHTED SCORE
HYFL L	0	224	Center	-711.5
			Lowest Energy	-936.3

KALATA B 9

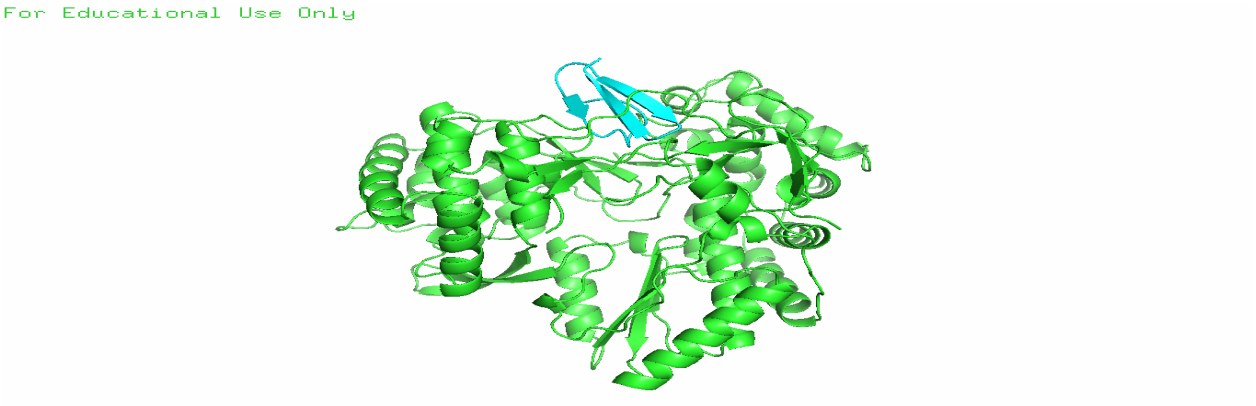

FIG 4.115 3d docking visualization of pathogenic proteins (NS5B CHAIN A) with Kalata B9 Pathogenic proteins are presented in green color and cyclotides are shown in blue color

Table 4.72 Kalata B9 docking score with NS5B chain A

CYCLOTIDE	CLUSTER	MEMBERS	REPRESENTATIVE	WEIGHTED SCORE
KALATA B9	0	214	Center	-651.3
			Lowest Energy	-988.6

KALATA B10

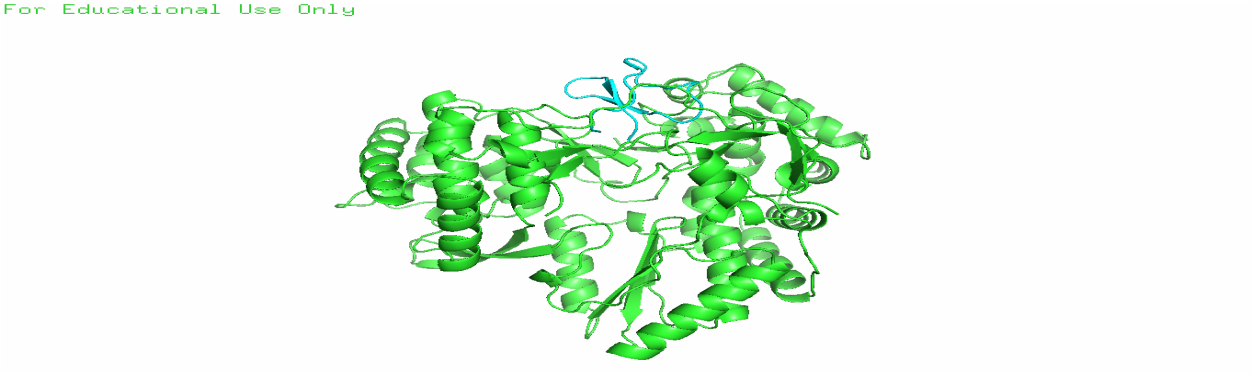

FIG 4.116 3d docking visualization of pathogenic proteins (NS5B CHAIN A) with Kalata B10 Pathogenic proteins are presented in green color and cyclotides are shown in golden color

Table 4.73 Kalata B10 docking score with NS5B chain A

CYCLOTIDE	CLUSTER	MEMBERS	REPRESENTATIVE	WEIGHTED SCORE
KALATA B10	0	178	Center	-726.7
			Lowest Energy	-864.2

KALATA B13

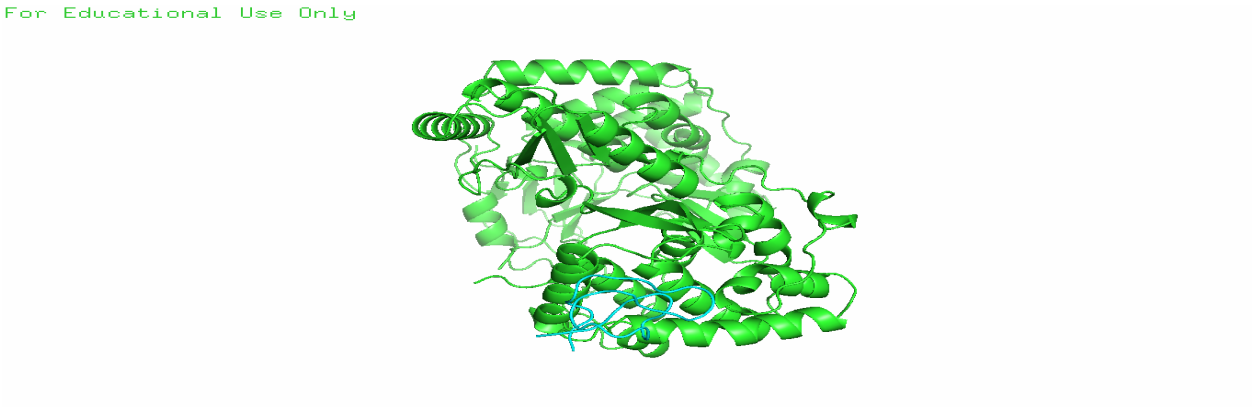

FIG 4.117 3d docking visualization of pathogenic proteins (NS5B CHAIN A) with Kalata B13
Pathogenic proteins are presented in green color and cyclotides are shown in blue color

Table 4.74 Kalata B13 docking score with NS5B chain A

CYCLOTIDE	CLUSTER	MEMBERS	REPRESENTATIVE	WEIGHTED SCORE
KALATA B13	0	320	Center	-677.4
			Lowest Energy	-811.4

KALATA B14

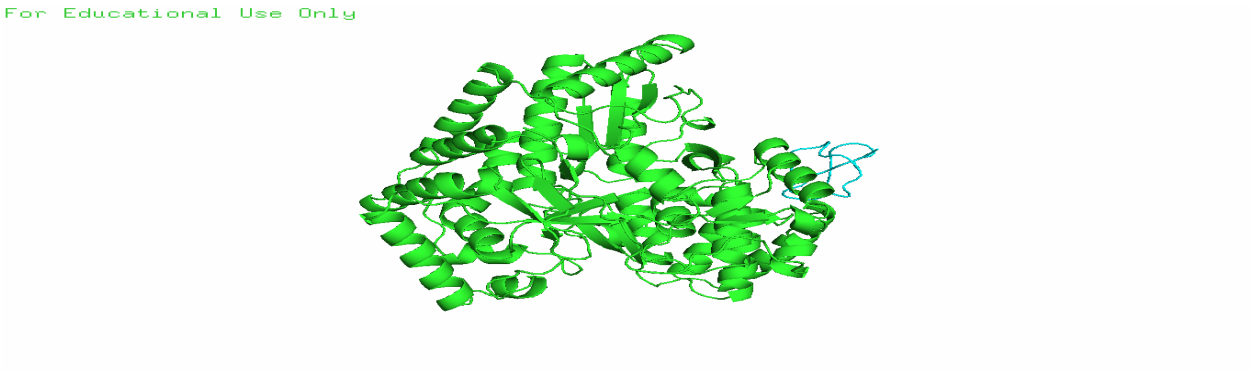

FIG 4.118 3d docking visualization of pathogenic proteins (NS5B CHAIN A) with Kalata B14
Pathogenic proteins are presented in green color and cyclotides are shown in blue color

Table 4.75 Kalata B14 docking score with NS5B chain A

CYCLOTIDE	CLUSTER	MEMBERS	REPRESENTATIVE	WEIGHTED SCORE
KALATA B14	0	331	Center	-674.5
			Lowest Energy	-787.7

KALATA B16

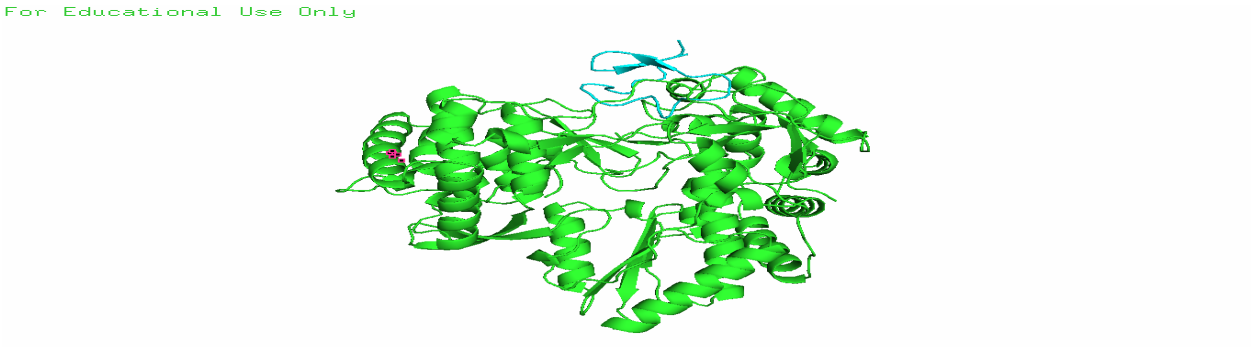

FIG 4.119 3d docking visualization of pathogenic proteins (NS5B CHAIN A) with Kalata B116
Pathogenic proteins are presented in green color and cyclotides are shown in blue color

Table 4.76 Kalata B16 docking score with NS5B chain A

CYCLOTIDE	CLUSTER	MEMBERS	REPRESENTATIVE	WIGHTED SCORE
KALATA B16	0	399	Center	-945.1
			Lowest Energy	-954.2

KALATA B17

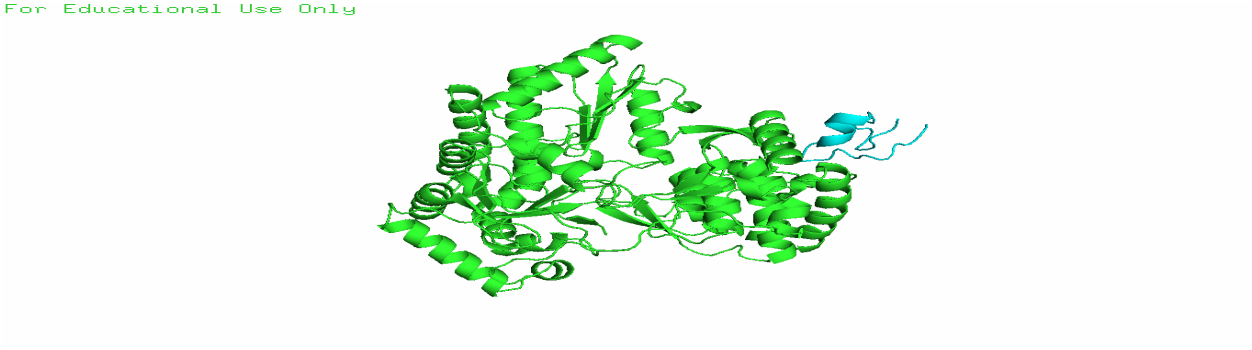

FIG 4.120 3d docking visualization of pathogenic proteins (NS5B CHAIN A) with Kalata B17
Pathogenic proteins are presented in green color and cyclotides are shown in blue color

Table 4.77 Kalata B17 docking score with NS5B chain A

CYCLOTIDE	CLUSTER	MEMBERS	REPRESENTATIVE	WEIGHTED SCORE
KALATA B17	0	190	Center	-738.4
			Lowest Energy	-829.1

KALATA B18

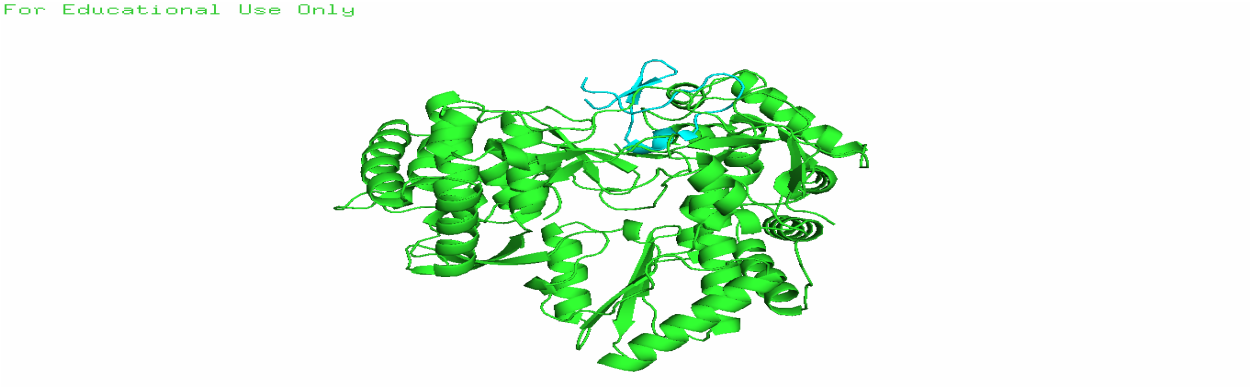

FIG 4.121 3d docking visualization of pathogenic proteins (NS5B CHAIN A) with Kalata B18 Pathogenic proteins are presented in green color and cyclotides are shown in blue color

Table 4.78 Kalata B18 docking score with NS5B chain A

CYCLOTIDE	CLUSTER	MEMBERS	REPRESENTATIVE	WEIGHTED SCORE
KALATA B18	0	299	Center	-739.3
			Lowest Energy	-957.8

PHYB A

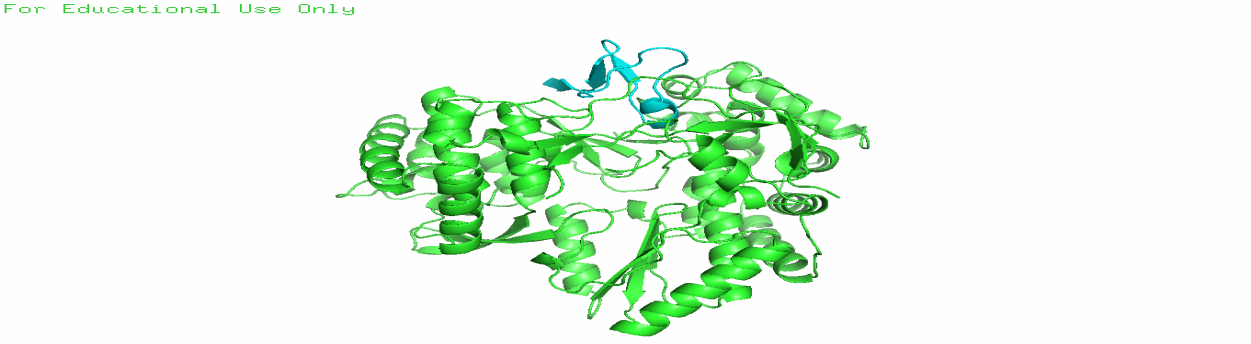

FIG 4.122 3d docking visualization of pathogenic proteins (NS5B CHAIN A) with Phyb A Pathogenic proteins are presented in green color and cyclotides are shown in blue color

Table 4.79 Phyb A docking score with NS5B chain A

CYCLOTIDE	CLUSTER	MEMBERS	REPRESENTATIVE	WEIGHTED SCORE
PHYB A	0	209	Center	-744.5
			Lowest Energy	-826.7

PHYB B

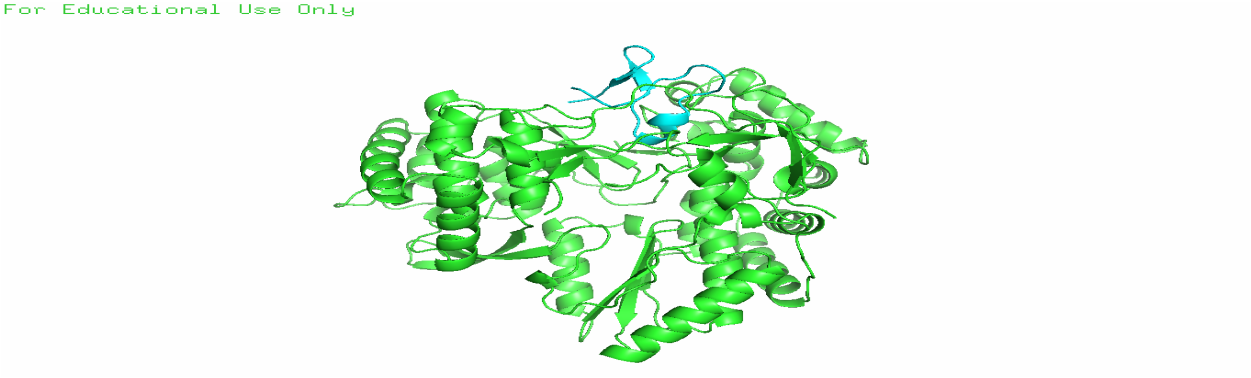

FIG 4.123 3d docking visualization of pathogenic proteins (NS5B CHAIN A) with Phyb B Pathogenic proteins are presented in green color and cyclotides are shown in blue color

Table 4.80 Phyb B docking score with NS5B chain A

CYCLOTIDE	CLUSTER	MEMBERS	REPRESENTATIVE	WEIGHTED SCORE
PHYB B	0	253	Center	-779.4
			Lowest Energy	-1011.2

PHYB C

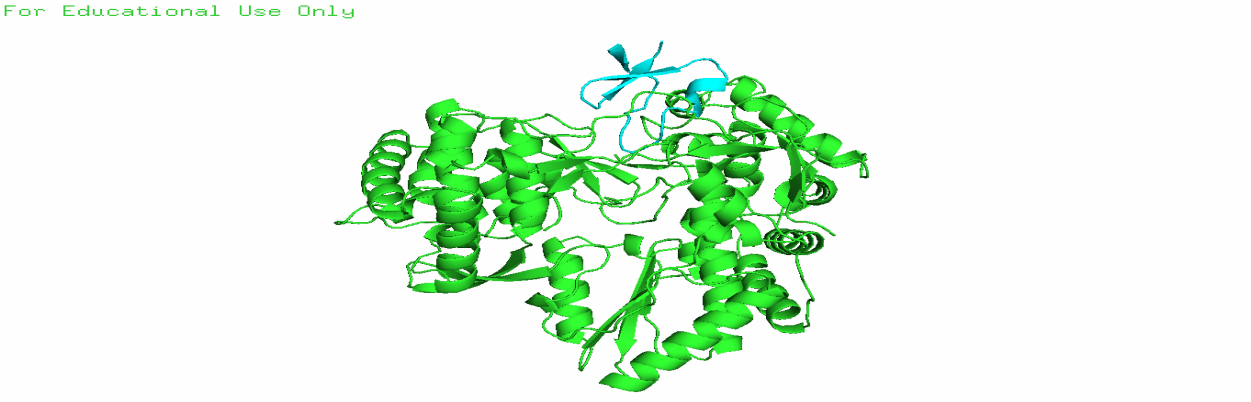

FIG 4.124 3d docking visualization of pathogenic proteins (NS5B CHAIN A) with Phyb C Pathogenic proteins are presented in green color and cyclotides are shown in blue color

Table 4.81 Phyb C docking score with NS5B chain A

CYCLOTIDE	CLUSTER	MEMBERS	REPRESENTATIVE	WEIGHTED SCORE
PHYB C	0	194	Center	-728.7
			Lowest Energy	-903.8

PHYB D

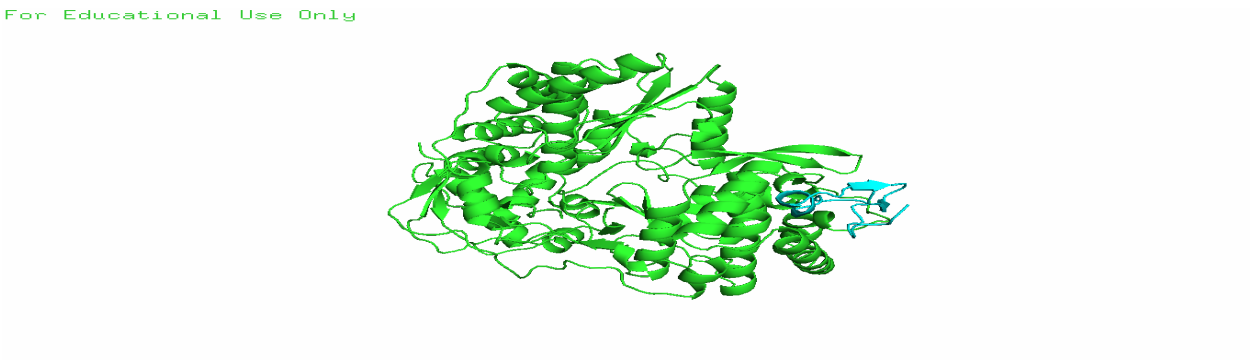

FIG 4.125 3d docking visualization of pathogenic proteins (NS5B CHAIN A) with Phyb D Pathogenic proteins are presented in green color and cyclotides are shown in blue color

Table 4.82 Phyb D docking score with NS5B chain A

CYCLOTIDE	CLUSTER	MEMBERS	REPRESENTATIVE	WEIGHTED SCORE
PHYB D	0	208	Center	-717.9
			Lowest Energy	-815.9

PHYB E

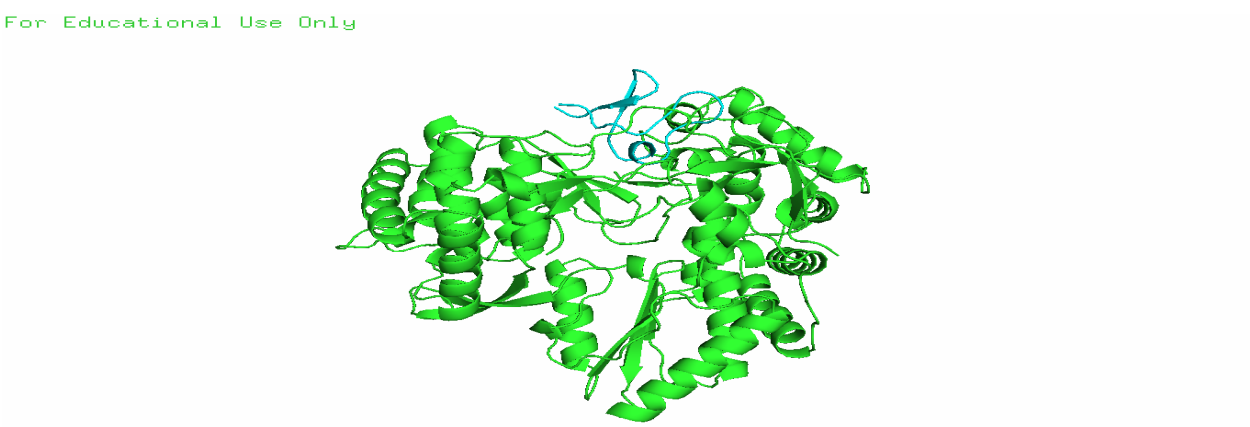

FIG 4.126 3d docking visualization of pathogenic proteins (NS5B CHAIN A) with Phyb E Pathogenic proteins are presented in green color and cyclotides are shown in blue color

Table 4.83 Phyb E docking score with NS5B chain A

CYCLOTIDE	CLUSTER	MEMBERS	REPRESENTATIVE	WEIGHTED SCORE
PHYB E	0	285	Center	-842.2
			Lowest Energy	-990.2

PHYB F

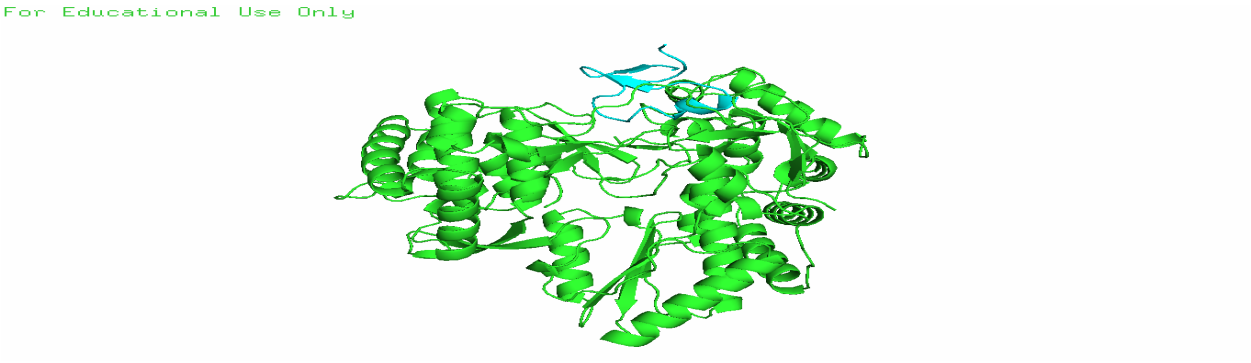

FIG 4.127 3d docking visualization of pathogenic proteins (NS5B CHAIN A) with Phyb F Pathogenic proteins are presented in green color and cyclotides are shown in blue color

Table 4.84 Phyb F docking score with NS5B chain A

CYCLOTIDE	CLUSTER	MEMBERS	REPRESENTATIVE	WEIGHTED SCORE
PHYB F	0	261	Center	-764.4
			Lowest Energy	-995.7

PHYB G

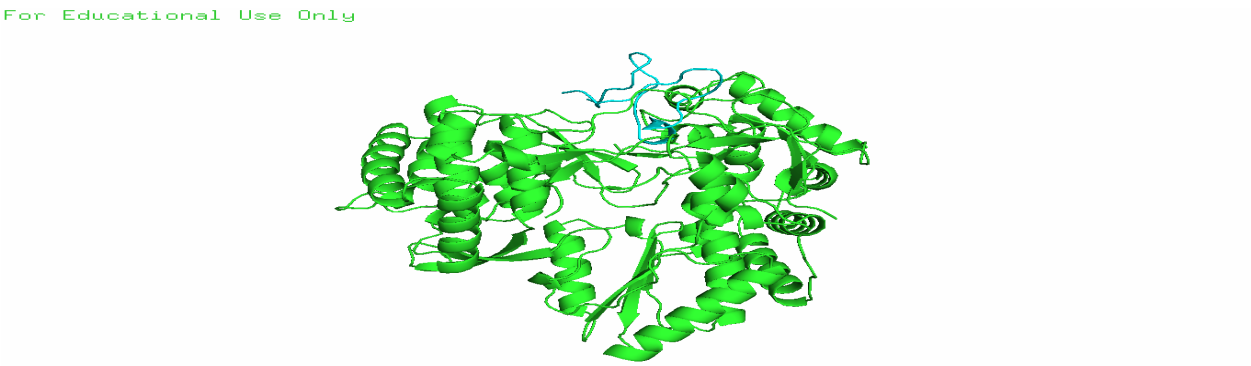

FIG 4.128 3d docking visualization of pathogenic proteins (NS5B CHAIN A) with Phyb G Pathogenic proteins are presented in green color and cyclotides are shown in blue color

Table 4.85 Phyb G docking score with NS5B chain A

CYCLOTIDE	CLUSTER	MEMBERS	REPRESENTATIVE	WEIGHTED SCORE
PHYB G	0	231	Center	-777.2
			Lowest Energy	-901.1

PHYB H

FIG 4.129 3d docking visualization of pathogenic proteins (NS5B CHAIN A) with Phyb H Pathogenic proteins are presented in green color and cyclotides are shown in blue color

Table 4.86 Phyb H docking score with NS5B chain A

CYCLOTIDE	CLUSTER	MEMBERS	REPRESENTATIVE	WEIGHTED SCORE
PHYB H	0	240	Center	-656.3
			Lowest Energy	-760.8

PHYB I

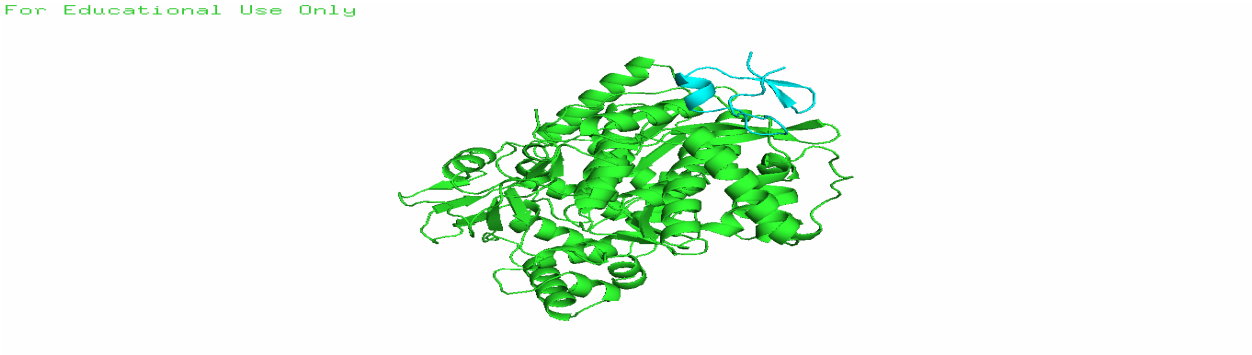

FIG 4.130 3d docking visualization of pathogenic proteins (NS5B CHAIN A) with Phyb I Pathogenic proteins are presented in green color and cyclotides are shown in blue color

Table 4.87 Phyb I docking score with NS5B chain A

CYCLOTIDE	CLUSTER	MEMBERS	REPRESENTATIVE	WEIGHTED SCORE
PHYB I	0	175	Center	-713.6
			Lowest Energy	-754.5

PHYB J

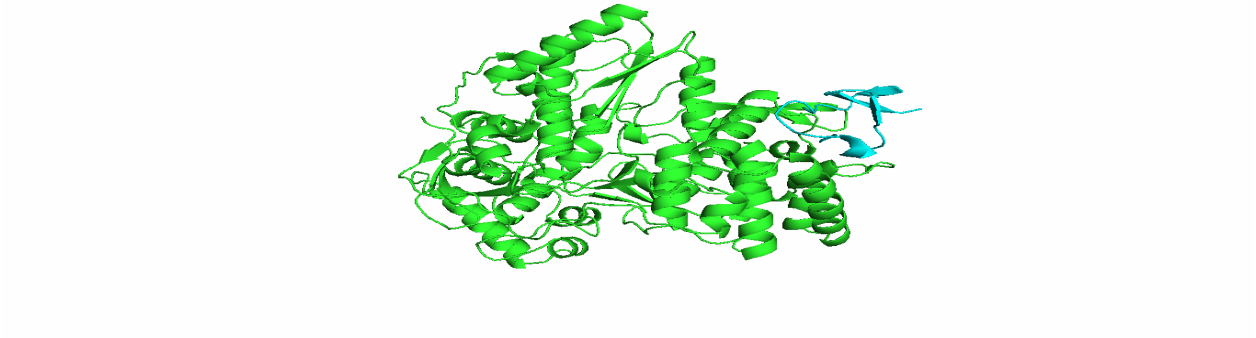

FIG 4.131 3d docking visualization of pathogenic proteins (NS5B CHAIN A) with Phyb J Pathogenic proteins are presented in green color and cyclotides are shown in blue color

Table 4.88 Phyb J docking score with NS5B chain A

CYCLOTIDE	CLUSTER	MEMBERS	REPRESENTATIVE	WEIGHTED SCORE
PHYB J	0	222	Center	-661.3
			Lowest Energy	-801.9

PHYB L

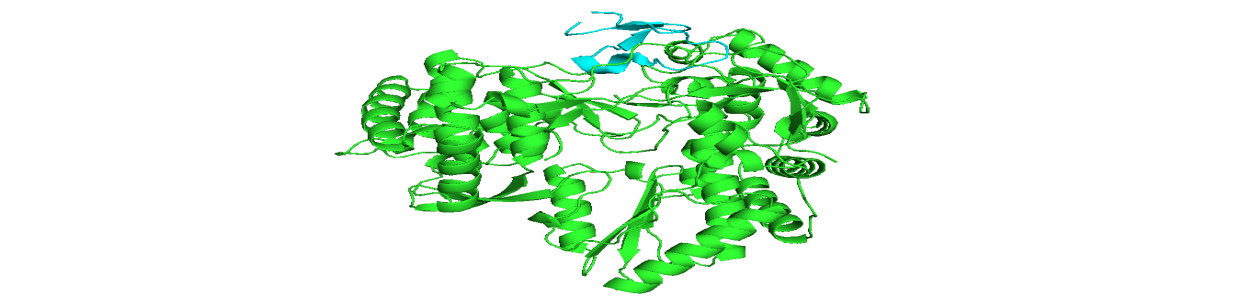

FIG 4.132 3d docking visualization of pathogenic proteins (NS5B CHAIN A) with Phyb L Pathogenic proteins are presented in green color and cyclotides are shown in blue color

Table 4.89 Phyb L docking score with NS5B chain A

CYCLOTIDE	CLUSTER	MEMBERS	REPRESENTATIVE	WEIGHTED SCORE
PHYB L	0	277	Center	-831.5
			Lowest Energy	-1015.7

Vian 3

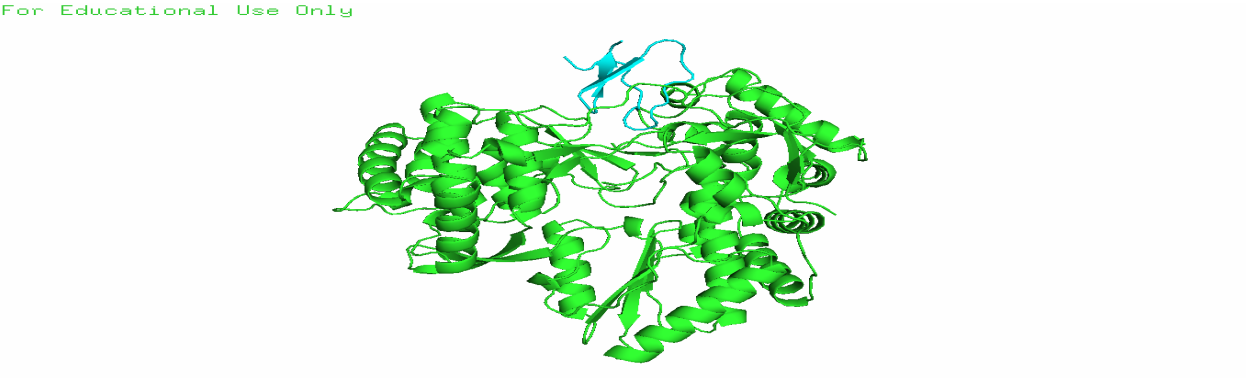

FIG 4.133 3d docking visualization of pathogenic proteins (NS5B CHAIN A) with VIAN 3 Pathogenic proteins are presented in green color and cyclotides are shown in blue color

Table 4.90 VIAN 3 docking score with NS5B chain A

CYCLOTIDE	CLUSTER	MEMBERS	REPRESENTATIVE	WEIGHTED SCORE
VIAN 3	0	418	Center	-668.8
			Lowest Energy	-865.7

Vian 5

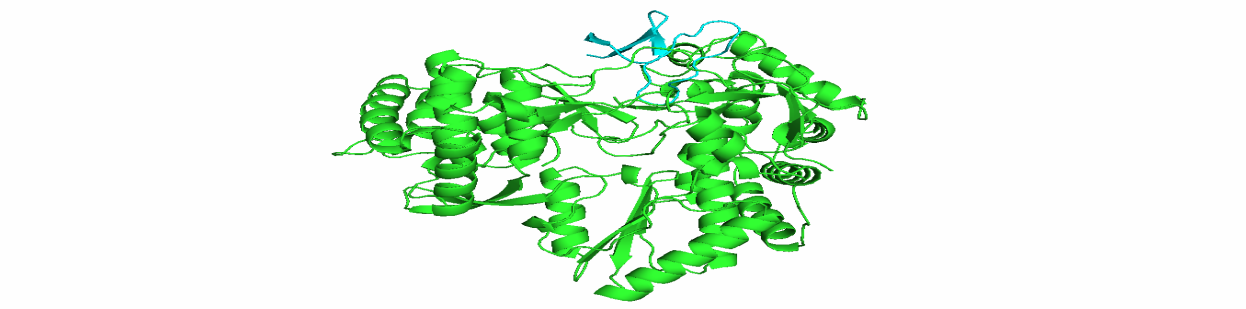

FIG 4.134 3d docking visualization of pathogenic proteins (NS5B CHAIN A) with VIAN 5 Pathogenic proteins are presented in green color and cyclotides are shown in blue color

Table 4.91 VIAN 5 docking score with NS5B chain A

CYCLOTIDE	CLUSTER	MEMBERS	REPRESENTATIVE	WEIGHTED SCORE
VIAN 5	0	244	Center	-713.5
			Lowest Energy	-956.4

Vian 6

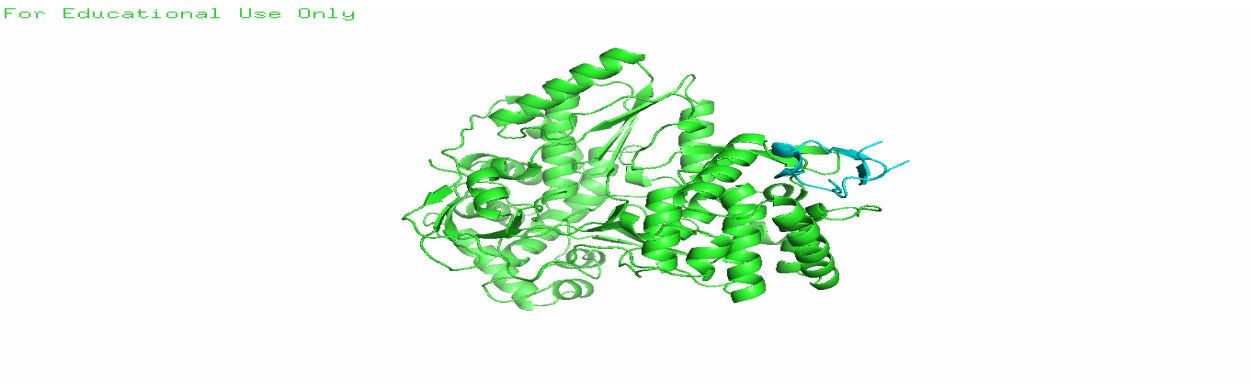

FIG 4.135 3d docking visualization of pathogenic proteins (NS5B CHAIN A) with VIAN 6 Pathogenic proteins are presented in green color and cyclotides are shown in blue color

Table 4.92 VIAN 6 docking score with NS5B chain A

CYCLOTIDE	CLUSTER	MEMBERS	REPRESENTATIVE	WEIGHTED SCORE
VIAN 6	0	273	Center	-749.8
			Lowest Energy	-798.6

Vian 7

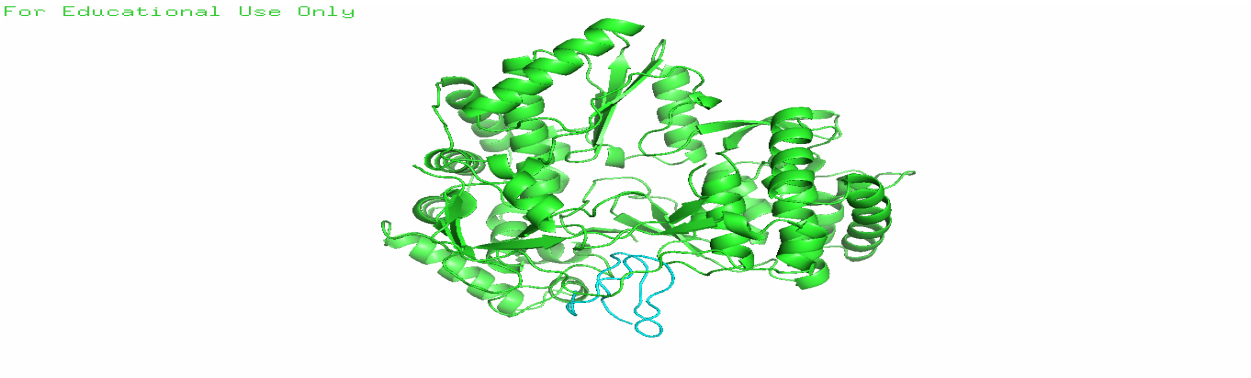

FIG 4.136 3d docking visualization of pathogenic proteins (NS5B CHAIN A) with VIAN 7 Pathogenic proteins are presented in green color and cyclotides are shown in blue color

Table 4.93VIAN 7docking score with NS5B chain A

CYCLOTIDE	CLUSTER	MEMBERS	REPRESENTATIVE	WEIGHTED SCORE
VIAN 7	0	345	Center	-802.6
			Lowest Energy	-999.9

Vian 9

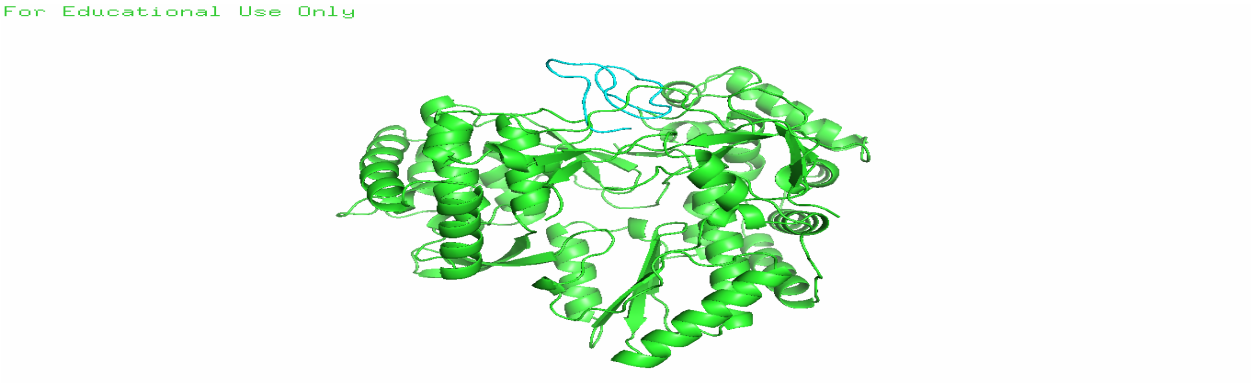

FIG 4.137 3d docking visualization of pathogenic proteins (NS5B CHAIN A) with VIAN 9 Pathogenic proteins are presented in green color and cyclotides are shown in blue color

Table 4.94 VIAN 9 docking score with NS5B chain A

CYCLOTIDE	CLUSTER	MEMBERS	REPRESENTATIVE	WEIGHTED SCORE
VIAN 9	0	213	Center	-587.4
			Lowest Energy	-758.7

Vian 10

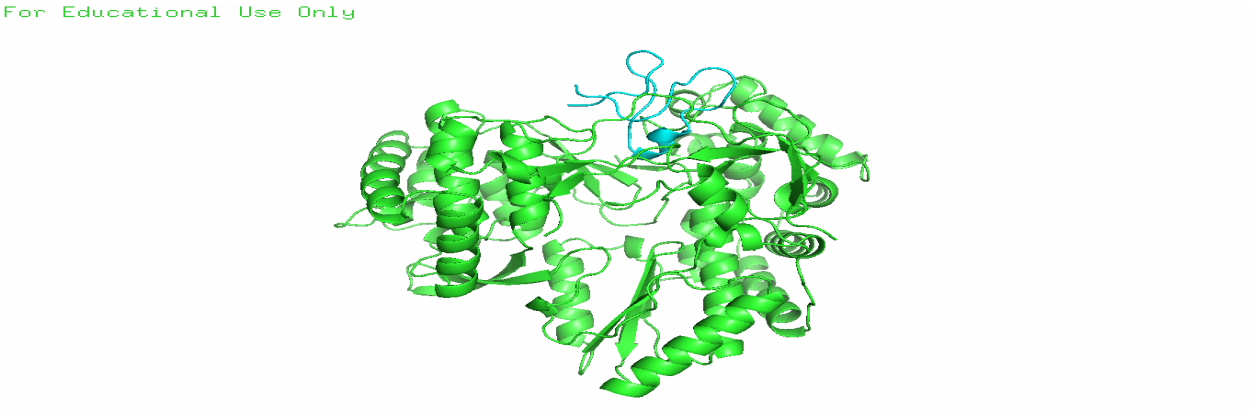

FIG 4.138 3d docking visualization of pathogenic proteins (NS5B CHAIN A) with VIAN 10 Pathogenic proteins are presented in green color and cyclotides are shown in blue color

Table 4.95 VIAN 10 docking score with NS5B chain A

CYCLOTIDE	CLUSTER	MEMBERS	REPRESENTATIVE	WEIGHTED SCORE
			Center	-751.0

VIAN 10	0	296	Lowest Energy	-929.6

Vian 11

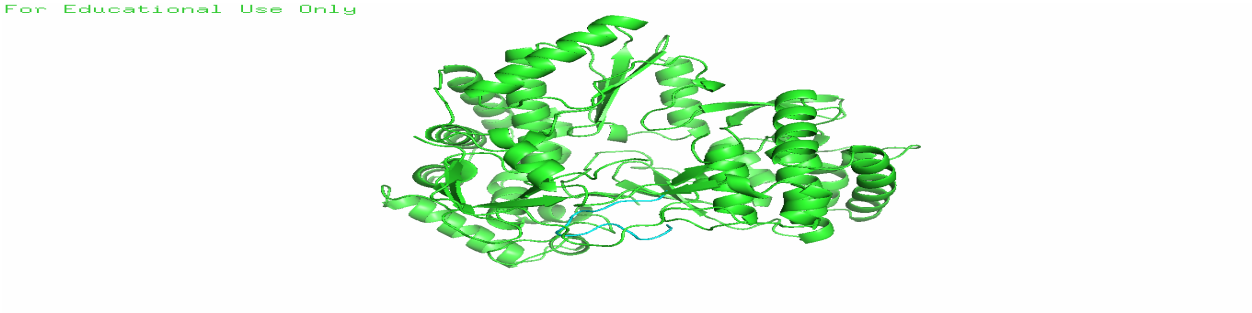

FIG 4.139 3d docking visualization of pathogenic proteins (NS5B CHAIN A) with VIAN 11 Pathogenic protein are presented in green color and cyclotides are shown in blue color

Table 4.96 VIAN 11 docking score with NS5B chain A

CYCLOTIDE	CLUSTER	MEMBERS	REPRESENTATIVE	WEIGHTED SCORE
VIAN 11	0	216	Center	-789.5
			Lowest Energy	-953.9

4.8. TOP LOWEST ENERGY PROTEIN-PROTEIN DOCKING COMPLEX SELECTION BEFORE MD SIMULATION

The complexes presented in Table were chosen as the best because they represent the complexes with the minimum binding energy among all the complexes yielded by docking calculations. Chain a of NS5A showed the lowest energy when interacting with Phyb L, and chain A of NS5B, when interacting with Circular E, showed the lowest binding energy. Figure 2A illustrated 3D docking visualization of Chain a of NS5A+Phyb L, and Figure 2B presents 3D docking visualization of Chain A of NS5B+Circulin E. Figure 3 shows the interaction analysis by DIMPLOT in Ligplus. Figure 4 shows the 2D & 3D structure of selected cyclotides Phyb L and Circulin E. Table 4 presents mutation, toxicity & allergenicity prediction of Phyb L and Circulin E and Table 5 presents their physiochemical properties.

Table 4.97: Docking score of top cyclotides.

Docking score of top cyclotides selected as drug candidate.

Pathogenic Protein	Cyclotide	Representative	Weighted Score
NS5A	Phyb L	Center	-747.5
		Lowest Energy	-1037.8
NS5B	Circulin E	Center	-734.1
		Lowest Energy	-1059.7

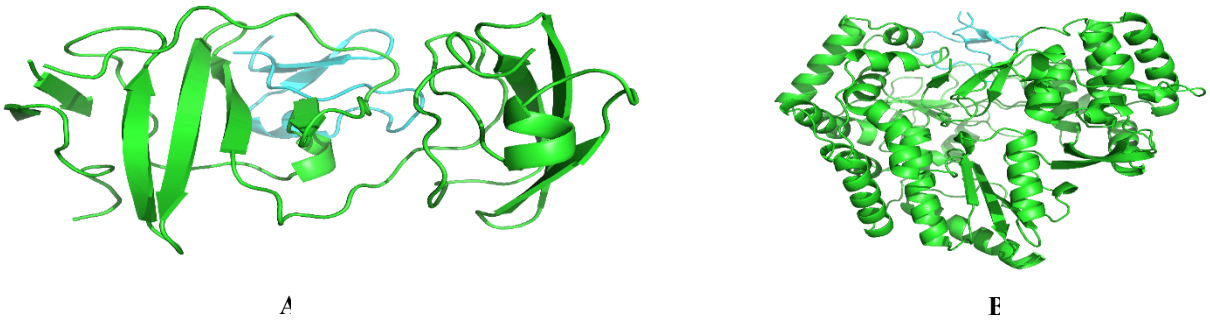

Fig 4.140: 3D docking visualization of pathogenic proteins with top cyclotides. Pathogenic proteins are presented in green color and cyclotides are shown in blue color. **(A):** 3D docking visualization of Chain A of NS5A+Phyb L, and **(B)** 3D docking visualization of Chain A of NS5B+Circulin E

4.9. ACTIVE SITE INTERACTION ANALYSIS

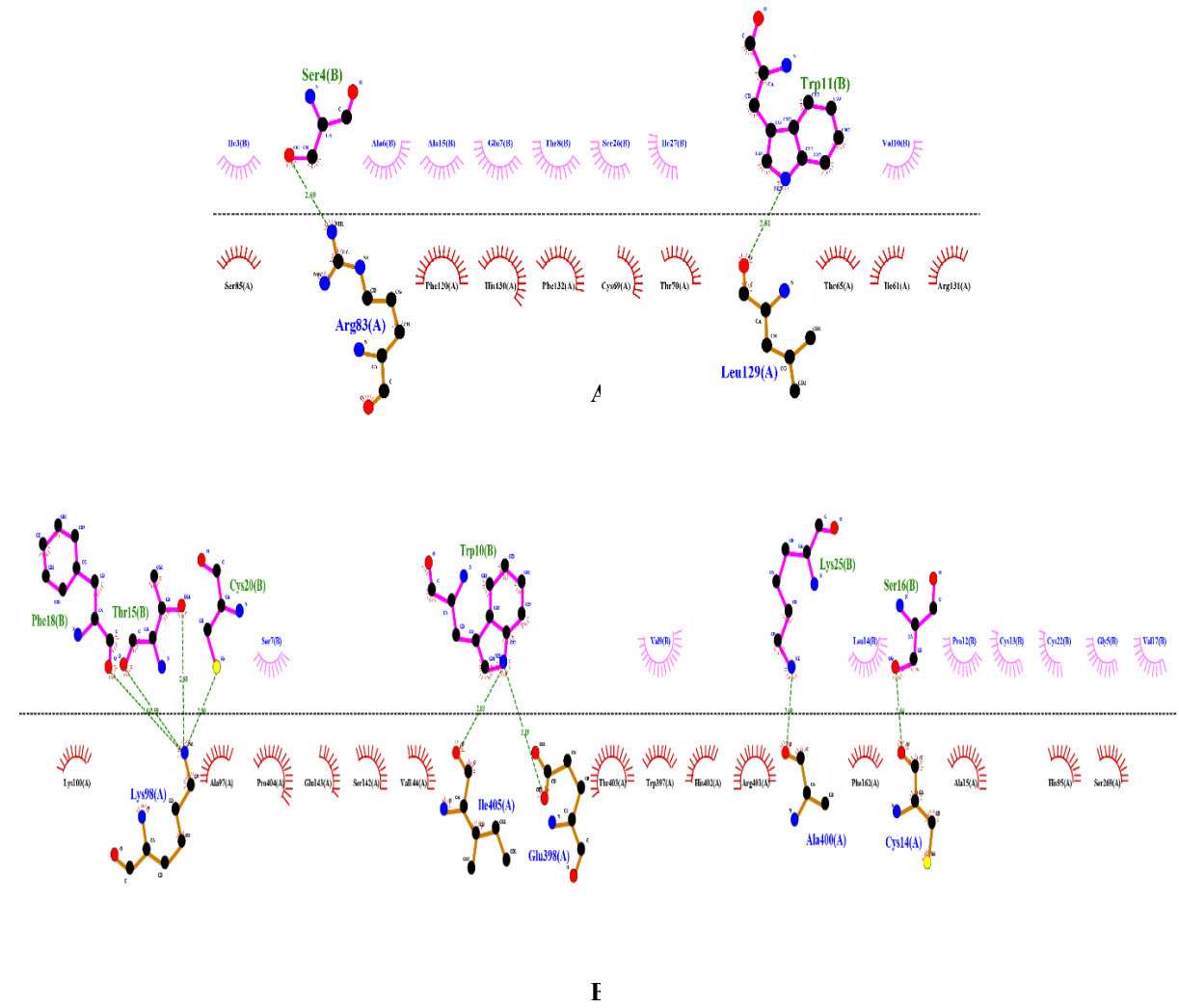

Figure 4.141: Figure shows the interaction analysis by DIMPLOT in Ligplus. **(A):** The green color lines represent hydrogen bonds with bond length, which denote the areas of ligand (Phyb L) contact with the proteins' (NS5A) residues, including Arg83(A) and Leu129(A), and **(B):** The green color lines represent hydrogen bonds with bond length, which denote the areas of ligand (Circulin E) contact with the proteins' (NS5B) residues, including Lys98(A), Ile405(A), Glu398(A), Ala400(A), and Cys14(A).These bonds are useful for adding extra stability to the ligand in its binding pocket.

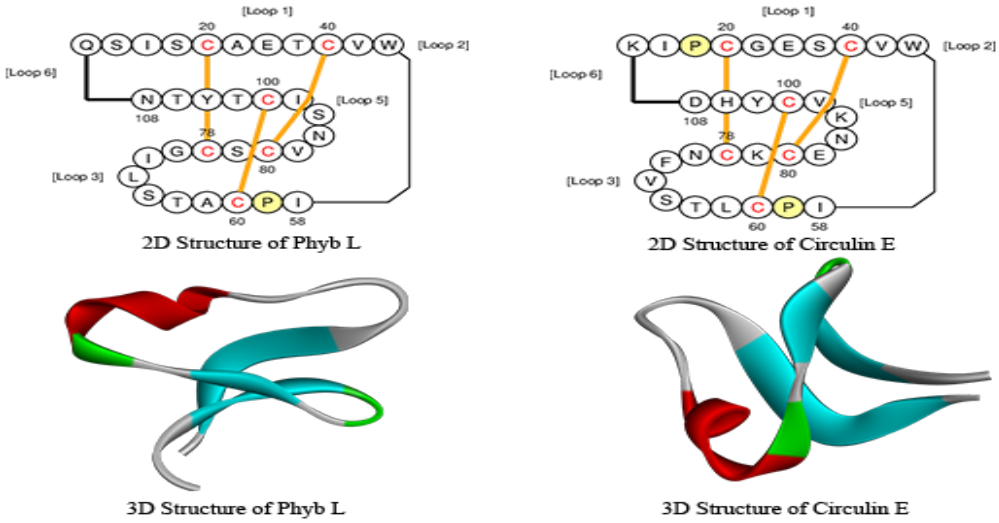

Figure 4142. 2D & 3D structure of selected cyclotides Phyb L and Circulin E

Table 4.98 Mutation, toxicity, and allergenicity of Phyb L and Circulin E

Status of mutation, toxicity, and allergenicity of Phyb L and Circulin E				
Peptide	**Mutation Position**	**SVM Score**	**Toxicity**	**Allergenicity**
Phyb L	No Mutation	-0.63	Non-Toxin	Non-Allergen
Circulin E	No Mutation	-0.99	Non-Toxin	Non-Allergen

Table 4.99. Physiochemical Properties of Phyb L and Circulin E

Physiochemical Properties of Top Cyclotides Based on Docking Score			
	Properties	**Values (Phyb L)**	**Values (Circulin E)**
Atomic and Amino-Acid Composition	Number of Amino Acids	32	30
	Total Number of Atoms	454	463
	Formula	C_{140} H_{224} N_{36} O_{48} S_6	C_{148} H_{228} N_{38} O_{43} S_6
	Molecular Weight	3371.89	3420.03
State of Charge on Residues	Negatively Charged Residues (Asp + Glu)	1	3
	Positively Charged Residues (Arg + Lys)	0	3
Extinction Coefficients (M^{-1} cm^{-1} at 280 nm) Measured in Water	Assuming all pairs of Cys residues form cystines,	Ext. Coefficient: 7365 Abs 0.1% (=1 g/1): 2.184	Ext. Coefficient: 7365 Abs 0.1% (=1 g/1): 2.153
	Assuming all Cys residues are reduced	Ext. Coefficient: 6990 Abs 0.1% (=1 g/1): 2.073	Ext. Coefficient: 6990 Abs 0.1% (=1 g/1): 2.044
Estimated Half-Life	Mammalian reticulocytes, In-Vitro	0.8 hours	1.3 hours
	Yeast, In-Vivo	10 minutes	3 minutes
	Escherichia coli, In-Vivo	10 hours	3 minutes
Protein Stability Indices	Aliphatic Index	85.31	68.0
	Instability Index	38.66 (Stable Protein)	26.79 (Stable Protein)
Protein Hydrophobicity & Isoelectric Parameters	GRAVY (Grand Average of Hydropathicity)	0.744	0.090
	Theoretical pI	4.00	6.71

4.10. MOLECULAR DYNAMIC SIMULATION

4.10.1. NS5A-PHYL B COMPLEX MOLECULAR DYNAMIC SIMULATION

The RMSD analysis in Figure 4.143 A shows that the ligand and the receptor undergo conformational changes before they become stable. The receptor is comparatively more stable, with an average RMSD of around 2Å. At the same time, the ligand is relatively flexible, with an average RMSD of about 3Å and fluctuating towards the end of the simulation. The RMSF graph in Figure 4.143 B shows high flexibility at the N-terminus (up to 6 Å) and C-terminus of the receptor, with the core region being more stable (below 2Å). The ligand exhibits significant flexibility in its initial residues (0-30, peaking at 3-4Å), stabilizing afterwards. These observations indicate dynamic initial interactions with eventual stabilization in the binding site. Figure 4.143 C presents the radius of gyration (Rg) analysis, reveals that the ligand first increases from 8.2 Å to about 8.75 Å, stabilizing between 8.5 Å and 9.0 Å with some fluctuations, with mild variations, suggesting adaptability. The receptor's Rg at first oscillates between 16 Å and 20 Å and then settles at around 17 Å. 5 Å, thus ensuring that the structure of the scaffold remains consistent and dense. The hydrogen bond (H-bond) analysis for the protein-peptide complex over the simulation time presented in Figure 4.143 D reveals dynamic interaction patterns. Initially, H-bonds fluctuate between 0 and 3, indicating variable interactions during the first 20,000 ps. As the simulation progresses, from 20,000 to 60,000 ps, the number of H-bonds increases and becomes more stable, fluctuating between 1 and 5. Notably, after 60,000 ps, the H-bond count increases, frequently reaching 6 to 8, suggesting a more stable and robust binding interaction between the protein and peptide. Figure 4.144 illustrates Principal Component Analysis (PCA) and Dynamic Cross-Correlation Matrix (DCCM) in Protein Structure Dynamics.

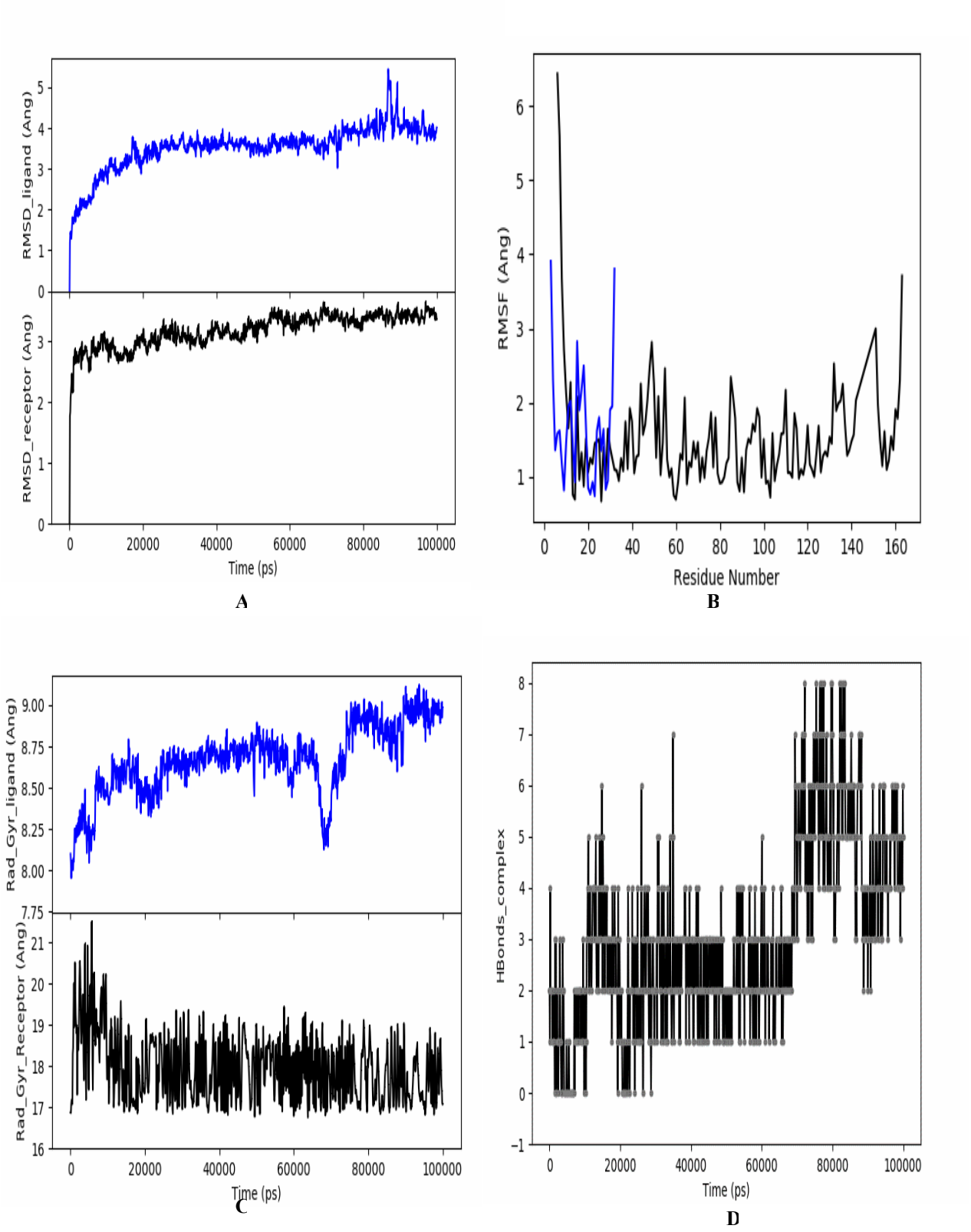

Fig 4.143: Molecular Dynamic Simulations Results of NS5A-Phyb L complex. **(A):** RMSD Values of Complex, **(B)**: RMSF Values of Complex, **(C):** Radius of Gyration of MD Simulation Complex, and, **(D):** H-bonds complex of MD Simulation.

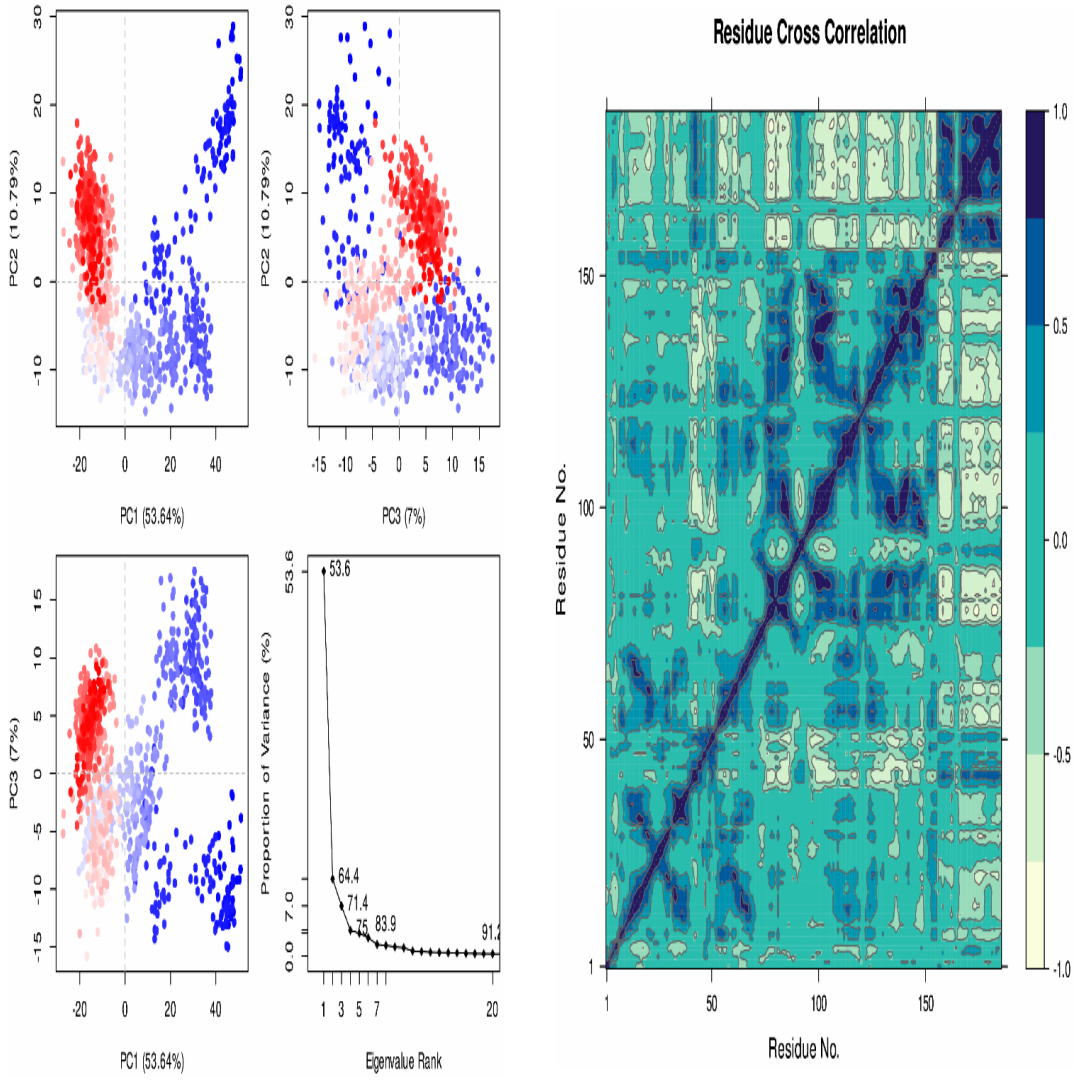

Figure 4.144: (A): The first three panels show the clustering of data points along PC1 vs PC2 (53.64% vs 10.79% variance explained), PC2 vs PC3 (10.79% vs 7% variance explained), and PC1 vs PC3 (53.64% vs 7% variance explained), respectively, illustrating the separation of distinct conformations. The fourth panel displays the scree plot, showing the proportion of variance explained by each principal component, with the first few components capturing the most significant variation. The first principal component (PC1) explains 53.6% of the variance, followed by 10.7% for PC2, 7% for PC3, and progressively lower values for subsequent components, and **(B):** The Dynamic Cross-Correlation Matrix (DCCM) chart shows the correlation of atomic displacement between residues in different parts of the protein structure. The color scale varies from -1 to 1, where blue represents positive correlations, meaning that the motions are correlated; beige represents negative correlations, meaning that the motions are anti-correlated; and green represents near zero correlations, meaning that the motions are uncorrelated. The diagonal corresponds to self-correlations, and the other elements of the matrix correspond to the cross-correlations between different residues.

4.10.2. NS5B-CIRCULIN E COMPLEX MOLECULAR DYNAMIC SIMULATION

The RMSD analysis in Figure 4.145A shows that the ligand and the receptor also need to undergo conformational changes at the beginning and remain stable. The ligand has a higher fluctuation, and the RMSD value reaches a plateau around 3 to 4Å, which shows that the binding pose is quite flexible. The receptor part has reasonable stability, with RMSD fluctuating and having stable structural integrity. The RMSF analysis presented in Figure B reveals that the receptor has high mobility at the N-terminus (up to 4. 5 Å) and at the C-terminus (around 4 Å). In comparison, the middle part of the receptor is more rigid (1-2 Å). The ligand has a relatively high flexibility in the first 40 residues, ranging from 0 to 40 Å, with a peak at around 3 Å, then the flexibility decreases. Figure C shows the radius of gyration of the simulation; for the ligand (top subplot, blue), the Rg oscillates around 8. 4 Å, which is somewhat flexible, and rises steadily to 8.8 Å over the simulation, which indicates a minor expense. For the receptor (bottom subplot, black), the Rg first increases to 23.4 Å and then remains almost constant at 23.0 Å, which is in good agreement with the compact structure with some variations. The hydrogen bond (H-bond) analysis for the protein-peptide complex over the simulation time presented in Figure D defines that at the beginning, the number of H-bonds ranges from 2 to 5, which shows that the interactions are not constant in the first 40,000 ps. From 40,000 to 60,000 ps in the simulation, the number of H-bonds rises, and it is between 4 and 7 more often, which indicates a more stable and more robust binding interaction. At 60,000 ps, the number of H-bonds remains relatively unstable and oscillates between 3 and 7, which indicates that the interaction is still relatively high. This means that the complex becomes more stable and interacts more over time. Figure 4.146 illustrates Principal Component Analysis (PCA) and Dynamic Cross-Correlation Matrix (DCCM) in Protein Structure Dynamics.

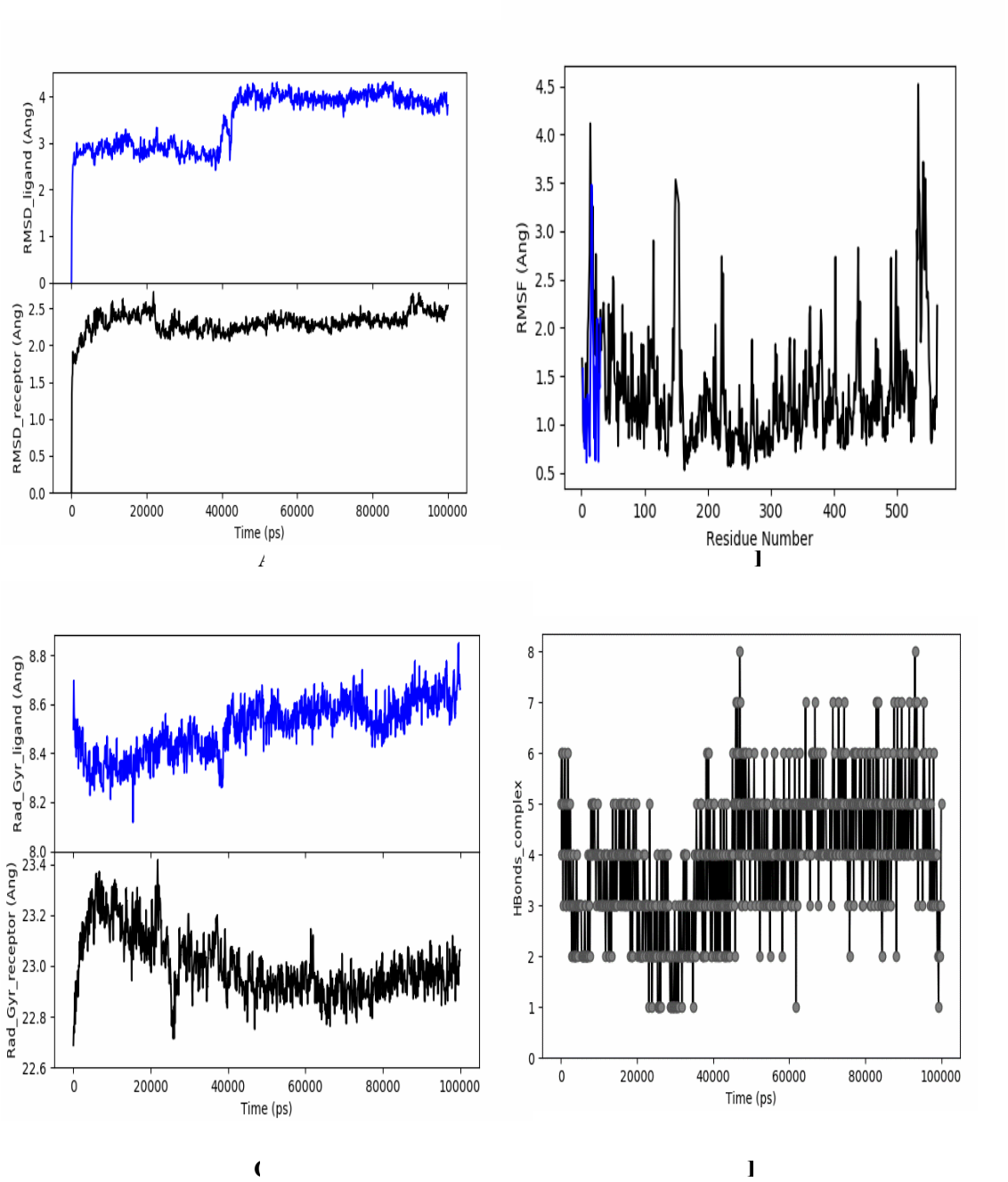

Figure 4.145: Molecular Dynamic Simulations Results of NS5B-Circulin E complex. **(A):** RMSD Values of Complex, **(B)**: RMSF Values of Complex, **(C):** Radius of Gyration of MD Simulation Complex, and, **(D):** H-bonds complex of MD Simulation

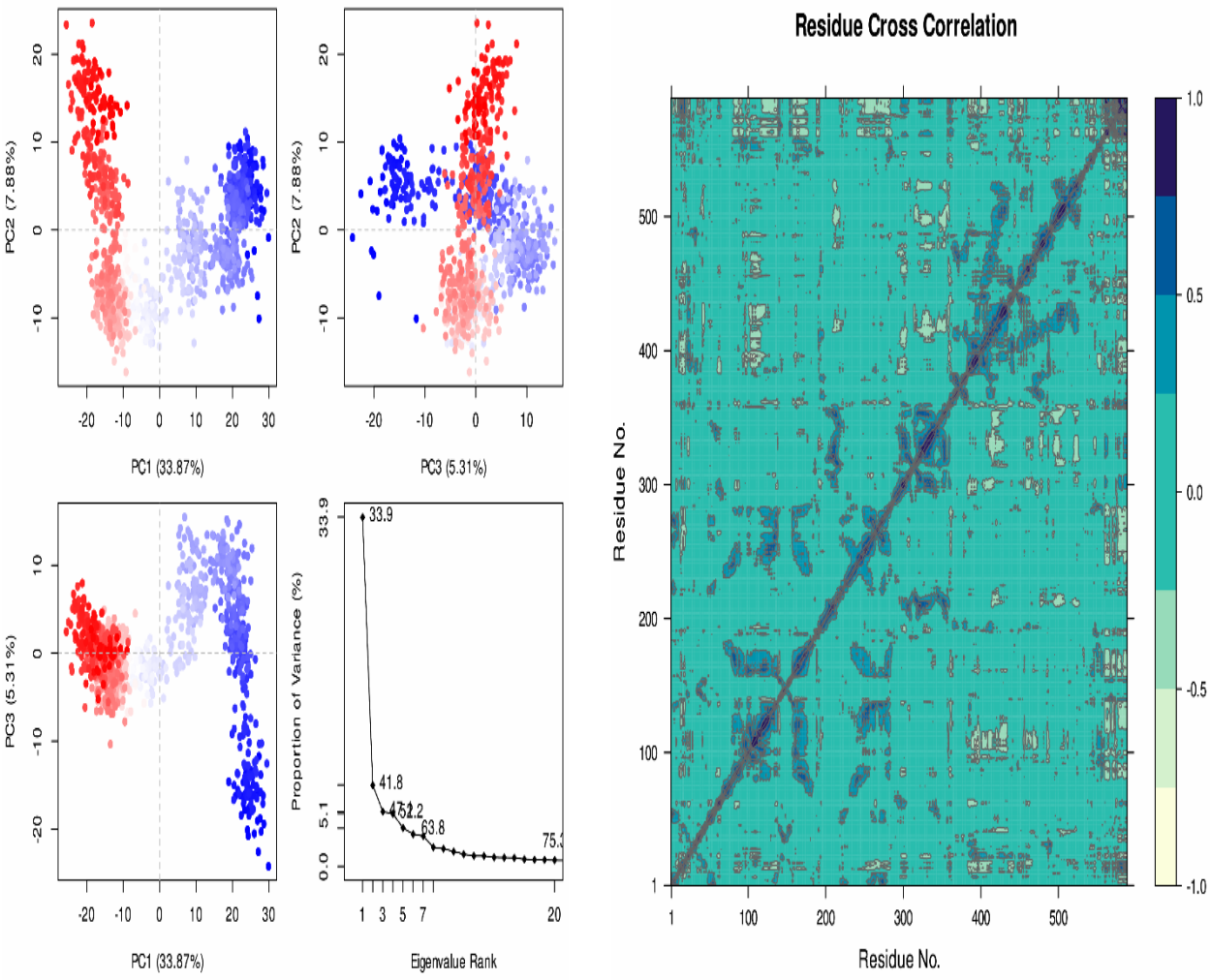

Figure 4.146: (A): The first three panels show the clustering of data points along PC1 vs. PC2 (33.87% vs. 8.78% variance explained), PC2 vs. PC3 (8.78% vs. 5.31% variance explained), and PC1 vs. PC3 (33.87% vs. 5.31% variance explained), respectively, illustrating the separation of distinct conformations. The fourth panel displays the scree plot, showing the proportion of variance explained by each principal component, with the first few components capturing the most significant variation. The first principal component (PC1) explains 33.9% of the variance, followed by 8.2% for PC2, 5.2% for PC3, and progressively lower values for subsequent components, and **(B):** The Dynamic Cross-Correlation Matrix (DCCM) chart shows the correlation of atomic displacement between residues in different parts of the protein structure. The color scale varies from -1 to 1, where blue represents positive correlations, meaning that the motions are correlated; beige represents negative correlations, meaning that the motions are anti-correlated; and green represents near zero correlations, meaning that the motions are uncorrelated. The diagonal corresponds to self-correlations, and the other elements of the matrix correspond to the cross-correlations between different residues.

10.4. MM-GBSA ENERGY CALCULATION RESULTS

The MM-GBSA energy results show the binding free energy (ΔG_{bind}) for two complexes: NS5A-Phyb L (-46.4648) and NS5B-Circulin E (-935.7883). The ΔG_{bind} values are the overall binding enthalpy; negative values depict favorable binding. The individual energy components, including Coulomb, Covalent, Hbond (hydrogen bond), Lipo (lipophilic interactions), Packing, SelfCont (self-contact), Solv-GB (solvation), and vdW (van der Waals interactions), give information about the individual contribution of the energy components for each ligand. These components represent the different forces and the interaction between the ligand and the target proteins.

Table 4.100: MM-GBSA energy results

MM-GBSA energy results		
Energies (kcal/mol)	**Compound (NS5A-Phyb L)**	**Compound (NS5B-Circulin E)**
ΔG_{bind}	-46.4648	-935.7883
ΔG_{bind} Coulomb	-48.2306	184.2841
ΔG_{bind} Covalent	0.8489	-30.7469
ΔG_{bind} H_{bond}	-1.7356	-40.0357
ΔG_{bind} Lipo	-17.4771	-361.0248
ΔG_{bind} Packing	-0.0036	0.0323
ΔG_{bind} SelfCont	0.2656	1.9201
ΔG_{bind} Solv-GB	49.8535	-157.4554
ΔG_{bind} vdW	-29.9858	-532.7619

CHAPTER 5

DISCUSSION

In current research toxin proteins NS5A and NS5B were extracted from the Protein Data Bank (PDB) and then purified, and the obtained structures were of good quality and suitable for the subsequent computational analysis. Water molecules and ligands were removed by Biovia Discovery Studio Visualizer in order to have structures of proteins that were free from these elements and suitable for further analysis. When the physicochemical properties analysis of the protein was done using ProtParam, the following information was obtained. The theoretical pI of NS5A was estimated to be 6.64 which indicates that at slightly acidic to neutral pH conditions, while that of NS5B has a pI of 9.06; conversely, it showed neutrality at a high pH level. Hence, it is anticipated that NS5A and NS5B have different conformations based on the pH of the environment to which they are exposed, which is a significant aspect of comprehending the roles of the proteins.

Upon the analysis of the docking that was done using ClusPro, several cyclotides were found to have a high binding affinity towards NS5A and NS5B and a low energy score. Phyb L originates in the *Petunia x hybrida* plant and occurs naturally boasts a cyclic cystine knot structure and exceptional stability, rendering it impervious to protease cleavage [68]. In the current study, Phyb L had an excellent binding with the NS5A protein with a score of -1037.8, which indicates the strong binding energy of Phyb L, therefore, can be considered as an antiviral agent for the development of new drugs for the treatment of viral diseases through targeting the NS5A protein. Circulin E is a natural product and a cyclotide found in plants of the Rubiaceae family. Circulin E is a cyclic peptide (cyclotide) derived from the *Chassalia parvifolia* plant. It was demonstrated that as a member of the circulin family, it could inhibit the cytopathic effects of in vitro HIV-1 infection [69]. The current study shows that Circulin E has a high binding affinity with the NS5B protein, with a minimum energy of -1059.7. This strong binding affinity suggests it can be used as an antiviral compound, especially in drug formulations targeting the NS5B protein in HCV infection.

Desmond was used to perform molecular dynamics simulations that assisted in identifying the stability and the binding interactions of the binds in these complexes. The RMSD values of the Phyb L-NS5A complex were almost similar for the protein and ligand, and the hydrogen bonds formed in the simulation were higher, which indicates that the binding interaction is stable. Similarly, for the Circulin E-NS5B complex, the RMSD values were not much varying, and the hydrogen bonds were not much varying, indicating that the complex's interactions were stable and efficient. This simulation stability makes the audience confident in the reliability of our research and findings.

The MM-GBSA analysis shows that the NS5A-Phyb L complex displays a moderate binding energy of -46.4648 kcal/mol, and the lowest binding energy of -935.7883 kcal/mol was observed for the complex formed between NS5B-Circulin E. Due to this high binding affinity of NS5B, Circular E could very well be a potent inhibitor of the NS5B protein, thus being a potential drug candidate for HCV treatment. This suggests that the moderate binding of NS5A might also have antiviral effects but may need further enhancement for better therapeutical outcomes [70]. The difference in Coulomb and vdW interactions between the two complexes is also seen, and in particular, much stronger in the NS5B complex, which testifies to the contribution of electrostatic and van der Waals forces to this binding. The positive energy values, including ΔG_{bind} Solv-GB for NS5A-Phyb L (49.8535 kcal/mol) and ΔG_{bind} Coulomb for NS5B-Circulin E (184.2841 kcal/mol), are destabilizing. Nevertheless, these positive contributions are small in comparison to the strong negative interactions that enable the ligands to remain stably bound. The overall binding energy remains negative, which means that the positive components do not over-dominate the overall binding energy [71]. These findings indicate that targeting NS5B may lead to more potent antiviral effects, while the antiviral effect of the NS5A may be enhanced by better structural optimization.

Research conducted by Shams, Kanwal [72] identified cyclotides Kalata B2, Kalata B12, and Cycloviolacin O14, with binding energies of -11 kcal/mol, -9.8 kcal/mol, and -8.4 kcal/mol, respectively, using MOE docking software. These cyclotides also suppressed NS5A expression in HepG2 cells. The percent inhibition of NS5A by Kalata B12 was the highest at 100 nM with 75% inhibition. Their study also endorses cyclotides as potential antiviral agents; however, it was conducted in vitro, while the

current work employed insilico analysis. In the current work, cyclotides, namely Phyb L and Circular E, had good binding energy with NS5A and NS5B proteins, the binding energy being -1037.8 and -1059.7, respectively; the bindings were also stable in the MD simulations. In addition, these cyclotides were expected to be non-toxic and non-allergenic, hence suitable for use in treating illnesses. Both studies focus on the HCV NS5A protein, considered for inhibition in treating the disease, and the cyclotides as potential antiviral agents. Thus, future research should be done to integrate these methods and perform in vivo experiments and clinical trials to prove the effectiveness of cyclotides in the treatment and their non-toxicity.

A research by Dhanasekaran, Selvadoss [73] centered on the binding interactions of structurally different Phyto-therapeutics with the catalytic residues of the HCV NS5B polymerase, based on their research, natural substances such as arjunolic acid can effectively combat viruses due to their high binding affinity (-8.78 kcal/mol) and stability. The present study delves deeply into the three-dimensional structures, GRAVY values (-0.364 for NS5A and -0.272 for NS5B), isoelectric points (pI values of 6.64 for NS5A and 9.06 for NS5B), and interactions between the toxin proteins NS5A and NS5B and different cyclotides. In both investigations, molecular docking and molecular dynamics simulations were employed to determine stable and likely conformations, illuminating dynamic interactions and the final stabilization of protein-drug candidates complexes. These discoveries advance a better knowledge of protein behavior and the creation of tailored antiviral treatments when combined with the specific physiochemical characteristics and interaction energies offered in recent studies.

CONCLUSION

The study of molecular docking using ClusPro and MD simulations with Desmond provides a detail approach to understanding the molecular interactions of cyclopeptides with viral proteins. The cyclopeptides (circulin E, PHYB L) targeting NS5A and NS5B proteins of HCV showed promising binding affinity and stability, suggesting its potential as a dual-targeting antiviral agent.

Thus, it is concluded that the cyclotides could be the potential inhibitor against NS5A, NS5B protease of HCV and it could be helpful in designing the inhibitory drugs with simple structural modifications against HCV.

Limitations

A limitation is the lack of information about the level of cyclotides' biological activity in different strains of HCV and the organisms infected with it. The viral family Hepatitis C Virus (HCV) is characterized by high genetic variability, which can influence the effectiveness of antiviral medication. The study is quite particular concerning the interactions of cyclotides with NS5A/NS5B proteins; however, the different genotypes of HCV are not considered. Further, the insilico approach has no information on the pharmacokinetics and pharmacodynamics of cyclotides in organisms, which are vital, especially for their use in drug development. These factors also indicate that more detailed biological and clinical studies should be conducted to determine the practical relevance of the outcomes.

REFERENCES

1. Roudot-Thoraval, F., *Epidemiology of hepatitis C virus infection.* Clinics and research in hepatology and gastroenterology, 2021. **45**(3): p. 101596.
2. Negro, F., *Natural history of hepatic and extrahepatic hepatitis C virus diseases and impact of interferon-free HCV therapy.* Cold Spring Harbor Perspectives in Medicine, 2020. **10**(4).
3. Malik, F., *Treating children and adolescents with hepatitis C: policies and practices*. 2022, UCL (University College London).
4. Farhan, M., et al., *National hepatitis registry in Pakistan: a dire need for hepatitis surveillance and control.* Tropical Medicine and Health, 2023. **51**(1): p. 41.
5. Davis, G.L., et al., *Aging of hepatitis C virus (HCV)-infected persons in the United States: a multiple cohort model of HCV prevalence and disease progression.* Gastroenterology, 2010. **138**(2): p. 513-21, 521.e1-6.
6. Heiza, M., K. Elmola, and B. Salama, *Unsafe practices associated with HCV infection among adults: a case control study.* International Journal of Preventive Medicine, 2021. **12**.
7. Organization, W.H., *Training modules on Hepatitis B and C screening, diagnosis and treatment.* 2020.
8. Pawlotsky, J.M., *Use and interpretation of virological tests for hepatitis C.* Hepatology, 2002. **36**(5B): p. s65-s73.
9. Pawlotsky, J.M., *Molecular diagnosis of viral hepatitis.* Gastroenterology, 2002. **122**(6): p. 1554-1568.
10. Lindenbach, B.D. and C.M. Rice, *The ins and outs of hepatitis C virus entry and assembly.* Nature Reviews Microbiology, 2013. **11**(10): p. 688-700.
11. Tabata, K., C.J. Neufeldt, and R. Bartenschlager, *Hepatitis C virus replication.* Cold Spring Harbor perspectives in medicine, 2020. **10**(3).
12. Guntipalli, P., et al., *Worldwide prevalence, genotype distribution and management of hepatitis C.* Acta gastroenterol. belg, 2021. **84**(4): p. 637-56.

13. Geddawy, A., et al., *Direct acting anti-hepatitis C virus drugs: clinical pharmacology and future direction.* Journal of translational internal medicine, 2017. **5**(1): p. 8-17.
14. Moradpour, D. and F. Penin, *Hepatitis C virus proteins: from structure to function.* Hepatitis C virus: from molecular virology to antiviral therapy, 2013: p. 113-142.
15. Elazar, M., et al., *Amphipathic helix-dependent localization of NS5A mediates hepatitis C virus RNA replication.* Journal of virology, 2003. **77**(10): p. 6055-6061.
16. Gale Jr, M.J., et al., *Evidence that hepatitis C virus resistance to interferon is mediated through repression of the PKR protein kinase by the nonstructural 5A protein.* Virology, 1997. **230**(2): p. 217-227.
17. Belema, M., et al., *Discovery and development of hepatitis C virus NS5A replication complex inhibitors.* Journal of medicinal chemistry, 2014. **57**(5): p. 1643-1672.
18. Cheemerla, S. and M. Balakrishnan, *Global epidemiology of chronic liver disease.* Clinical liver disease, 2021. **17**(5): p. 365-370.
19. Moustafa, R., *Characterization of functional determinants in the C-terminal part of hepatitis C virus E1 glycoprotein ectodomain*. 2019, Université de Lille.
20. Bartenschlager, R., V. Lohmann, and F. Penin, *The molecular and structural basis of advanced antiviral therapy for hepatitis C virus infection.* Nature Reviews Microbiology, 2013. **11**(7): p. 482-496.
21. Chen, S., et al., *Flaviviridae virus nonstructural proteins 5 and 5A mediate viral immune evasion and are promising targets in drug development.* Pharmacology & Therapeutics, 2018. **190**: p. 1-14.
22. Sesmero, E. and I.F. Thorpe, *Using the hepatitis C virus RNA-dependent RNA polymerase as a model to understand viral polymerase structure, function and dynamics.* Viruses, 2015. **7**(7): p. 3974-3994.
23. Venkataraman, S., B.V. Prasad, and R. Selvarajan, *RNA dependent RNA polymerases: insights from structure, function and evolution.* Viruses, 2018. **10**(2): p. 76.

24. Kulkarni, A.S., *Mechanisms of action and resistance to novel inhibitors of the Hepatitis C virus RNA-dependent RNA polymerase*. 2015: McGill University (Canada).
25. Gould, A., et al., *Cyclotides, a novel ultrastable polypeptide scaffold for drug discovery.* Current pharmaceutical design, 2011. **17**(38): p. 4294-4307.
26. Mammari, N., et al., *Plant-derived antimicrobial peptides as potential antiviral agents in systemic viral infections.* Pharmaceuticals, 2021. **14**(8): p. 774.
27. Vilas Boas, L.C.P., et al., *Antiviral peptides as promising therapeutic drugs.* Cellular and Molecular Life Sciences, 2019. **76**: p. 3525-3542.
28. Moosavy, S.H., et al., *Epidemiology, transmission, diagnosis, and outcome of Hepatitis C virus infection.* Electronic physician, 2017. **9**(10): p. 5646.
29. Jirasko, V., et al., *Structural and functional characterization of nonstructural protein 2 for its role in hepatitis C virus assembly.* Journal of Biological Chemistry, 2008. **283**(42): p. 28546-28562.
30. Alvisi, G., V. Madan, and R. Bartenschlager, *Hepatitis C virus and host cell lipids: an intimate connection.* RNA biology, 2011. **8**(2): p. 258-269.
31. McDonald, S.A., et al., *Projections of the current and future disease burden of hepatitis C virus infection in Malaysia.* PLoS One, 2015. **10**(6): p. e0128091.
32. Appel, N., et al., *From structure to function: new insights into hepatitis C virus RNA replication.* Journal of Biological Chemistry, 2006. **281**(15): p. 9833-9836.
33. Romero-López, C. and A. Berzal-Herranz, *Structure-function relationship in viral RNA genomes: The case of hepatitis C virus.* 2014.
34. Shaheen, M.A. and M. Idrees, *Evidence-based consensus on the diagnosis, prevention and management of hepatitis C virus disease.* World journal of hepatology, 2015. **7**(3): p. 616.
35. Patel, J., *An Investigation of the Complexes Formed Between the Hepatitis C Virus E1 and E2 Glycoproteins*. 1999: University of Glasgow (United Kingdom).
36. Hezode, C., et al., *Resistance analysis in patients with genotype 1–6 HCV infection treated with sofosbuvir/velpatasvir in the phase III studies.* Journal of hepatology, 2018. **68**(5): p. 895-903.

37. Song, Y., *Regulation of Hepatitis C Virus translation by the viral internal ribosome entry site and the 3′-untranslated region.* 2006.
38. Katze, M.G., Y. He, and M. Gale, *Viruses and interferon: a fight for supremacy.* Nature Reviews Immunology, 2002. **2**(9): p. 675-687.
39. Bulankina, A.V., R.M. Richter, and C. Welsch, *Regulatory role of phospholipids in hepatitis C virus replication and protein function.* Pathogens, 2022. **11**(1): p. 102.
40. Lee, W.P., et al., *Ser38-His93-Asn91 triad confers resistance of JFH1 HCV NS5A-Y93H variant to NS5A inhibitors.* The FEBS Journal, 2024. **291**(6): p. 1264-1274.
41. Li, H.-C., C.-H. Yang, and S.-Y. Lo, *Hepatitis C viral replication complex.* Viruses, 2021. **13**(3): p. 520.
42. Neumann, S., et al., *How do viruses control mitochondria-mediated apoptosis?* Virus research, 2015. **209**: p. 45-55.
43. Choi, B.-H. and H.S. Yoon, *FKBP38-Bcl-2 interaction: a novel link to chemoresistance.* Current opinion in pharmacology, 2011. **11**(4): p. 354-359.
44. Hollingworth, R. and R.J. Grand, *Modulation of DNA damage and repair pathways by human tumour viruses.* Viruses, 2015. **7**(5): p. 2542-2591.
45. Dash, S., Y. Aydin, and C.M. Stephens, *Hepatitis C Virus NS5B RNA-dependent RNA polymerase inhibitor: an integral part of HCV antiviral therapy*, in *Viral Polymerases*. 2019, Elsevier. p. 211-235.
46. Samanta, S., *Structure-function studies of viral RNA-dependent RNA polymerases.* Structure, 2018. **2018**: p. 09-18.
47. Barakat, K.H., et al., *Detailed computational study of the active site of the hepatitis C viral RNA polymerase to aid novel drug design.* Journal of chemical information and modeling, 2013. **53**(11): p. 3031-3043.
48. Luo, G., et al., *De novo initiation of RNA synthesis by the RNA-dependent RNA polymerase (NS5B) of hepatitis C virus.* Journal of virology, 2000. **74**(2): p. 851-863.
49. Zając, M., et al., *Hepatitis C–New drugs and treatment prospects.* European journal of medicinal chemistry, 2019. **165**: p. 225-249.

50. Jennings, C., et al., *Biosynthesis and insecticidal properties of plant cyclotides: the cyclic knotted proteins from Oldenlandia affinis.* Proceedings of the National Academy of Sciences, 2001. **98**(19): p. 10614-10619.
51. Gunasekera, S., et al., *Chemical synthesis and biosynthesis of the cyclotide family of circular proteins.* IUBMB life, 2006. **58**(9): p. 515-524.
52. Craik, D.J., R.J. Clark, and N.L. Daly, *Potential therapeutic applications of the cyclotides and related cystine knot mini-proteins.* Expert opinion on investigational drugs, 2007. **16**(5): p. 595-604.
53. Saether, O., et al., *Elucidation of the primary and three-dimensional structure of the uterotonic polypeptide kalata B1.* Biochemistry, 1995. **34**(13): p. 4147-4158.
54. Koehbach, J., et al., *Cyclotide discovery in Gentianales revisited—identification and characterization of cyclic cystine‐knot peptides and their phylogenetic distribution in Rubiaceae plants.* Peptide Science, 2013. **100**(5): p. 438-452.
55. Barry, D.G., et al., *Solution structure of the cyclotide palicourein: implications for the development of a pharmaceutical framework.* Structure, 2004. **12**(1): p. 85-94.
56. Bobardt, M.D., et al., *Hepatitis C virus NS5A anchor peptide disrupts human immunodeficiency virus.* Proceedings of the National Academy of Sciences, 2008. **105**(14): p. 5525-5530.
57. Pallaghy, P.K., et al., *A common structural motif incorporating a cystine knot and a triple‐stranded β‐sheet in toxic and inhibitory polypeptides.* Protein Science, 1994. **3**(10): p. 1833-1839.
58. Qin, Q., et al., *Identification of candidates for cyclotide biosynthesis and cyclisation by expressed sequence tag analysis of Oldenlandia affinis.* Bmc Genomics, 2010. **11**: p. 1-11.
59. Berman, H.M., et al., *The protein data bank.* Nucleic acids research, 2000. **28**(1): p. 235-242.
60. Baroroh, U., et al., *Molecular interaction analysis and visualization of protein-ligand docking using Biovia Discovery Studio Visualizer.* Indonesian Journal of Computational Biology (IJCB), 2023. **2**(1): p. 22-30.

61. Martinez, G.S., et al., *Multiple Protein Profiler 1.0 (MPP): A webserver for predicting and visualizing physiochemical properties of proteins at the proteome level.* arXiv preprint arXiv:2312.00796, 2023.
62. Chauhan, B., B. Sharma, and H. Singh, *Swiss-model: a web-based computational tool for designing of protein structures.* 2020.
63. Alekseenko, A., et al., *Protein–protein and protein–peptide docking with ClusPro server.* Protein Structure Prediction, 2020: p. 157-174.
64. Tao, Y., et al., *PyVibMS: a PyMOL plugin for visualizing vibrations in molecules and solids.* Journal of Molecular Modeling, 2020. **26**: p. 1-12.
65. Shivanika, C., et al., *Molecular docking, validation, dynamics simulations, and pharmacokinetic prediction of natural compounds against the SARS-CoV-2 main-protease.* Journal of biomolecular structure & dynamics, 2020: p. 1.
66. Di Micco, S., et al., *Garcinol and related polyisoprenylated benzophenones as topoisomerase II inhibitors: biochemical and molecular modeling studies.* Journal of natural products, 2019. **82**(10): p. 2768-2779.
67. Chinnasamy, S., et al., *Molecular docking and molecular dynamics simulation studies to identify potent AURKA inhibitors: assessing the performance of density functional theory, MM-GBSA and mass action kinetics calculations.* Journal of Biomolecular Structure and Dynamics, 2020. **38**(14): p. 4325-4335.
68. Poth, A.G., et al., *Cyclotides associate with leaf vasculature and are the products of a novel precursor in petunia (Solanaceae).* Journal of Biological Chemistry, 2012. **287**(32): p. 27033-27046.
69. Gustafson, K.R., et al., *New Circulin Macrocyclic Polypeptides from Chassalia p arvifolia.* Journal of natural products, 2000. **63**(2): p. 176-178.
70. Barbaro, G., et al., *Highly active antiretroviral therapy: current state of the art, new agents and their pharmacological interactions useful for improving therapeutic outcome.* Current pharmaceutical design, 2005. **11**(14): p. 1805-1843.
71. Rastelli, G., et al., *Fast and accurate predictions of binding free energies using MM-PBSA and MM-GBSA.* Journal of computational chemistry, 2010. **31**(4): p. 797-810.

72. Shams, F., et al., *Cyclopeptide Kalata B12 as HCV-NS5A potent Inhibitor: Cyclopeptide Kalata B12 as HCV-NS5A Potent Inhibitor*. Pakistan BioMedical Journal, 2022: p. 267-271.

73. Dhanasekaran, S., et al., *Regulation of NS5B Polymerase Activity of Hepatitis C Virus by Target Specific Phytotherapeutics: An In-Silico Molecular Dynamics Approach.* Cell Biochemistry and Biophysics, 2024: p. 1-20.